

Universidade Federal do Rio Grande – FURG

Instituto de Oceanografia

Programa de Pós-Graduação em Oceanologia

Geoquímica do Arsênio em Sedimentos do Estuário da Lagoa dos Patos

Larissa Pinheiro Costa

Tese apresentada ao Programa de Pós-Graduação em
Oceanologia, como parte dos requisitos para a obtenção do
Título de Doutor.

Orientador: *Prof. Dr. Nicolai Mirlean*

Universidade Federal do Rio Grande (FURG), Brasil.

Rio Grande, RS, Brasil

Janeiro, 2020

Geoquímica do Arsênio em Sedimentos do Estuário da Lagoa dos Patos (RS)

Tese apresentada ao Programa de Pós-Graduação em Oceanologia, como parte dos
requisitos para a obtenção do Título de Doutor.

Larissa Pinheiro Costa

Rio Grande, RS, Brasil

Janeiro, 2020

© A cópia parcial e a citação de trechos desta tese são permitidas sobre a condição de que
qualquer pessoa que a consulte reconheça os direitos autorais do autor. Nenhuma
informação derivada direta ou indiretamente desta obra deve ser publicada sem o
consentimento prévio e por escrito do autor.

Costa, Larissa Pinheiro

Geoquímica do Arsênio em Sedimentos do Estuário da Lagoa dos Patos (RS)./

Larissa Pinheiro Costa. – Rio Grande: FURG, 2020.

Número de páginas p.127

Tese (Doutorado) – Universidade Federal do Rio Grande.

Doutorado em Oceanologia. Área de Concentração: Geoquímica

1. Arsênio. 2. Estuário 3. Bioturbação 4. Bioirrigação

Agradecimentos

Ao longo destes quatro anos de doutorado aprendi muito, tanto academicamente quanto pessoalmente. As batalhas, estresses e momentos de ansiedade não poderiam ter sido vencidos se eu não tivesse a ajuda de diversas pessoas. E é a estas pessoas que dedico mais esta conquista.

Primeiramente agradeço aos colegas de laboratório e todo o pessoal do LOG pelo apoio e carinho. Em especial a Elisa Seus, que mais do que técnica do laboratório também se tornou uma grande amiga, sempre me ajudando de muito bom humor, torcendo por mim e fazendo o melhor para me ajudar.

Ao meu orientador Prof. Nicolai Mirlean, por ter aceitado esta orientação e ter acreditado nos meus sonhos, especialmente quando decidi fazer o Programa de Doutorado Sanduíche. Muito obrigado por toda atenção e orientação.

Aos meus irmãos Lucas, Izadora e Pedro Henrique, pelos momentos tranquilos e divertidos. Iza, obrigado pelas noites de series e descanso e por ter sido minha família no Natal longe de casa. Lucas, obrigada pelas tuas piadas irritantes e engraçadas. Pedro Henrique, obrigado por esse sorriso lindo e amor sincero.

As minhas amigas que escutaram todos as minhas reclamações, me acalmara e sempre se orgulharam de mim. Especialmente, Thaís Silveira, Bianca Maio e Daniela Flores. Obrigado por tanto.

Por fim, e não menos importante, agradeço a Prof. Dr. Karen Johannesson por me receber nos USA, por toda ajuda e principalmente por acreditar no meu trabalho. Aos meus colegas na Tulane University, especialmente Segun e Jackie (I miss our meetings!). A melhor amiga que ganhei, Enyiah, que eu sinto saudade diária. A Prof. Elisabeth Gleckler por me receber e tornar meus dias mais alegres. A todos os amigos que fiz nesse ano de intercâmbio em New Orleans, a essa cidade especial que me conquistou e que me ensinou tanto.

Agradeço também a CAPES por essa oportunidade e ao Programa de Pós-Graduação em Oceanologia da FURG por toda estrutura disponibilizada e a todos os professores que fizeram parte desta jornada.

Índice

Agradecimentos	i
Lista de Figuras.....	v
Lista de Tabelas	vii
Resumo.....	viii
Abstract	x
1. Introdução Geral	1
1.1. Toxicidade do Arsênico	2
1.2. Geoquímica do Arsênio	4
1.3. O cenário atual do estudo da geoquímica do Arsênio no Brasil	8
2. Hipótese.....	10
3. Objetivos.....	10
3.1. Objetivos Específicos	10
4. Área de Estudo.....	11
5. Material e Métodos	14
5.1. Coleta e Amostragem de Sedimentos e Testemunhos.....	14
5.2. Análises Químicas e Geológicas	18
5.3. Análise de Arsênio e Elementos Metálicos	20
5.4. Caracterização mineralógica dos nódulos de Fe-Mn	22
5.5. Análise de Água Intersticial.....	23
CAPÍTULO I: Distribution and geochemistry of arsenic in sediments of the world's largest choked estuary: The Patos Lagoon, Brazil.....	26
Abstract	26
Introduction	26
Study Area	30
Materials and Methods	32

Results	35
Salt marshes	35
Shallow open water areas	40
Discussion.....	45
Salt marshes	45
Shallow open water areas	47
Conclusion	50
Acknowledgments.....	52
References	52
CAPÍTULO II: Effects of bioirrigation and salinity on arsenic distributions in ferruginous concretions from salt marsh sediment cores (southern Brazil)	61
Abstract	61
Introduction	61
Study Area	64
Methods	65
Sampling approach.....	65
Sediment sampling and analysis	66
Pore water analysis.....	69
Results	70
Sediment geochemistry	70
Pore water chemistry	76
Discussion.....	79
Controls on As distribution in salt marshes sediments	79
Pore water redox cycling	83
Conclusion	85
Acknowledgments.....	86
References	86

CAPÍTULO III: Arsenic environmental threshold surpass in estuarine sediments: effects of bioturbation	93
Abstract	93
Introduction	93
Methods and Materials	95
Results and Discussion.....	97
Acknowledgements	99
References	99
6. Considerações Finais e Conclusão	102
7. Referências Bibliográficas.....	104
ANEXOS	117

Lista de Figuras

Figura 1- Diagrama Eh-pH para as espécies de As em meio aquoso, no sistema As-O ₂ -H ₂ O a 25°C e 1 bar de pressão total (Smedley e Kinnburgh, 2002) AsH ₃	5
Figura 2- Localização da Lagoa dos Patos com destaque para região estuarina.....	11
Figura 3 - Localização dos pontos amostrados no estudo dos efeitos da salinidade; Capítulo 1.....	15
Figura 4 – Amostragem testemunho de marisma ocupada por <i>N. granulata</i> . A: testemunho entre 8 – 18 cm de profundidade (escala em preto – 10 cm); B: amostras seccionadas em 1 cm e separadas em placas de petri; C: amostra seca, pontos avermelhados indicam presença de nódulos de Fe-Mn.....	17
Figura 5 - Amostras coletadas na Ilha da Pólvora; A – local ocupado por <i>S. alterniflora</i> (SA) B – local ocupado por <i>N. granulata</i> (DA); Capítulo 3. Círculos amarelos (A) e marcações brancas (B) representam locais onde sedimento foi coletado para análise.....	18
Figura 6 – Nódulos de Fe-Mn observados visualmente, amostra de nódulos extraídas da profundidade de 13 cm para marisma ocupada por <i>S. alterniflora</i>	23
CAPÍTULO I: Distribution and geochemistry of arsenic in sediments of the world's largest choked estuary: The Patos Lagoon, Brazil	
Figure 1 – Patos Lagoon estuary and samples location. Sites labeled with “M” represent locations where salt marsh sediment cores were collected, whereas those labeled with “Z” show the sites where sediment cores were collected from beneath open water.....	30
Figure 2 – Arsenic, manganese and iron vertical distribution for marshes areas (M1, M2 and M3).....	38
Figure 3 – Arsenic, total organic carbon and fine grains vertical distribution for marshes areas (M1, M2, and M3).....	39
Figure 4 – Arsenic, manganese and iron vertical distribution for shallow open water areas (Z1, Z2, and Z3).....	43
Figure 5 – Arsenic, total organic carbon and fine grains vertical distribution for shallow open areas (Z1, Z2, and Z3).....	44
Figure 6 – Arsenic, free sulfides, AVS and CRS vertical distribution in shallow open water areas (Z1, Z2, and Z3).....	49

CAPÍTULO II: Effects of bioirrigation and salinity on arsenic distributions in ferruginous concretions from salt marsh sediment cores (southern Brazil)

Figure 1 – Patos Lagoon estuary showing our sampling locations. Site labeled with “NG” represents location where the crab <i>Neohelice granulata</i> is chiefly responsible for bioturbation, whereas location labeled with “SA” shows the sampling site occupied by <i>Spartina alterniflora</i>	65
Figure 2 – Sediment cores collected from the NG (A) and the SA (B) sites of the Pólvora Island salt marsh. Ferruginous nodules/concretions subsamples from 15 cm depth in each core are also shown.....	67
Figure 3 – Percentage of fine grain sediment, total organic carbon (TOC) content, and redox potential (Eh) as a function of depth for sediment cores collected from the NG (A) and SA (B) sites in the Pólvora Island salt marsh.....	72
Figure 4 – Arsenic, manganese, and iron content in ferruginous sediment nodules as a function of depth for sediment cores collected from the NG (A) and SA (B) sites within the Pólvora Island salt marsh. See Figure 1 for locations of the cores.....	73
Figure 5 – Optical microscope images of the insides of ferruginous nodules from the NG (A) and SA (B) cores, obtained from a depth of 17 cm. The nodules contain occluded quartz grains, examples of which are circled on each nodule sample. Magnification of 2.5x and 1.6x for NG and SA, respectively.....	74
Figure 6 – Mineralogical characteristics of a nodule from 17 cm depth – SA location. A) SEM image shows no internal structure, Nevertheless, quartz grains (Qz) can be observed within the ferruginous nodule (arrow in panel A). B) EDS analysis shows high intensities of Fe, Si, Ca, Al, and Ti. C) X-ray diffraction analyses (XRD) indicate the presence of quartz, muscovite, kaolinite, dickite, and albite.....	75
Figure 7 – pH, Mn, and Fe concentrations in pore water as a function of depth at sites for sediment cores collected in Pólvora Island. A: NG core collected during brackish water period. B: NG core collected during fresh water period. C: SA core collected during brackish water period. D: SA core collected during fresh water period.....	78
Figure 8 – Arsenic content in sediment nodules normalized by iron content and the percentage of nodules as functions of depth for sites NG (A) and SA (B).....	82
CAPÍTULO III: Arsenic environmental threshold surpass in estuarine sediments: effects of bioturbation	
Figure 1 - Study area. Sampling points: DA- area populated by <i>Neohelice granulata</i> crabs; SA- area occupied by <i>Spartina alterniflora</i>	95

Lista de Tabelas

Tabela 1 – Limites de detecção e precisão (% RSD – desvio padrão relativo) para as análises químicas e geológicas.....19

Tabela 2- Limites de detecção e precisão (% RSD – desvio padrão relativo) para as análises de arsênio e elementos metálicos.....22

CAPÍTULO I: Distribution and geochemistry of arsenic in sediments of the world's largest choked estuary: The Patos Lagoon, Brazil

Table 1 - Geochemical parameters for marsh sediments on fluvial domain – M locations. The upper numbers are the concentration range, and the mean \pm SD for the entire core is presented within parentheses.....36

Table 2 – Geochemical parameters for shallow open water areas sediments on fluvial domain – Z locations. The upper numbers are the concentration range, and the mean \pm SD for the entire core is presented within parentheses.....41

CAPÍTULO II: Effects of bioirrigation and salinity on arsenic distributions in ferruginous concretions from salt marsh sediment cores (southern Brazil)

Table 1 - Analytical quality control data, average and standard deviation obtained for 3 replicates of the standard reference material MESS-4.....69

Table 2 – Geochemical parameters for marsh nodules, salt water period. The upper numbers are the concentration range, and the mean \pm SD for the entire core is presented within parentheses.....71

Table 3 – Iron, manganese contents and pH for NG and SA pore water. The upper numbers are the concentration range, and the mean \pm SD for the entire core is presented within parentheses.....77

CAPÍTULO III: Arsenic environmental threshold surpass in estuarine sediments: effects of bioturbation

Table 1 - Concentrations of elements in different extractions from sediments in crab (DA) and spartina (SA) areas. The concentration range is shown as the numerator, and the mean \pm SD is presented as the denominator.....97

Resumo

Este estudo apresenta resultados acerca da geoquímica do arsênio (As) no estuário da Lagoa dos Patos, onde predominam zonas rasas de alta produtividade biológica sob um regime hidrológico irregular. Para compreender a geoquímica do metaloide no estuário, investigou-se a relação dos processos diagenéticos/biológicos na distribuição do As. Testemunhos foram coletados em três locais dentro do estuário para analisar possíveis alterações no conteúdo de As com o gradiente de salinidade. Dois testemunhos foram coletados em cada localidade, um em água rasa sem vegetação e o outro em uma marisma. Juntamente com As, quantificamos o tamanho das partículas, potencial redox (Eh), manganês (Mn), ferro (Fe), carbono orgânico total (COT), concentrações de sulfeto livre (dissolvido), os sulfetos voláteis ácidos (AVS) e os sulfetos redutíveis em cromo (CRS). Ademais, para estudar os efeitos da bioturbação/bioirrigação testemunhos foram obtidos durante um período dominado por água polihalina, em dois ambientes diferentes de uma marisma: um não vegetado colonizado por caranguejos (*Neohelice granulata*) e um local vegetado por *Spartina alterniflora*. Especificamente, determinamos a porcentagem de nódulos em cada intervalo de profundidade, juntamente com o conteúdo de As, Fe e Mn dos nódulos, que foi analisado por espectrometria ICP-MS. A mineralogia dos nódulos foi investigada por microscópio eletrônico de varredura (MEV) com sistema EDS, e por difratômetria de raios-X. Os resultados demonstraram que nódulos são compostos principalmente por quartzo, filossilicatos e óxidos/oxi-hidróxidos amorfos de Fe-Mn. Nos sedimentos de zonas rasas, elevadas concentrações de As, Fe e Mn ocorrem em profundidades entre 40 cm e 50 cm (abaixo da superfície). Perfis verticais de Eh, sulfetos livres e CRS para testemunhos de zona rasa mostraram distribuição semelhante em profundidades de 50 cm, sugerindo que a formação de pirita é um importante reservatório para o As em sedimentos de águas rasas abertas. Nas marismas do estuário, a bioturbação/bioirrigação dos sedimentos leva à penetração de oxigênio abaixo da fronteira das zonas óxica e subóxica e à subsequente formação de óxi-hidróxidos de Fe-Mn em maior profundidade, onde a distribuição do As está fortemente correlacionada com a do Fe. Variações das concentrações de Fe e Mn da água intersticial foram analisadas, para períodos dominados por água polihalina e oligohalina. Os resultados do estudo da água inestrelcial mostraram que nas marismas ocupadas por *S. alterniflora*, o crescimento desta planta apresenta maior impacto na geoquímica do As, se comparado

aos efeitos da salinidade, devido à sulfato redução e a consequente redução do pH da água intersticial. Maiores concentrações de Fe foram observadas nas águas intersticiais durante o período de água polihalina, o que correspondeu à época de crescimento da *S. alterniflora* no estuário. O oposto ocorre em zonas ocupadas por *N. granulata*, onde maiores concentrações de Fe são observadas durante período oligohalino. Constatou-se também que áreas com sedimentos biologicamente perturbados podem superar concentrações de As estipuladas pelo legislativo, onde a formação de anomalias é resultado da redistribuição diagenética do metaloide, e não tem caráter antropogênico. Este estudo demonstra diferenças nas condições geoquímicas para os diferentes tipos de bioirrigação em sedimentos de marismas, além de diferenças nas condições geoquímicas para marismas e águas rasas abertas que podem ter implicações importantes para a distribuição de As em sedimentos estuarinos. Estudos futuros devem incluir taxas de sulfato redução e conteúdo de pirita, para assim fornecer uma melhor compreensão sobre a geoquímica e destino final do Fe e, consequentemente do As.

Palavras-chave: Arsênio, Marismas, Sulfetos Livres, Bioturbação, Óxidos/Oxihidróxidos de Ferro-Manganês.

Abstract

This study presents results on arsenic (As) geochemistry in Patos Lagoon estuary, where shallow areas of high biological productivity, under an irregular hydrological regime dominate. To understand the metalloid geochemistry in the estuary, we investigated the relationship of diagenetic/biological processes in As distribution. Cores were obtained from three sites within the estuary to analyze possible changes in As content with the salinity gradient. Two cores were collected at each location, one in shallow open water and another in a salt marsh. Together with As, we quantified particle size, redox potential (Eh), manganese (Mn), iron (Fe), total organic carbon (TOC), free sulfide (dissolved) concentrations, acid volatile sulfides (AVS) and reducible chromium sulfides (CRS). In addition, to study the effects of bioturbation/bioirrigation, cores were obtained during a period dominated by polyhaline water, in two different environments of a salt marsh: a non-vegetated colonized by crabs (*Neohelice granulata*) and a site vegetated by *Spartina alterniflora*. Specifically, we determined the percentage of nodules at each depth interval, along with the As, Fe, and Mn content of the nodules, that were analyzed by ICP-MS. Nodules mineralogy was investigated by scanning electron microscope (SEM) with EDS system and, by X-ray diffractometer. The results showed that the nodules are mainly composed of quartz, phyllosilicates and Fe-Mn amorphous oxides/oxyhydroxides. In shallow areas, a subsurface peak of As, Fe and Mn occurs at depths between 40 cm and 50 cm. Vertical profiles of Eh, free sulfides and CRS for these cores showed similar distribution at depths of 50 cm, suggesting that pyrite formation is an important reservoir for As in open shallow water sediments. In the estuary marshes, sediment bioturbation/bioirrigation leads to oxygen penetration below the oxic/suboxic barrier and subsequent Fe-Mn oxy-hydroxide precipitation, where As distribution is strongly correlated with Fe. Variations of Fe and Mn concentrations of interstitial water were also analyzed, for periods dominated by polyhaline and oligohaline water. Interstitial water results showed that *Spartina alterniflora* growth appears to have a greater impact on sediment geochemistry, when compared to salinity changes, due to sulfate reduction and associated decrease in interstitial water pH. Higher Fe concentrations were observed in interstitial waters during the polyhaline period, which corresponded to *S. alterniflora* growing season in the estuary. The opposite occurs in areas occupied by *N. granulata*, where higher Fe concentrations are observed during the

oligohaline period. It was also found that areas with biologically disturbed sediments may exceed As concentrations stipulated by the legislative, where the formation of anomalies is a result of the diagenetic redistribution of the metalloid, and has no anthropogenic character. This study demonstrates clear differences in geochemical conditions for different types of bioirrigation in marshes sediments, and differences in geochemical conditions for marshes and open shallow waters that may have important implications for As distribution in estuarine sediments. Future studies should include sulfate reduction rates and pyrite content, thus providing a better understanding of the geochemistry and ultimate fate of Fe and, consequently of As.

Key-words: Arsenic, Marshes, Free Sulfides, Bioturbation, Iron-Manganese oxides/oxyhydroxide.

1. Introdução Geral

As zonas costeiras são áreas consideradas propícias para o desenvolvimento de diversas atividades humanas, como, por exemplo, navegação, pesca, descarte de efluentes domésticos e industriais além de recreação. Os estuários integram a zona costeira, constituindo-se em ecossistemas que desempenham um importante papel na ciclagem de compostos orgânicos e inorgânicos (Medeiros *et al.*, 2005).

Sedimentos vêm sendo muito estudados ao longo dos anos devido a sua grande capacidade de adsorção de espécies orgânicas e inorgânicas na superfície mineral, que faz com que funcionem como repositórios de diversos contaminantes (Medeiros *et al.*, 2005). O equilíbrio das espécies associadas à superfície mineral depende das condições físico-químicas do meio, onde qualquer alteração facilita os processos de dessorção e solubilização dos elementos químicos, tornando-os biodisponíveis (Basílio, 2005). Sendo assim, torna-se importante entender, através de estudos da interação entre diferentes variáveis geoquímicas e físico-químicas, o comportamento e mobilidade de compostos tóxicos em sedimentos estuarinos.

Tais estudos são interessantes não apenas por avaliações das concentrações totais de metais, metaloides e ametais nos compartimentos ambientais, mas também para compreender a mobilidade e/ou biodisponibilidade dos elementos potencialmente tóxicos (Soares, 2011). As principais fontes naturais de metais/metaloides são o intemperismo sobre o material crustal, que os liberam nas formas dissolvida e/ou particulada e a atividade vulcânica, além da queima de florestas e a atividade biogênica (Davis *et al.*, 2003). As emissões antropogênicas para o meio ambiente são múltiplas, mas decorrem principalmente da mineração e da atividade industrial (Lima, 2008). Essas atividades antrópicas proporcionam influxos de um grande número de metais contaminantes nos ambientes naturais, em adição às fontes naturais, podendo provocar danos à saúde humana e biota.

A abundância normal de um elemento sem influência antrópica é denominada *background*, enquanto o limiar (*threshold*) é o valor superior da sua oscilação (Rohde, 2004). Quando um elemento ou substância apresenta concentrações acima dos valores de *background* este é considerado um contaminante, podendo ser potencialmente nocivo à biota (Gough, 1993). O estabelecimento de níveis de base (*background*) de elementos de interesse ambiental, devem ser levados em consideração. Estes níveis além de fornecer um panorama acerca da característica

geoquímica de ambientes costeiros, fornecem também parâmetros confiáveis de avaliação da qualidade ambiental (Soares, 2011). Nas áreas estuarinas, um cuidado adicional deve ser tomado, devido à dinâmica promovida pela ação das marés, fluxo dos rios e bioturbação. A contaminação metálica em sedimentos é potencialmente vulnerável, considerando-se que sua imobilização é relativamente instável, podendo ocorrer sua remobilização para o sistema (água e biota), sob determinadas modificações nas condições ambientais, principalmente com mudanças de pH e Eh. Destaca-se ainda que diversos processos bióticos e abióticos podem ser responsáveis por esse fenômeno, tornando biodisponíveis os metais e possibilitando sua bioacumulação e transferências na trama trófica (Jesus *et al.*, 2004).

O Arsênio (As) está entre os elementos mais nocivos à saúde humana, e os processos que levam à mobilidade do As em zonas costeiras e estuarinas devem ser estudados a fim de identificar os fatores que levam ao enriquecimento deste metalóide em sedimentos (Smith *et al.*, 2000; Sharma e Sohm, 2009). Sendo assim, propõem-se o estudo dos processos de distribuição do As em sedimentos e seu comportamento geoquímico durante a diagênese.

Sabe-se que os mecanismos de adsorção ou coprecipitação com óxidos/oxi-hidróxidos de Fe (III) sejam uma causa primária de elevadas concentrações de As em sedimentos (Pierce e Moore, 1982; Kneebone *et al.*, 2002; Smedley e Kinniburgh, 2002; Chaillou *et al.*, 2003; Bednar *et al.*, 2005; Ying *et al.*, 2012). Entretanto, como os sistemas estuarinos são meios que apresentam alta complexidade em termos de suas condições geoquímicas, as condições redox variam em resposta a muitos fatores (por exemplo, bioturbação, entrada de água doce e condições meteorológicas), e consequentemente a geoquímica de elementos sensíveis às condições redox, como S, Fe, Mn e As podem variar consideravelmente. Todos estes parâmetros físico-químicos, geológicos e geoquímicos devem ser levados em consideração na interpretação e compreensão da redistribuição e acumulação do As em sedimentos estuarinos.

1.1. Toxicidade do Arsênico

Nas últimas décadas o As tem sido o foco de atenção pública devido aos problemas de saúde, considerados semelhantes à uma epidemia, que vêm ocorrendo pelo consumo de água subterrânea contaminada por milhões de pessoas, principalmente em Bangladesh e Bengala Ocidental (Das *et al.*, 1996; Dhar *et al.*, 1997; Khan *et al.*, 1997). O efeito tóxico das espécies de As depende, principalmente, de sua forma química. O As inorgânico é considerado como

carcinogênico humano (Grupo I) (ASTDR, 2007) e, a toxicidade das espécies de As (III) é considerada superior à das espécies de As (V), por exemplo (Barra *et al.*, 2000). Além disso, o As também pode formar compostos orgânicos, que ocorrem devido à metilação (Cullen e Reimer, 1989). Esse processo de metilação do As inorgânico constitui um importante mecanismo de redução de sua toxidez. Os compostos inorgânicos são 100 vezes mais tóxicos que as espécies químicas metiladas (Mabuchi *et al.*, 1980).

As possíveis vias de exposição humana ao As são por meio de ingestão de água e comida contaminada, inalação de gases e ingestão de pó (Kendall *et al.*, 2003). Entretanto, a mais importante via de exposição humana é a ingestão de água (ASTDR, 2007). Uma longa exposição, principalmente aos compostos inorgânicos de As, pode conduzir a problemas cardiovasculares e neurológicos, além de alguns tipos de câncer (ASTDR, 2007). Em áreas contaminadas, por exemplo, em Bangladesh, o teor de As em águas subterrâneas pode chegar a $2500 \mu\text{g L}^{-1}$ (Ahmad *et al.*, 1997; Biswas *et al.*, 1999).

O valor de referência da Organização Mundial da Saúde (WHO, 2011) para o As em água potável é de $10 \mu\text{g L}^{-1}$, o mesmo estabelecido no Brasil através da CONAMA (2005 e 2008). Apesar disso, alguns países ainda mantêm o limite de $50 \mu\text{g L}^{-1}$, como Bangladesh e Índia (Rahman *et al.*, 2015). A combinação da alta toxicidade e ampla ocorrência do As gerou uma preocupação para o efetivo monitoramento deste elemento não só em água mas também em solo (Melamed, 2005). No Brasil, a resolução CONAMA 454/2012 (CONAMA, 2012) estabelece os níveis de arsênio para sedimento dragado apenas. Em águas doce, as concentrações de arsênio em sedimento seco não podem ultrapassar 17 mg kg^{-1} (Nível 2); e em águas salobras as concentrações não podem ser superiores a 70 mg kg^{-1} (Nível 2). O nível 2 representa o limiar acima do qual há maior probabilidade de efeitos adversos à biota (CONAMA, 2012). Já considerando o nível 1, limiar abaixo do qual há menor probabilidade de efeitos adversos à biota (CONAMA, 2012), os níveis de As não podem ultrapassar $5,9 \text{ mg kg}^{-1}$ e 19 mg kg^{-1} , para águas doce e salina, respectivamente.

Nos alimentos marinhos a presença de As não é crítica, visto que há uma pequena proporção de As na forma inorgânica, predominando os compostos orgânicos não tóxicos como a arsenobetaína e arsenocolina, presentes em peixes, frutos do mar e algas (Edmonds e Francesconi, 1987). A presença das espécies inorgânicas de As foi reportada em algumas culturas agrícolas por meio do sistema água-solo-planta (Khan *et al.*, 2010). Feldmann e Krupp (2011) apontam que em

peixe o As ocorre principalmente na forma não tóxica (85%) e, em contraste, no arroz as espécies tóxicas de As predominam (69%).

1.2. Geoquímica do Arsênio

O arsênio (As) é um elemento amplamente distribuído na crosta terrestre e existe a uma concentração média mundial de cerca 5 mg kg^{-1} (Flora, 2015). O As encontra-se na crosta principalmente na forma de arsenopirita (FeAsS) e em alguns outros minerais de sulfeto (por exemplo, ouro pigmento (As_2S_3), realgar (As_4S_4)), embora ocorra como constituinte em mais de 200 minerais de menor abundância (Garelick *et al.*, 2008). Estes minerais são relativamente raros em ambientes naturais, com maiores concentrações em áreas de mineralização onde ocorrem em estreita associação em minerais de outros elementos traço, tais como Ag, Au, Cd, Pb, P, Sb, Mo e W (Smedley e Kinniburgh, 2002). Devido a essa elevada capacidade de associação com outros elementos o As raramente é encontrado no meio como um elemento nativo (O'Day, 2004).

Este elemento é considerado como um metaloide que apresenta valência de 3-, 0, 3+ e 5+. O As está presente na natureza numa variedade de formas químicas, incluindo espécies orgânicas e inorgânicas, como resultado de sua participação em complexos biológicos, processos químicos e algumas aplicações industriais, como a manufatura de certos vidros, materiais semicondutores e fotocondutores, entre outros (Mirlean *et al.*, 2003, 2012; Sá *et al.*, 2015). As formas inorgânicas consideradas as mais comuns no ambiente abrangem as espécies químicas mais tóxicas nas formas de arsenato (AsO_4^{3-}) e arsenito (AsO_3^{3-}) (O'Day, 2004). Na Figura 1, o diagrama de estabilidade termodinâmica das principais espécies de As em função do pH e do potencial de oxirredução (Eh) em meio aquoso é apresentado. Trata-se de uma representação gráfica das possíveis fases de equilíbrio estáveis das diferentes espécies de arsênio onde os parâmetros físico-químicos, pH e Eh, são os principais responsáveis pela distribuição das espécies de As.

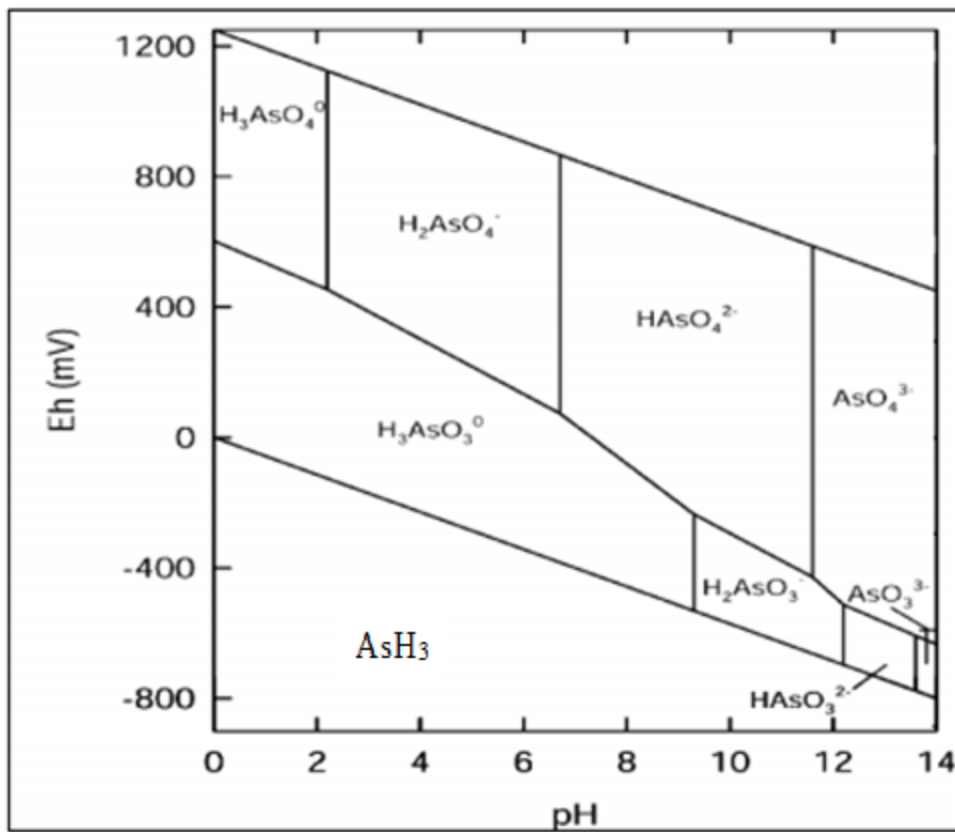


Figura 1- Diagrama Eh-pH para as espécies de As em meio aquoso, no sistema As-O₂-H₂O a 25°C e 1 bar de pressão total (Smedley e Kinnburgh, 2002) AsH₃

Os processos de mobilização de As que ocorrem naturalmente desempenham um papel importante em sua redistribuição no ambiente e muitos estudos foram realizados para melhor quantificar os processos responsáveis pela sua mobilização (Shimada, 1996; Sullivan e Aller, 1996; Nickson *et al.*, 2000; Smith *et al.*, 2000; Planer-Friedrich *et al.*, 2007; Choi *et al.*, 2009; Ravenscroft *et al.*, 2009; He *et al.*, 2010; Sailo e Mahanta, 2014). Os sulfetos de As, que são as principais formas minerais do metaloide, podem ser oxidados em condições superficiais, liberando o arsênio para as águas (Fagnani e Guimarães, 2011). As formas do arsênio trivalente (As⁺³; arsenito) e pentavalente (As⁺⁵; arsenato) (oxiânions) são muito solúveis, por isso atingem elevados teores – sem que ocorram processos de precipitação de minerais – e são as formas dominantes nas águas (Chaillou *et al.*, 2003). Ainda assim, apesar da grande solubilidade, as formas trivalentes e pentavalentes são suscetíveis de serem adsorvidas pela superfície de minerais metálicos, como os minerais de ferro (Fe) (Pierce e Moore, 1982; Mirlean *et al.*, 2003; Hatje *et al.*, 2010)

Embora vários processos possam liberar As dos sólidos, uma transição de condições óxicas para subóxicas e a correspondente recuperação de óxidos/óxi-hidróxidos de Fe (III) e Mn (IV), parecem ser um meio dominante, mas não exclusivo, pelo qual são geradas altas concentrações de As dissolvido (Bhattacharyya *et al.*, 2003; Smith *et al.*, 2006; Ravenscroft *et al.*, 2009; He *et al.*, 2010). Estudos demonstram que em níveis redox mais altos (500-200 mV), a solubilidade do As é baixa e ocorre principalmente (65-98%) em solução, como os oxiâniões do arsenato (por exemplo, H_2AsO_4^- , HAsO_4^{2-}) (Figura 1; Magalhães, 2007). Sob condições moderadamente reduzidas (0-100 mV), a solubilidade do As é controlada pela dissolução de óxidos/óxi-hidróxidos de ferro e subsequente liberação do As adsorvido e/ou co-precipitado para solução (Masscheleyn *et al.*, 1991, 2010). Já em ambientes com condições redox inferiores a -200 mV, o teor de As solúvel aumenta 13 vezes em comparação com 500 mV (Masscheleyn *et al.*, 1991). Sob condições redutoras (ou seja, ferruginosas), as espécies de arsenito (H_3AsO_3 e H_2AsO_3^-) são predominantes (Figura 1; Sharma e Sohn, 2009).

Apesar de o estado redox de um sistema ser importante, a mobilidade e o transporte do As no ambiente são dominados por reações de adsorção que ocorrem na superfície de minerais reativos de óxido/óxi-hidróxido de Fe e Mn, com o oxiânião de arsenita geralmente exibindo menor afinidade por superfícies minerais do que o oxiânião de arsenato (Smedley e Kinniburgh, 2002; Dixit e Hering, 2003). Em águas sulfídricas (condições anóxicas), o As forma complexos com íons de sulfeto dissolvidos, onde espécies tioarsênicas (tioarsenatos e tioarsenitos) podem ser bastante móveis (Widerlund e Ingri, 1995; Planer-Friedrich *et al.*, 2007; Helz e Tossell, 2008).

Em sedimentos, uma grande porção do As encontra-se trapeado na camada óxica, formando uma zona sedimentar (0-2 cm) que é relativamente rica neste metaloide (Chaillou *et al.*, 2003). Entretanto, estudos de Mirlean *et al.* (2012) apontam concentrações significativas de As em sedimentos costeiros do Brasil de até 1,5 m de profundidade, onde a variação dos níveis de As foi relacionada à distribuição de materiais calcários, refletindo as circunstâncias paleogeográficas que promovem os recifes locais. Outros estudos (Riedel *et al.*, 1987; Masscheleyn *et al.*, 1991), apontam ainda que altas concentrações de As em zonas sedimentares mais profundas (ex. 15 cm) está associado à presença de plantas e organismos que promovem a circulação de oxigênio, através da água intersticial, até zonas mais profundas. Winderlund & Ingri (1995), estudaram geoquímica do As em sedimento do Estuário do Rio Kalix, norte da Suécia, e constaram que os óxidos de Fe (III) persistiram na zona anóxica do sedimento e atuaram como carreadores de As até

profundidades de 10-15 cm. Chaillou *et al.* (2003) interpretaram o comportamento do metalóide em sedimentos lamosos da Baía de Biscay (França) e destacam o impacto da diagênese do As em registros geoquímicos de ambientes sedimentares modernos, apontando erros na interpretação de suas origens (antrópicas/naturais). Portanto, o comportamento químico e consequências ambientais do As e de diferentes metais pesados depende dos processos de fixação nos carreadores geoquímicos, onde os óxidos/óxi-hidróxidos de Fe (III) se destacam pela capacidade de fixação e de liberação (Mirlean *et al.*, 2012).

Observa-se que as mudanças das condições de óxido-redução nos sedimentos e a ocorrência dos processos diagenéticos/biológicos são importantes parâmetros na transformação e distribuição do As. A oxidação da matéria orgânica dos sedimentos produz um ambiente redutor, que pode também provocar liberação do As adsorvido nos óxidos/óxi-hidróxidos de Fe (Salomons *et al.*, W e Forstner, 1984; Förstner, 1987; Bowell, 1994). Neste sentido, torna-se importante também o estudo dos processos de sulfato-redução, que estão direta ou indiretamente associados à degradação da matéria orgânica e desenvolvimento de zonas redutoras.

Sendo assim, ferro (Fe) e enxofre (S) são elementos-chave na biogeoquímica de sedimentos estuarinos, onde a redução de Fe (III) e sulfato (SO_4^{2-}) são importantes para o entendimento dos processos de dissolução de elementos sensíveis às mudanças redox, como As (O'Day *et al.*, 2004; Jorgensen e Kasten, 2006; Machado *et al.*, 2008; S. Wang *et al.*, 2012; Nóbrega *et al.*, 2013). A estratificação redox é comum em sedimentos marinhos e estuarinos, com condições geralmente mais redutoras com o aumento da profundidade (Clark *et al.*, 1998; Vidal-Durà *et al.*, 2018). Os sulfetos (fases dissolvidas e minerais) gerados pelas reações redox podem ter destinos diferentes nos sedimentos estuarinos, incluindo re-oxidação em sulfato e, na presença de ferro reativo, precipitação como sulfetos de ferro, por exemplo, FeS e FeS₂ (Yücel *et al.*, 2010; Nóbrega *et al.*, 2013). Minerais de sulfeto de ferro autigênico como mackinawita, greigita e pirita têm sido extensivamente estudados devido ao seu importante papel no controle da biodisponibilidade e toxicidade de elementos traço em ambientes estuarinos (Huerta-Diaz e Morse, 1992; Otero e Macias, 2003; Machado *et al.*, 2008). Ademais, cabe ressaltar que os sulfetos de Fe amorfo e a mackinawita (FeS) são comumente agrupados como a fração de sulfetos voláteis em ácido (AVS, *acid volatile sulfides*), enquanto a pirita (FeS₂) está associada à fração de sulfetos redutíveis de cromo (CRS, *chromium reducible sulfides*) (Huerta-Diaz *et al.*, 1998).

A acumulação de As nas fronteiras redox em sedimentos também já foi documentada e a

associação com sulfeto de hidrogênio foi observada em condições anóxicas (Brannon e Patrick, 1987; Moore *et al.*, 1988). Alguns estudos apontam que o As associado aos sulfetos em sedimentos estuarinos ocorre próximo ao limite entre a zona subóxica e zona sulfídrica, onde a incorporação de As em pirita (FeS_2) ou arsenopirita (FeAsS) é comumente proposta como mecanismo diagenético precoce para a remoção de As da água intersticial (Huerta-Diaz e Morse, 1992; Sá *et al.*, 2015). Devido à sua alta sensibilidade redox, a diagênese do arsênio também pode ser fortemente afetada pelas dinâmicas hidrológicas dos sistemas estuarinos e de marismas, que podem mudar diurna ou sazonalmente (Beck *et al.*, 2008; Telfeyan *et al.*, 2017).

1.3. O cenário atual do estudo da geoquímica do Arsênio no Brasil

No Brasil, altas concentrações de As em valores superior dos limites toleráveis foram encontradas em sedimentos marinhos e de praias ao longo da linha da costa do estado do Espírito Santo, em profundidades de até 1,5m (Mirlean *et al.*, 2012). Na costa brasileira a distribuição de As foi estudada, juntamente com Fe e CaCO_3 (Mirlean *et al.*, 2013) O estudo abrangeu praias da zona equatorial (2°S) até praias do estado do Rio de Janeiro (28°S). As altas concentrações de As total (até 120 mg kg^{-1}), que excedem os limiares ambientalmente aceitáveis, foram encontradas nas areias da praia e nos sedimentos superficiais próximos à costa. Mirlean *et al.* (2013) apontam que as concentrações totais de As são mais altas nas areias das praias das costas dos estados da Bahia e Espírito Santo, onde correlações positivas entre As e carbonato de cálcio nas areias da praia sugerem que bioclastos calcários participam na retenção do metalóide e seu acúmulo em sedimentos costeiros. Em lagos e pantânos interdunas brasileiros, o estudo de Mirlean *et al.* (2014) foi o primeiro a encontrar enriquecimento de As em aquíferos e sedimentos no delta do rio Paraíba do Sul, no norte do estado do Rio de Janeiro (RJ) (Baeyens *et al.*, 2019). Neste estudo, foram encontrados até 270 mg kg^{-1} de As em lagos e pantânos interdunas. Além disso, constatou-se que altas concentrações de As na parte inferior dos testemunhos estava associadas a minerais sulfetados (Mirlean *et al.*, 2014).

No estuário da Lagoa dos Patos, estudos de Estudos de Baisch *et al.* (1988), Travassos *et al.* (1993) e Baisch (1994) discutem a especiação de metais no estuário da Lagoa dos Patos, indicando que óxi-hidróxidos e, secundariamente sulfetos e matéria orgânica são os principais carreadores de metais nos sedimentos do estuário, em condições superficiais. Pesquisas de Mirlean *et al.* (2003); Farias (2011); Bento *et al.* (2013) indicam a contaminação do sedimento em

suspensão do canal, principalmente por As e/ou Cd, no estuário da Lagoa dos Patos, poluição esta que deriva das fábricas de fertilizantes localizadas na cidade de Rio Grande. Wallner-Kersanach *et al.* (2015) apontam que o sedimento desta região apresenta altas concentrações de As, acima do estabelecido pela legislação, principalmente em vários locais ao redor da área urbana, industrial e portuária da cidade.

O órgão regulador que controla a qualidade do sedimento marinho no Brasil (CONAMA) vem demonstrando interesse nas distribuições de As na zona costeira e plataforma continental, principalmente devido às limitações ambientais que são impostas em operações de dragagem nas zonas portuárias (Mirlean *et al.*, 2012). A CONAMA 454/12, legislação brasileira que trata da qualidade do sedimento no Brasil propondo limites máximos permitidos de contaminantes nessa matriz foi atualizada em 2012. Os novos limites legislativos estabelecidos para concentração de As em sedimento marinhos é de 19 mg kg⁻¹ (nível 1) (CONAMA, 2012). O nível 1 é o limiar abaixo do qual há menor probabilidade de efeitos adversos à biota.

A geoquímica ambiental do As é complexa, em virtude das grandes diferenças entre as propriedades dos seus compostos de origem natural ou antropogênica. O aspecto bioquímico mais observado no meio ambiente é a metilação. O As inorgânico pode ser convertido em formas metiladas no meio ambiente, que são liberadas no meio aquoso, tornando-se disponível para aumentar os níveis de As na cadeia alimentar. Como a biodisponibilidade e os efeitos fisiológicos/toxicológicos do metaloide dependem de sua forma química, o conhecimento da especiação e transformação no meio ambiente torna-se muito importante, necessitando de métodos adequados para a separação e determinação das espécies de As (Barra *et al.*, 2000).

Entretanto, entender a dinâmica e a disponibilidade dos elementos-traço, bem como suas concentrações nos ecossistemas naturais, tem sido um grande desafio uma vez que processos geoquímicos podem levar a redução significativa ou aumento da toxicidade de elementos como o As. Para estudos que envolvem concentrações de metais e metaloides em sedimento, o pH e o Eh são importantes parâmetros para determinar se o elemento estudado estará solúvel na água intersticial ou terá precipitado.

Ressalva-se que o monitoramento da qualidade do sedimento requer conhecimento dos valores de *background* dos componentes em questão. Normalmente, as estações de amostragem de sedimentos de fundo são selecionadas em zonas próximas (frequentemente em reservas biológicas) que estão livres de impacto antropogênico e onde são esperadas baixas concentrações

dos componentes. Porém, como já citado anteriormente, nestas áreas podem ocorrer anomalias na concentração de As em decorrência ao enriquecimento promovido pela bioturbação/bioirrigação. A má interpretação dos resultados das áreas de *background* pode levar a representações erradas da distribuição do elemento, e consequentemente, a erros em projetos de monitoramento.

No entanto, não existem trabalhos que apontem o efeito da bioturbação/bioirrigação na redistribuição do As e acumulação em sedimentos estuarinos na Lagoa dos Patos. Ademais, são inexistentes as pesquisas que abordam a geoquímica do arsênio durante a diagênese, apontando o papel das barreiras óxicas e sulfídricas na redistribuição deste metaloide, levando em conta todos os outros fatores acima citados. Este estudo torna-se de extrema importância, principalmente considerando zonas rasas do estuário de alta produtividade biológica visando um regime hidrológico irregular.

2. Hipótese

A formação de anomalias de As sem impacto antropogênico evidente em sedimentos rasos do estuário é resultado da redistribuição do metaloide durante a diagênese precoce e depende dos processos de sua acumulação nas barreiras geoquímicas que respondem aos efeitos da bioturbação e, onde os óxi-hidróxidos ou sulfetos de Fe assumem principal importância como fixadores do metaloide.

3. Objetivos

O objetivo principal desta tese é o estudo dos processos da diagênese que controlam a distribuição do As nos sedimentos estuarinos que levam ao aparecimento de anomalias do metaloide acima do nível legislativo.

3.1. Objetivos Específicos

1. Avaliar as variações espaciais dos parâmetros geoquímicos e dos metais (Fe, Mn) e As.

2. Estudar as variações de Fe, Mn e As nos perfis dos sedimentos em zonas rasas e em zonas sob o efeito da bioturbação e/ou bioirrigação.
3. Descrever os processos de sulfato redução e oxidação nos sedimentos em zonas do estuário com diferentes gradientes salinos, apontando a contribuição da bioturbação e/ou bioirrigação nesses processos.
4. Estudar a distribuição do As e seus suportes geoquímicos ao longo do perfil de sedimentos, levando em consideração o papel das barreiras óxica e sulfídrica nesta distribuição.
5. Apontar os processos de redistribuição do metaloide durante o diagênese precoce e sua possível liberação para água intersticial.

4. Área de Estudo

A Lagoa dos Patos (Figura 2) localiza-se na planície costeira do Rio Grande do Sul e tem sua região estuarina situada na parte sul da Lagoa ($31^{\circ}41'$ e $32^{\circ}12'$ S, $51^{\circ}49'$ e $52^{\circ}15'$ W), possuindo uma área de aproximadamente 900 km^2 (Calliari, 1998). É considerada a maior laguna do tipo estrangulado do mundo (Kjerfve, 1994).

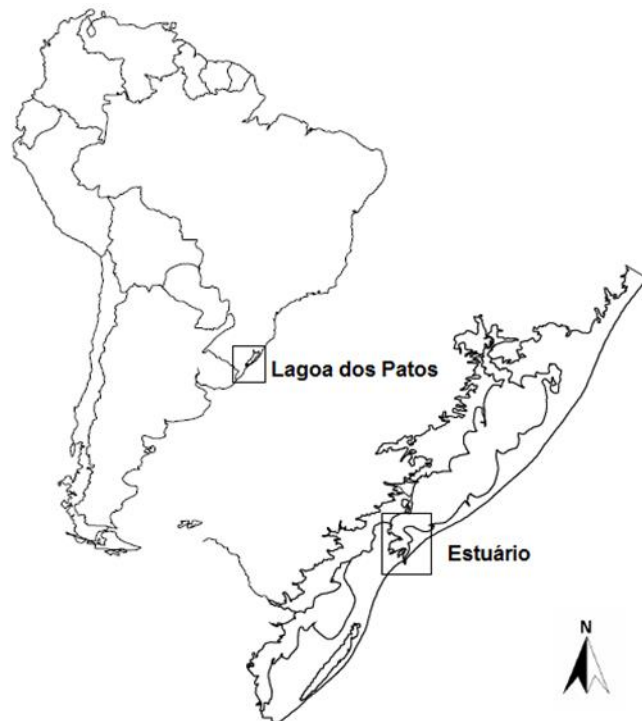


Figura 2- Localização da Lagoa dos Patos com destaque para região estuarina.

Esta considerável bacia hidrográfica produz, nas estações chuvosas, vazões da ordem de 10.000 m³ do estuário ao Oceano Atlântico. Contudo a circulação estuarina é muito variável. Devido à maré astronômica de baixa amplitude - aproximadamente 0,4m, os fatores mais importantes que regem a circulação estuarina são a descarga fluvial e a direção e intensidade dos ventos (Fernandes *et al.*, 2004; Marques *et al.*, 2010). Por exemplo, quando predominam os ventos de nordeste, todo o estuário permanece relativamente doce por períodos prolongados. Por outro lado, durante períodos sem chuva e sob um vento sudeste, o estuário é preenchido principalmente por águas salinas (Moller *et al.*, 1996; Marques *et al.*, 2010).

O estuário da Lagoa dos Patos é um sistema de micro maré (variação das marés < 0,5 m) e exibe variações sazonais caracterizadas por altos níveis de água e baixas salinidades (0–5) durante o inverno/primavera e níveis baixos de água e altas salinidades (20–30) durante o verão/outono (Moller *et al.*, 1996, 2001). A média anual de salinidade no estuário é 13, com valores instantâneos variando de 0 a 34 (Castello, 1985). Gradientes verticais são observados e o estuário pode variar desde o tipo cunha salina até bem misturado (Möller e Castaing 1999, Fernandes *et al.* 2003). As mudanças nos períodos de água doce *versus* dominância de água salobra/salina no estuário impactam especificamente o desenvolvimento da vegetação, bem como os processos geoquímicos que ocorrem nos sedimentos do estuário da Lagoa dos Patos (Mirlean e Costa, 2017).

Os principais rios contribuintes são os rios Taquari e o Jacuí, que correm pelo rio Guaíba, e rio Camaquã até a lagoa (Marques *et al.*, 2009). Na porção estuarina existe a predominância de regiões rasas com profundidades entre 1 e 5 m, tendo profundidade máximas de 18 m ao longo do canal, de largura entre 0,5 e 3 km, que comunica a laguna com o Oceano Atlântico (Baisch, 1994). As enseadas associadas às margens do estuário são definidas por um número elevado de bancos e esporões arenosos recurvados, que formam uma feição típica das áreas rasas, com profundidades menores de 1 m (Calliari, 1998).

O material inorgânico acumulado na Lagoa dos Patos tem sua constituição principal como sendo de quartzo, vários feldspatos, calcita e argilominerais (Hartmann e Calliari, 1996). A fonte deste material é principalmente as rochas polimetamórficas, ígneas e sedimentares, pré-cambrianas e paleozoicas do embasamento cristalino além das sequências sedimentares, ígneas, paleozoicas e mesozoicas da Bacia do Paraná (Vilwock, 1994). Outras fontes importantes de material para a

região lagunar tem origem no Rio Camaquã e desembocadura do Canal São Gonçalo (Calliari, 1998). O matéria orgânico é constituído por: frústulas de diatomáceas, restos de conchas, foraminíferos e material vegetal (Hartmann, 1988). Em se tratando de elemento químico, destaca-se por ordem de grandeza a presença de silício, alumínio, ferro, potássio, titânio, cálcio e cloro (Hartmann e Calliari, 1996). Parâmetros oceanográficos do estuário permitem destacar a existência de uma circulação estuarina do Tipo A (homogênea), de alta turbidez e baixa transparência (10 cm) (Hartmann e Calliari, 1996).

O estuário da Lagoa dos Patos destaca-se ainda pela sua importância ecológica determinante para a região, sendo um ambiente de alta complexidade ecológica e de grande importância como criadouro natural para inúmeras espécies, muitas delas importantes à atividade pesqueira fundamental para o contexto sócio-econômico da região (Portz, 2005). Este estuário possui mais de 7.000 ha de marismas, onde *Spartina alterniflora* e *S. densiflora* são as espécies vegetais dominantes (Costa *et al.*, 2003; Marangoni and Costa, 2012). A *S. alterniflora* ocorre em marismas de áreas oligohalinas até eurihalinas, nas zonas frequentemente alagadas (30–80 % dos dias do ano) das enseadas protegidas (Copertino *et al.*, 1997). Ainda segundo Cupertino *et al.* (1997) a *S. alterniflora* é uma planta robusta na base, sendo sua parte aérea composta por folhas com bainhas glabras e caule formado pelas bainhas foliares. Observa-se também que a parte subterrânea apresenta numerosas raízes de absorção, concentrando-se principalmente nos 30 cm superficiais do sedimento, podendo atingir profundidades superiores a 50 cm (Rabelo, 1994).

Ao longo das marismas adjacentes, o caranguejo (*Neohelice granulata*) apresenta importante papel ecológico, controlando ou afetando diferentes aspectos físicos e químicos (por exemplo, microtopografia, química de sedimentos e drenagem) do ambiente estuarino (Iribarne *et al.*, 2000). O *Neohelice granulata* (Dana, 1851) é um caranguejo encontrado em marismas e manguezais da costa sul do Atlântico, do Rio de Janeiro (Brasil) à Patagônia (Argentina) (Melo, 1996), e é um dos Brachyura mais abundantes em marismas da região estuarina da Lagoa dos Patos. Este caranguejo apresenta grande importância como bioturbador de áreas entremarés de estuários tropicais e subtropicais, já que suas escavações aumentam os níveis de oxigenação e drenagem do solo (Gregati e Negreiros-Franozo, 2009).

Os locais estudados neste trabalho no estuário da Lagoa Patos foram escolhidos porque não estão sujeitos aos efeitos diretos de efluentes domésticos e industriais (Niencheski *et al.*, 1994; Windom *et al.*, 1999), permitindo-nos investigar a distribuição natural do As dentro do sistema.

Para estudos dos efeitos dos gradientes de salinidade em zonas rasas e zonas de marisma foram coletados testemunhos em locais de águas rasas e abertas livre de vegetação, que são de regiões onde a profundidade da água varia de dezenas de centímetros a um metro. Os testemunhos de sedimentos coletados em zona de marisma foram obtidos proximamente aos locais de amostragem em águas abertas e rasas e são dominados por *Spartina sp.* e colônias de caranguejos *Neohelice granulata*, como descrito acima. Além disso, dois ambientes de uma marisma foram examinados para os períodos de água polihalina e de água oligohalina com base em diferentes atividades biológicas: uma zona ocupada por *S. alterniflora* e outra por *N. granulata*, com o objetivo de investigar os efeitos das diferentes bioturbações/biorrigações submetidas a regime hidrológico irregular. Por fim, para investigação dos níveis de As acima do legislativo, foram escolhidos dois pontos amostrais; um localizado em zonas rasas (lamina d'água < 0.2 m, inundada no momento da coleta) e ocupadas por *S. alterniflora*, e outro localizado em águas com maiores profundidades (lamina d'água 0.2 – 1.0 m) e ocupadas por *N. granulata*.

5. Material e Métodos

5.1. Coleta e Amostragem de Sedimentos e Testemunhos

Para estudar o efeito da salinidade na redistribuição do As em sedimentos estuarinos (Capítulo 1), as amostras de sedimentos foram coletadas em setembro de 2016, quando o estuário era dominado por descarga fluvial (ou seja, período de água oligohalina). Condições de salinidade variando entre 0 e 8 prevaleceram no local do estudo por cerca de um mês antes do início da amostragem, de acordo com a rede do sistema de monitoramento SiMCosta. Três zonas do estuário foram examinadas com base nas condições gerais de salinidade (Figura 3): (1) o baixo estuário (maior salinidade; 20 a 30); (2) estuário médio (salinidade intermediária; 5-10); (3) estuário alto (água doce; 0 - 5), obtendo amostras representativas do gradiente estuarino no momento da coleta do testemunho.

Segundo Filgueras (2009) existe uma classificação de estuários baseada na zonação da salinidade, que considera os diferentes graus de mistura entre água doce e salgada. Para esta classificação, a região dominada exclusivamente pela água doce continental é denominada zona limnética, com salinidade abaixo de 0,5, passando pela região oligohalina (0,5 a 5), mesohalina (5

a 18) polihalina (18 a 30) e eurihalina (acima de 30), podendo existir também a região hiperhalina (acima de 40). Portanto, o “estuário baixo” também é caracterizado pela presença prolongada de águas com salinidade entre 18 a 30, e considerado uma região polihalina; o “estuário médio” é caracterizado principalmente por águas mesohalinas; e o “estuário alto” é predominantemente caracterizado por uma região oligohalina.

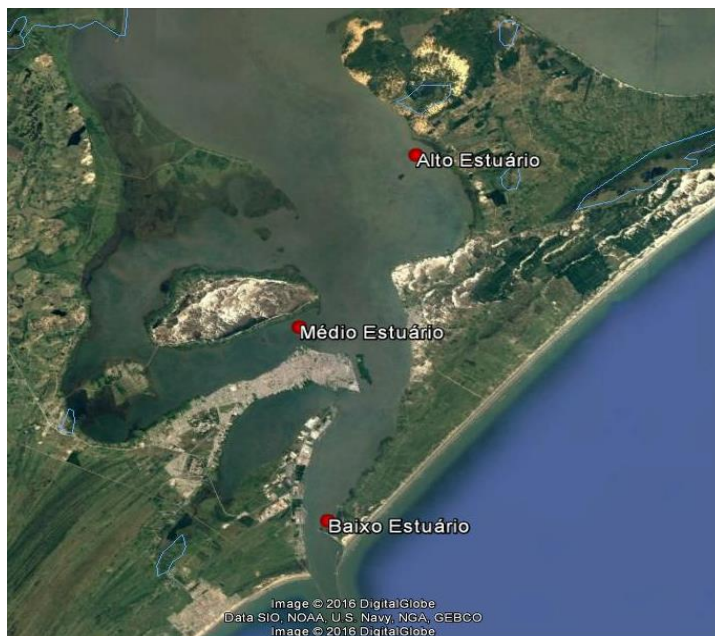


Figura 3 - Localização dos pontos amostrados no estudo dos efeitos da salinidade; Capítulo 1.

Os testemunhos de águas rasas e abertas que correspondem ao estuário baixo (polihalino), médio (mesohalino) e alto (oligohalino) são rotulados como Z1, Z2 e Z3, respectivamente, enquanto os testemunhos correspondentes as marismas de estuário baixo, médio e alto são designados M1, M2 e M3, respectivamente. Cada testemunho tinha entre 60 e 66 cm de comprimento e foram coletados em tubos de PVC (8 cm de diâmetro), hermeticamente fechados e transportados verticalmente para o laboratório, onde foram abertos longitudinalmente e envoltos em filme plástico. Os testemunhos foram posteriormente cortados ao meio, com uma metade sendo seccionada em subamostras de 2 cm e usados imediatamente para análise de Eh e sulfetos livres e, posteriormente, para a medição do conteúdo de As, Fe e Mn dos sedimentos. A outra metade de cada um dos 6 testemunhos também foi seccionada com 2 cm de espessura e imediatamente congelada para posterior análise do conteúdo de sulfetos dos sedimentos (isto é, AVS e CRS).

Já para avaliar a influência da salinidade e bioturbação/biorrigação na distribuição dos óxi-hidróxidos de Fe/Mn (nódulos) (Capítulo 2), as amostras de sedimentos foram coletadas em abril e outubro de 2018, quando o estuário da Lagoa de Patos estava dominado, respectivamente, pela influência do influxo de água marinha (ou seja, período polihalino) e descarga fluvial (ou seja, período oligohalino). Condições de salinidade variando entre 20 e 30 prevaleceram no local do estudo por cerca de um mês antes do início da amostragem do período polihalino (de acordo com a rede do sistema de monitoramento SiMCosta). Para o período de água oligohalina, as condições de salinidade estavam abaixo de 3, por um mês antes da amostragem.

Para a análise de nódulos, foram coletados testemunhos em duas zonas/ambientes da marisma, examinados no período de água polihalina com base em diferentes atividades biológicas: uma zona ocupada por *S. alterniflora* (SA) e outra por *N. granulata* (NG), localizadas na Ilha da Pólvora. Para cada local (ou seja, SA e NG), a composição da água intersticial foi analisada para os períodos de água polihalina e de água oligohalina através da coleta de testemunhos para os respectivos períodos. Cada testemunho tinha cerca de 35 cm (Figura 4) de comprimento e foi coletado em tubos de PVC, que foram hermeticamente fechados e transportados verticalmente para o laboratório. O tratamento dos sedimentos foi realizado imediatamente após a coleta da amostra. Cada sub-amostra foi coletada em um intervalo de 1 cm, as mesmas foram transferidas para uma placa de petri, destinadas para secagem (Figura 4) e tratamento dos nódulos.



Figura 4 – Amostragem testemunho de marisma ocupada por *N. granulata*. A: testemunho entre 8 – 18 cm de profundidade (escala em preto – 10 cm); B: amostras seccionadas em 1 cm e separadas em placas de petri; C: amostra seca, pontos avermelhados indicam presença de nódulos de Fe-Mn.

Para o estudo dos efeitos da bioturbação no acúmulo de As acima do nível legislativo em sedimentos estuarinos (Capítulo 3), dois blocos de sedimentos ($35 \times 35 \times 35$ cm; Figura 5) foram amostrados, nos locais SA e DA (SA representa local ocupado por *S. alterniflora* e DA uma área ocupada pelo caranguejo *N. granulata*) usando uma *box core* inoxidável quadrangular e transportados imediatamente para o laboratório. A amostragem foi realizada na superfície recém-exposta dos blocos de sedimentos, representando as zonas óxicas e subóxicas/anóxicas do sedimento. Utilizou-se uma seringa plástica para amostrar aproximadamente 5 g de material de sedimento em cada ponto da parede do bloco, as subamostras foram imediatamente congeladas para tratamento posterior. Foram coletadas 21 e 36 amostras para os blocos de sedimentos SA e DA, respectivamente.



Figura 5 - Amostras coletadas na Ilha da Pólvora; A – local ocupado por *S. alterniflora* (SA) B – local ocupado por *N. granulata* (DA); Capítulo 3. Círculos amarelos (A) e marcações brancas (B) representam locais onde sedimento foi coletado para análise.

5.2. Análises Químicas e Geológicas

As medidas do potencial redox (Eh) foram conduzidas através da utilização de um eletrodo combinado de Platina previamente calibrado com padrão 470 ± 5 mV. A determinação de sulfetos livres (S_2^- , HS^- , H_2S) em sedimentos foi realizada através de um potenciômetro de alta sensibilidade (ISE/pH/mV/ORP/temp. meter) conectado a um eletrodo combinado Ag/ HS^- (HI 4115) descrito por Kenneth, 2001. Todas as análises foram feitas imediatamente após a abertura dos testemunhos. Uma solução antioxidante básica para sulfetos (*Sulfide Antioxidant Buffer* - SAOB, Hanna Instruments®) e um padrão de sulfeto ($\text{Na}_2\text{S} \cdot 9\text{H}_2\text{O}$) foram previamente elaborados e utilizados para calibração do eletrodo de íon seletivo. O eletrodo foi calibrado após cada 12 leituras a partir de uma curva de calibração de três pontos ($100, 1000, 10000 \mu\text{mol L}^{-1}$). A medição

foi realizada em uma mistura contendo 2 g de sub-amostras de sedimentos e 5 mL de SAOB, imergindo o eletrodo diretamente na suspenção (Brooks, 2001).

Para determinação da condutividade das amostras, a água intersticial foi obtida das subamostras de sedimentos por centrifugação (3.000 rpm por 30 min). Após a centrifugação, o sobrenadante foi decantado e filtrado através de filtros de membrana de 0,45 µm. A condutividade das sub-amostras foi medida na água intersticial (intervalos de 4 cm) com um eletrodo de platina, célula de condutividade (Oakton®).

Análises AVS (*acid volatile sulphide*) foram realizadas seguindo os métodos descritos no *Draft analytical method for determination of acid volatile sulfide in sediment* (USEPA, 1991). Para CRS (*cromium reducible sulphide*), foi seguido o método descrito por Fossing e Jørgensen (1989). Mais especificamente, a quantificação de AVS e CRS foi feita por iodometria. A precisão, determinada pelo desvio padrão relativo (% RSD), para essas medições foi inferior a 5% e 10% para AVS e CRS, respectivamente (Tabela 1).

Outros parâmetros, como carbono orgânico total e granulometria foram determinados subsequentemente em alíquotas das amostras do testemunho. Especificamente, para a análises de carbono orgânico total (TOC) foram efetuadas segundo os métodos tradicionais de analisador de carbono Shimadzu, modelo TOC - L / SSM – 5000A. Para tal procedimento, empregou-se 30 mg de amostra de sedimento macerado. Este método possui um limite de detecção de $4 \mu\text{g kg}^{-1}$ (Tabela 1). Os resultados são apresentados em porcentagem de carbono orgânico de sedimentos secos e o desvio padrão relativo (% RSD) foi inferior a 5% para análises em triplicata (Tabela 1). As análises granulométricas do sedimento foram realizadas segundo métodos tradicionais de peneiragem e pipetagem, descritos pela ABNT, NBR 7181.

Tabela 1 – Limites de detecção e precisão (% RSD – desvio padrão relativo) para as análises químicas e geológicas

Método	Limite de detecção	% RSD
AVS	$2,0 \text{ mg kg}^{-1}$	< 5,0 %
CRS	$15,0 \text{ mg kg}^{-1}$	< 10,0 %
TOC	$4,0 \mu\text{g kg}^{-1}$	< 5,0 %

5.3. Análise de Arsênio e Elementos Metálicos

Para avaliação da concentração de As e investigação dos efeitos da salinidade (Capítulo 1) e concentração de As e metais em nódulos (Capítulo 2); As, Fe e Mn foram extraídos das amostras de testemunho e nódulos, seguindo o método EPA 3050B (USEPA, 1996). Resumidamente, as extrações foram realizadas em 1 g de amostra para aquelas provenientes dos testemunhos Z1, Z2, Z3, M1, M2 e M3 e 0,5 g de amostra foram utilizadas para extração dos nódulos dos pontos SA e NG. As amostras foram secas, maceradas e digeridas inicialmente a 95 ± 5 °C com 10 mL de HNO₃ ultrapuro (grau Optima™) 1:1 (v/v) durante 10 min. Posteriormente, 5 mL de HNO₃ ultrapuro (grau Optima™) concentrado (16N) foram adicionados à solução e deixados reagir por 2 horas. A solução foi ainda digerida por adição de 5 mL de 30% H₂O₂ e aquecimento por 2 horas. Posteriormente, as soluções foram diluídas até 50 mL com H₂O ultrapura Milli-Q (18,2 MΩ cm) e centrifugadas a 3000 rpm por pelo menos 10 minutos para separar o sobrenadante de qualquer material particulado restante. O sobrenadante foi então diluído por um fator de 1:10 usando 2% de HNO₃ (16N) e mantido refrigerado (4 °C) até a análise.

O arsênio total e o manganês foram analisados por espectrometria de massa com plasma indutivamente acoplado de alta resolução (ICP-MS) (Thermo Fisher Element 2) com uma câmara de pulverização PC3 (ESI) e auto-amostrador FAST (ESI) na Universidade de Tulane. A cada amostra, um padrão interno de 1 µg L⁻¹ de Scandium (High Purity Standards®) foi adicionado para monitorar a deriva do instrumento durante a análise. As curvas de calibração foram obtidas por diluições (0,1, 10, 100, 500, 1000 µg L⁻¹) a partir de uma solução padrão de múltiplos elementos (10 µg mL⁻¹) - Material de referência certificado Claritas PPT®. O limite de detecção para As e Mn para essa abordagem foi de 0,02 µg kg⁻¹ e 0,01 µg kg⁻¹, respectivamente (Tabela 2).

Devido às altas concentrações totais de Fe, as soluções extraídas foram diluídas por um fator de 1:400 (v/v) e medidas por espectrofotometria UV/VIS usando um espectrofotômetro DR 2800 da Hach Company®, método 8008 - Método FerroVer® (HACH, 2007). Para este método, um reagente de ferro, FerroVer, é adicionado a 10 mL de amostra, onde o ferro reage com o indicador de 1,10 fenantrolina no reagente para formar uma cor laranja proporcional à concentração de ferro (HACH, 2007). A absorção foi medida a 510 nm e o limite de detecção para as medidas de Fe foi de 0,02 mg kg⁻¹ (Tabela 2).

A exatidão e precisão das análises foram asseguradas pela extração e quantificação do material de referência de sedimentos marinhos MESS-4 (Conselho Nacional de Pesquisa do

Canadá (NRCC)), onde as recuperações de As, Fe e Mn estavam dentro dos limites de confiança de 95 % (Tabela 2). Para cada 20 amostras processadas, um branco foi realizado, e as concentrações aqui relatadas para todas as amostra foram subtraídas do branco. As amostras duplicadas adicionadas foram processadas rotineiramente (5 % de cada extração), com desvio padrão relativo (RSD) inferior a 5 %.

Para avaliação do efeito da bioturbação no acúmulo de As (Capítulo 3), a concentração total dos elementos (As, Fe e Mn) foi determinada de acordo com a Agência de Proteção Ambiental dos Estados Unidos - USEPA - método 3051 (USEPA, 2012). Sub-amostras de sedimentos (200 mg de peso úmido) também foram extraídas por 24 h em temperatura ambiente, utilizando 25 mL de uma solução de ascorbato (50 g de NaHCO₃, 50 g de citrato de Na, 20 g de ácido ascórbico para 1 L de solução; tamponado a pH 8) como descrito em Chaillou *et al.* (2003). Este procedimento remove as fases mais reativas de Fe (III) e seus metais traço associados (Hyacinthe *et al.*, 2001). Uma extração separada foi realizada usando 25 mL de HCl 1N para determinar o Mn e Fe solúvel em ácido e o teor de As associado.

O conteúdo de As para esta análise foi determinado por espectrometria de absorção atômica com atomização eletrotérmica (Perkin Elmer Analyst 800), com correção de fundo com efeito Zeeman longitudinal. Os níveis de Mn e Fe foram determinados por espectrometria de absorção atômica com chama (acetileno-ar). O menor limite de detecção dos elementos analisados As, Mn e Fe foi de 0,04 mg kg⁻¹, 20 mg kg⁻¹ e 40 mg kg⁻¹ (Tabela 2), respectivamente. Cada amostra de sedimento foi analisada em triplicata. A precisão determinada como o desvio padrão relativo (% RSD) foi inferior a 6,0%, 3,6% e 4,5% para As, Mn e Fe (Tabela 2), respectivamente. O material de referência (PACS-2, Conselho Nacional de Pesquisa do Canadá) foi analisado juntamente com cada conjunto de amostras para fins de controle de precisão.

Tabela 1- Limites de detecção e precisão (% RSD – desvio padrão relativo) para as análises de arsênio e elementos metálicos

Método	Elemento	Limite de detecção	% RSD
Espectrometria de massa com plasma indutivamente acoplado (ICP-MS)	As	0,02 µg kg ⁻¹	< 4,2 %
Espectrometria de massa com plasma indutivamente acoplado (ICP-MS)	Mn	0,01 µg kg ⁻¹	< 2,6 %
Espectrofotometria UV/VIS	Fe	0,02 mg kg ⁻¹	< 5,0 %
Espectrometria de absorção atômica com atomização eletrotérmica	As	0,04 mg kg ⁻¹	< 6,0 %
Espectrometria de absorção atômica com chama	Fe	20 mg kg ⁻¹	< 3,6 %
Espectrometria de absorção atômica com chama	Mn	40 mg kg ⁻¹	< 4,5 %

5.4. Caracterização mineralógica dos nódulos de Fe-Mn

Os nódulos ricos em Fe/Mn que caracterizam os sedimentos da marisma local (Capítulo 2), consistem em corpos discretos duros, geralmente de forma esférica, feitos de solo ou materiais de sedimentos que foram cimentados juntos por óxidos/óxi-hidróxidos de Fe e Mn (Gasparatos *et al.*, 2005). Os nódulos que ocorrem dentro de cada sub-amostra de 1 cm dos testemunhos foram separados do sedimento por peneiração úmida (peneira de 45 µm), lavados repetidamente com água deionizada e depois secos a 85 °C. Logo após, os nódulos foram coletados visualmente (Figura 6), pesados e armazenados em recipientes de vidro para análise futura. A outra metade do testemunho também foi seccionada em sub-amostras de 1 cm que foram secas a 45 °C e pesadas. Essas análises foram empregadas para calcular a porcentagem de nódulos em cada sub-amostra do testemunho, de acordo com a equação 1:

$$\% \text{ Nódulos} = \left(\frac{\text{peso seco dos nódulos}}{\text{peso seco total da subamostra}} \right) \times 100 \quad (1)$$

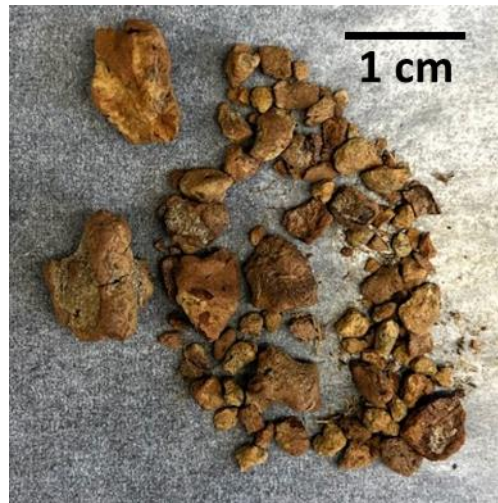


Figura 6 – Nódulos de Fe-Mn observados visualmente, amostra de nódulos extraídas da profundidade de 13 cm para marisma ocupada por *S. alterniflora*

Para cada local de amostragem (isto é, SA e NG; Capítulo 2), os nódulos (isto é, um do topo, meio e final dos respectivos testemunhos) foram escolhidos para posterior investigação microscópica, mineralógica e da estrutura interna. Os nódulos foram fraturados e as superfícies frescas quebradas foram examinadas por microscópio eletrônico de varredura (MEV) usando um MEH de alta resolução Hitachi 4800 com uma resolução de 1,0 nm a 15 kV. O MEV foi equipado com um sistema de espectroscopia de raios-X de energia dispersiva (EDS) para análise qualitativa. A análise forneceu imagens de alta resolução e composição elementar qualitativa para as superfícies dos nódulos. A mineralogia dos nódulos foi ainda examinada usando um difratômetro de raios-X (Scintag, XDS 2000, Cu K α , $\lambda = 0,154$ nm, U = 8,047 KeV, I = 38 mA) a uma taxa de varredura de 1°/min. O XRD foi equipado com um detector de estado sólido de alta resolução e trocador automático de amostras.

5.5. Análise de Água Intersticial

Amostras de água de intersticial foram extraídas dos testemunhos coletados nos locais de SA e NG nos períodos sazonais dominados por água oligohalina e água polihalina (Capítulo 2). Os testemunhos foram abertos longitudinalmente e manipulados dentro de uma *glove box* sob uma atmosfera inerte de N₂ para evitar qualquer oxidação da amostra. Os testemunhos foram seccionados em fatias de 3 cm de profundidade de 5 a 11 cm e em intervalos de 2 cm de profundidade de 11 a 20 cm, com as amostras superior (0-5 cm) e inferior (20-25 e 25-30 cm)

adicionadas para inferir melhor entendimento do limite óxico/subóxico nos sedimentos da marisma analisada. Sub-amostras foram colocadas em tubos Falcon de 50 mL e centrifugadas a 3000 rpm por pelo menos 30 min para separar a água intersticial do sedimento. A água intersticial adquirida foi então transferida para tubos Falcon de 10 mL e diluída por um fator de 1:10 usando 2% de HNO₃ (16N). Posteriormente, As, Fe e Mn foram analisados no ICP-MS (Thermo Fisher Element 2) com uma câmara de pulverização PC3 (ESI) e um amostrador automático FAST (ESI) na Universidade de Tulane, como já foi descrito acima. Os limites de detecção para As, Mn e Fe foram 0,02 µg kg⁻¹, 0,01 µg kg⁻¹ e 0,03 µg kg⁻¹, respectivamente.

ARTIGOS CIENTÍFICOS

Para a obtenção do título de Doutor pelo Programa de Pós-Graduação em Oceanologia, é requerido que o discente realize a submissão de pelo menos dois artigos científicos como primeiro autor em periódico indexado com corpo editorial. Desse modo, os resultados da pesquisa desenvolvida durante o período de doutorado e a discussão dos resultados serão apresentados em forma de artigos neste Capítulo. O primeiro manuscrito, de autoria de Larissa Costa, Nicolai Mirlean, Guilherme Quintana, Segun Adebayo e Karen Johannesson, é intitulado “*Distribution and geochemistry of arsenic in sediments of the world's largest choked estuary: The Patos Lagoon, Brazil*” e foi publicado no periódico “*Estuaries and Coasts*”. O segundo manuscrito, de autoria de Larissa Costa, Nicolai Mirlean, Guilherme Quintana, Segun Adebayo e Karen Johannesson, é intitulado “*Effects of bioirrigation and salinity on arsenic distributions in ferruginous concretions from salt marsh sediment cores (southern Brazil)*” e está em processo de revisão para publicação no periódico “*Regional Studies in Marine Science*”. Por fim, o terceiro manuscrito, de autoria de Larissa Pinheiro Costa, Nicolai Mirlean e Felipe Garcia, é intitulado “*Arsenic environmental threshold surpass in estuarine sediments: effects of bioturbation*” e foi publicado no periódico “*Bulletin of Environmental Contamination and Toxicology*”.

CAPÍTULO I: Distribution and geochemistry of arsenic in sediments of the world's largest choked estuary: The Patos Lagoon, Brazil

Estuaries and Coasts (2019) 42: 1896

DOI 10.1007/s12237-019-00596-0

Abstract

The arsenic (As) contents of sediment cores from the Patos Lagoon in southern Brazil were measured to better understand the biogeochemical cycling of As in the estuary. Sediment cores (ca. 60 cm) were obtained from three locations within the estuary to capture possible changes in As content across the salinity gradient (*i.e.*, where saline, brackish, and freshwater dominated). Two sediment cores were collected at each location, one beneath open water and the other from the fringing salt marsh. Along with As, we quantified the particle size, redox potential (Eh), manganese (Mn), iron (Fe), total organic carbon (TOC), free (dissolved) sulfide concentrations, acid volatile sulfides (AVS), and chromium reducible sulfides (CRS) contents. Bioturbation supports oxygen penetration to depths between 20 cm and 30 cm below the salt marsh surface, where an As- and Fe-rich zone was identified (3-fold higher As than mean As contents of the sediments). A similar subsurface peak of As, Fe and Mn occurs in the open water cores, albeit at greater depths between 40 cm to 50 cm below the surface. The subsurface peak has As concentrations that are 2-fold higher than the average for each core. Vertical profiles of Eh, free sulfides, and CRS for the shallow open water cores showed similar distribution at depths of 50 cm, suggesting that pyrite formation is an important sink for As in the open water cores. The data demonstrate clear differences in the geochemical conditions for salt marshes and shallow open waters that can have important implications for As distribution in estuarine sediments.

Key-words: Arsenic, Marshes, Free Sulfides, Bioturbation, Pyrite.

Introduction

Arsenic (As) is a widely distributed element in the Earth's crust and exists at an average concentration of approximately 5 mg kg⁻¹ (Flora, 2015). It is primarily found in arsenopyrite and in several other sulfide mineral (*e.g.*, orpiment, realgar), although it occurs as a constituent in more than 200 minerals (Garellick *et al.*, 2008). The mobilization process of naturally-occurring As plays

an important role in its redistribution in the environment and many studies have been undertaken to better quantify the processes responsible for mobilization (Shimada, 1996; Sullivan and Aller, 1996; Nickson *et al.*, 2000; Smith *et al.*, 2000; Nordstrom, 2002; Choi *et al.*, 2009; Ravenscroft *et al.*, 2009; He *et al.*, 2010; Sailo and Mahanta, 2014).

Although various processes may liberate arsenic from solids, a transition from oxic to anoxic conditions, and corresponding arsenic and iron/manganese reduction, appears to be a dominant, but not exclusive, means by which high concentrations of dissolved arsenic are generated (Bhattacharyya *et al.*, 2003; Smith *et al.*, 2006; Ravenscroft *et al.*, 2009; He *et al.*, 2010). Studies demonstrate that at higher redox levels (500-200 mV), arsenic solubility is low and it chiefly occurs (65-98 %) in solution as the arsenate oxyanions (*e.g.*, H_2AsO_4^- , HAsO_4^{2-}) (Magalhães, 2007). Under moderately reduced conditions (0-100 mV), arsenic solubility is controlled by the dissolution of iron oxides/oxyhydroxides, and subsequent release of sorbed and/or co-precipitated As to solution (Masscheleyn *et al.*, 1991, 2010). Upon reduction to -200 mV, the soluble arsenic content increases 13-fold as compared to 500 mV (Masscheleyn *et al.*, 1991). Under reducing conditions arsenite species (H_3AsO_3 and H_2AsO_3^-) are predominant (Sharma and Sohn, 2009). Although the redox state of a system is important, arsenic mobility and transport in the environment is dominated by adsorption reactions that occur at the surface of reactive iron and manganese oxide/oxyhydroxide minerals, with the arsenite oxyanion commonly exhibiting lower affinity for mineral surface sites than the arsenate oxyanion (Smedley and Kinniburgh, 2002; Dixit and Hering, 2003). In sulfidic waters, As forms complexes with dissolved sulfide ions, and these thioarsenic species (both thioarsenates and thioarsenites) may be quite mobile in these sulfidic waters (Planer-Friedrich *et al.*, 2007; Helz and Tossell, 2008; Strucker *et al.*, 2014).

In sediments, a large fraction of As is trapped in the metal oxide-rich layers, forming a sedimentary zone that is relatively rich in this metalloid (Chaillou *et al.*, 2003). In marine and estuarine sediments, layers rich in such Fe/Mn oxides/oxyhydroxides commonly occur at or near the sediment-water interface as upward diffusing pore waters rich in Fe(II) and/or Mn(II) react with the overlying, O_2 -rich water column (Burdige, 1993). However, some studies have pointed to substantial concentrations of As in coastal sediments up to 1.5 m deep (Mirlean *et al.*, 2012). This phenomenon is commonly associated with the presence of plants and animals that promote the circulation of oxygen through the interstitial water to greater depths in the sediments (Krantzberg,

1985; Mermilliod-Blondin *et al.*, 2004; Mermilliod-Blondin, 2011; Costa *et al.*, 2017). The depth of these “oxidized zones” varies as a function of the diffusive flux of oxygen, sediment organic matter content, physical heterogeneity in the subsurface from roots (bioirrigation), and bioturbation by benthic animals (Elderfield and Hepworth, 1975; Gaillard *et al.*, 1989; Burdige, 1993). Winderlund and Ingri (1995) reported that Fe (III)-oxides/oxyhydroxides might persist in the suboxic zone of the sediment and act as a carrier for arsenic down to depths of 10-15 cm. Consequently, changes in the redox conditions within the sediments, intensity of diagenetic reactions, and the activity of organisms are all important factors that are likely to impact the distribution of As in modern sediments.

Iron (Fe) and sulfur (S) are both key elements in the biogeochemistry of estuarine sediments, where both Fe (III) and sulfate reduction are important for organic matter decomposition (Van Capellen and Wang, 1996; O’Day *et al.*, 2004; Jørgensen and Kasten, 2006; Machado *et al.*, 2008; Nóbrega *et al.*, 2013). Redox stratification is common in marine and estuarine sediments, with conditions generally becoming more reducing with increasing depth (Froelich *et al.*, 1979; Clark *et al.*, 1998; Vidal-Durà *et al.*, 2018). Sulfides (*i.e.*, dissolved and mineral phases) generated by redox reactions can have different fates within estuarine sediments, including re-oxidation to sulfate and, in the presence of reactive iron, precipitation as iron sulfides, *e.g.*, FeS and FeS₂ (Yücel *et al.*, 2010; Nóbrega *et al.*, 2013). Authigenic iron sulfide minerals like mackinawite, greigite, and pyrite have been extensively studied because of their important role in controlling the bioavailability and toxicity of trace elements in estuarine environments (Huerta-Diaz and Morse, 1992; Otero and Macias, 2003; Machado *et al.*, 2008). Amorphous Fe-sulfide and mackinawite (FeS) are commonly grouped with the acid volatile sulfur (AVS) fraction of marine and estuarine sediments, whereas pyrite (FeS₂) is associated with the chromium reducible sulfide (CRS) fraction (Huerta-Diaz *et al.*, 1998).

Early diagenesis of As is thought to be largely controlled by redox reactions involving Fe, Mn, and organic matter, as well as hydrolysis and diffusive or advective fluxes (Sullivan and Aller, 1996). Accumulation of arsenic at redox boundaries in sediments has also been documented, and association with sulfide has been observed under anoxic conditions (Brannon and Patrick, 1987; Moore *et al.*, 1988). Some studies argued that arsenic associated with sulfide in estuarine sediments occurs near the redox boundary layer (sulfidic zone) and the incorporation of As in pyrite (FeS₂) or arsenopyrite (FeAsS) is commonly proposed as early diagenetic mechanisms for the removal of

As in pore water (Huerta-Diaz and Morse, 1992; Sá *et al.*, 2015). Because of its high redox sensitivity, arsenic diagenesis can also be strongly affected by hydrologic and geochemical dynamics of estuarine and salt marsh systems, which may change diurnally or seasonally and be largely decoupled from deeper pore waters (Beck *et al.*, 2008; Telfeyan *et al.*, 2017).

The redox conditions at the sediment-water interface may determine whether the sediment acts as a sink or a source for arsenic (Widerlund and Ingri, 1995). Iron and S cycles can affect the shallow subsurface (0-20 cm) redox geochemistry of pore water and can vary as a function of the hydrological regime (Charette and Sholkovitz, 2002; Otero and Macias, 2003; Roy *et al.*, 2010, 2011; Nóbrega *et al.*, 2013). Marine sediments with high organic matter content undergo SO_4^{2-} reduction, a process ubiquitous in the shallow subsurface but largely absent at greater depths (Mladenov *et al.*, 2015; Telfeyan *et al.*, 2017). Instead, at depth and in the absence of organic-rich sediments, Fe concentrations are elevated, suggesting that reduction of Fe (III) oxides/oxyhydroxides buffers redox conditions (Telfeyan *et al.*, 2017).

The mechanisms of adsorption or coprecipitation with Fe (III) oxides/oxyhydroxides are thought to be a primary cause of elevated arsenic in sediments after reductive dissolution of these minerals (Pierce and Moore, 1982; Kneebone *et al.*, 2002; Smedley and Kinniburgh, 2002; Chaillou *et al.*, 2003; Bednar *et al.*, 2005; Ying *et al.*, 2012). However, because estuarine systems are complex saline environments and present high complexity in terms of their geochemical conditions, with redox conditions varying in response to many factors (*e.g.*, bioturbation, freshwater input, and climate conditions), geochemistry of redox sensitive elements, such as S, Fe, Mn and As may vary considerably. Here, we present new As, Fe, and Mn data for sediment cores collected across the salinity gradient in the Patos Lagoon estuary in Brazil, to investigate the distribution of these redox sensitive elements as a function of salinity and redox conditions. The study aims to better understand the biogeochemical processes that influence As distribution in estuarine systems. Chemical analysis of total organic carbon (TOC), redox potential (Eh), free sulfides, AVS, CRS, and sediment grain size were carried out as a way of understanding local geochemistry. Implications of this study may help understanding complexities of trace element cycling in other major estuarine systems.

Study Area

Located along the southern Brazilian coast between 30-32 °S and 50-52°W, the Patos Lagoon (Fig. 1) is the largest choked coastal lagoon in the world, with a surface area of ca. 10,000 km² (Kjerfve, 1994). The Patos Lagoon estuary is a microtidal system (< 0.5 m tidal range) and exhibits seasonal variations characterized by high water levels and low salinities (0–5) during the rainy winter/spring season and low water levels and high salinities (20–30) during the summer/fall season (Moller *et al.*, 1996; Marques *et al.*, 2010). The main contributing rivers are the Taquari and Jacuí, which flow through the Guaíba River and Camaquã River into the lagoon (Marques *et al.*, 2009).

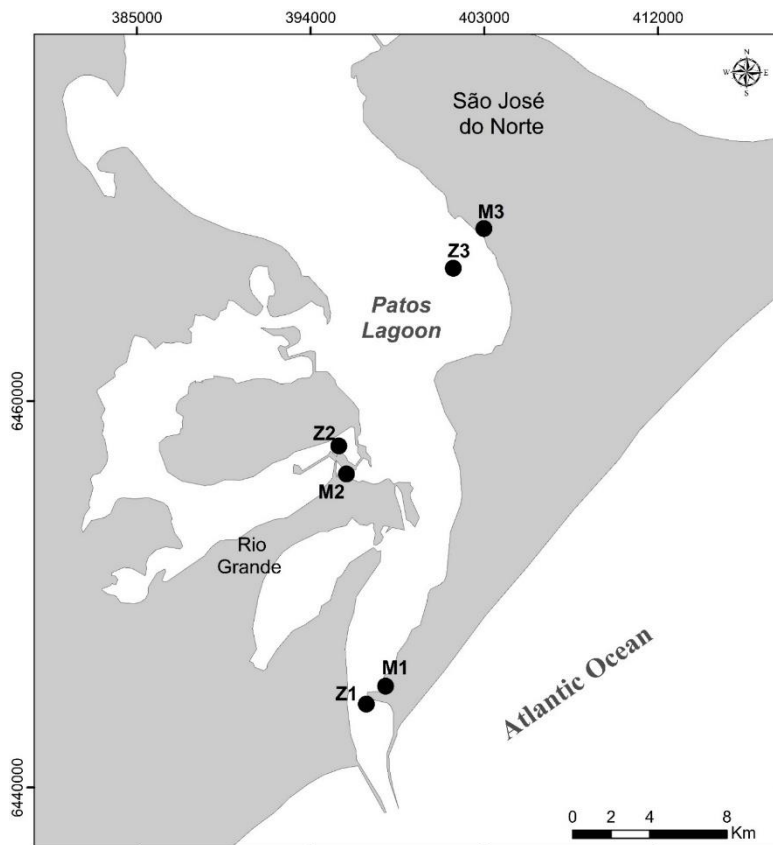


Figure 1 – Patos Lagoon estuary and samples location. Sites labeled with “M” represent locations where salt marsh sediment cores were collected, whereas those labeled with “Z” show the sites where sediment cores were collected from beneath open water.

Circulation within the Patos Lagoon estuary is chiefly driven by winds, and to a lesser extent, by river discharge to the lagoon (Moller *et al.*, 2001). For example, when winds from the northeast predominate, the entire estuary dramatically freshens and remains relatively fresh for prolonged periods. In contrast, during rainless periods and under a southeast wind, the estuary is chiefly filled with saline waters from the Atlantic Ocean (Moller *et al.*, 1996). The changing periods of fresh water versus and brackish/saline water dominance within the estuary specifically impacts development of vegetation, as well as geochemical processes occurring within the sediments of the Patos Lagoon estuary (Mirlean and Costa, 2017).

The southern Patos Lagoon estuary has over 7,000 ha of salt marshes where *Spartina alterniflora* and *S. densiflora* are the dominant plant species (Costa *et al.*, 2003; Marangoni and Costa, 2012). Along adjacent saltmarsh/mudflats, crabs (*Neohelice granulate*) have important ecological roles, controlling or affecting different physical and chemical aspects (*e.g.*, microtopography, sediment chemistry, and drainage) of the estuarine environment (Iribarne *et al.*, 2000). The *N. granulate* population densities are as high as 60 individual.m⁻², with the crabs excavating and maintaining semi-permanent open burrows, and removing large amounts of sediment during feeding and burrow maintenance (D'Incao *et al.*, 1992; Iribarne *et al.*, 2000; Rosa and Bemvenuti, 2005).

High As contents (up to 50 mg kg⁻¹) in Patos Lagoon estuarine sediments have previously been reported, and it is estimated that ca. 80 % of this As is bioavailable (Mirlean *et al.*, 2003; Niencheski *et al.*, 2014; Costa *et al.*, 2017). The source of the elevated As contents of the sediments is hypothesized to be related either to the fertilizer industry or natural enrichment from biological activity – *e.g.*, bioturbation (Mirlean *et al.*, 2003; Wallner-Kersanach *et al.*, 2016; Costa *et al.*, 2017).

The specific sites within the Patos Lagoon estuary studied in this contribution were chosen because they are not subjected to the direct effects of domestic and industrial effluents (Niencheski *et al.*, 1994; Windom *et al.*, 1999) thus allowing us to investigate the natural As cycling within the system (Fig. 1). Sediment cores collected from shallow, open water locations (*i.e.*, cores Z1, Z2, and Z3; Fig. 1) are from regions where water depth varies from tens of centimeters to one meter. The sediment cores collected from the fringing marshes (*i.e.*, M1, M2, and M3; Fig. 1) were obtained proximal to the shallow, open water sampling locations, and are dominated by *Spartina sp.* and *Neohelice granulate* crabs colonies, as described above. The shallow open water area (Z1, Z2, and Z3) are free of vegetation.

Materials and Methods

Sediment samples were collected in September 2016 when the estuary was dominated by fluvial discharge. Salinity conditions ranging between 0 and 8 prevailed at the study site for about a month before sampling commenced, according to the SiMCosta¹ monitoring system network. Three zones of the estuary were examined based on the general salinity conditions: (1) the low estuary (highest salinity; 20 -30); (2) mid estuary (intermediate salinity; 5 -10); (3) high estuary (freshwater; 0 – 5), thus obtaining samples representative of the estuarine gradient at the time of sediment core collection. Hence, the “low estuary” is also characterized by the prolonged presence of saline water, the “mid estuary” is chiefly characterized by moderately brackish water and the “high estuary” is predominantly fresh water.

The open water cores that correspond to the low (saline), mid (brackish), and high (fresh) estuary are labeled Z1, Z2, and Z3, respectively, whereas the corresponding marsh sediment cores for the low, mid, and high estuary are designated M1, M2, and M3, respectively (Fig. 1). Each core was between 60 and 66 cm long and were collected in PVC tubes (8 cm in diameter), which were hermetically sealed and transported vertically to the laboratory where they were opened longitudinally and wrapped with plastic film. The cores were subsequently cut in half, with one half being sectioned into 2 cm subsamples and used immediately for analysis of Eh and free sulfides (*i.e.*, $\Sigma S(-II) = H_2S^0 + HS^- + S^{2-}$) concentrations of the pore waters, and later for measurement of the As, Fe, and Mn contents of the sediments (see below). The other half of each of the 6 cores was also sectioned in 2 cm thickness and immediately frozen for further sulfide contents analysis of the sediments (*i.e.*, AVS = acid volatile sulfides, and CRS = chromium reducible sulfides).

The Eh was measured on the freshly exposed surface of the sediment core, using a naked Pt-electrode (Analion®). The sediment surface was covered with polyethylene film to prevent sediment oxidation and oxygen penetration during the measurement, and the electrode was then pushed through the film into the sediments, thus reducing the

¹ SiMCosta is a Brazilian Coast Monitoring System, which consist of an integrated network of floating or fixed platforms, equipped with instruments and sensors, with autonomous operation and capacity to collect real-time oceanographic and meteorological variables, transmitting them to a processing center at Federal University of Rio Grande (FURG)

influence of oxygen. The electrode was inserted directly into the sediment sample to a depth of approximately 2 centimeters. The Eh measurement in mV was then recorded after the reading had stabilized. The determination of free sulfides in the interstitial pore water was performed using a silver/sulfide combination ion selective electrode (model Hanna® 9616 BNC) coupled to an Orion™ ISE/pH/mV/Eh/temperature meter (model 209a; Brooks, 2001). A basic antioxidant solution for sulfides (Sulfide Antioxidant Buffer - SAOB, Hanna Instruments®) and a sulfide standard ($\text{Na}_2\text{S} \cdot 9\text{H}_2\text{O}$) were previously made and used for calibration of the ion selective electrode. The electrode was calibrated after every 12 readings from a three-point calibration curve (100, 1000, 10000 $\mu\text{mol L}^{-1}$). Measurement was performed in a solution containing 2g of sediment subsamples and 5 mL of SAOB by immersing the electrode directly into the solution. Pore water was obtained from the sediment subsamples by centrifugation at 3,000 rpm for 30 min. After centrifugation the supernatant was decanted and filtered through 0.45 μm membrane filters. The conductivity of the subsamples was measured in the interstitial pore water (intervals of 4 cm) with a platinum electrode, conductivity cell (Oakton®).

Acid volatile sulfides (AVS) analysis was carried out following the method described by USEPA 821-R-100 (U.S. EPA, 1991). For CRS (chromium reducible sulfur) we followed the method described by Fossing and Jørgensen (1989). More specifically, the AVS and CRS quantification were made by iodometry. These titration techniques determine excess of iodine concentration, but they do not directly determine the $\Sigma\text{S}^{\text{-II}}$ concentration. Therefore, $\Sigma\text{S}^{\text{-II}}$ is then calculated by the ratio of hydroxylamine used in relation to the standard. The precision determined as the relative standard deviation (% RSD) for these measurements was less than 5.0% and 10.0% for AVS and CRS, respectively.

Other parameters such as total organic carbon and percent of fine grains (clay and silt) were subsequently determined on aliquots of the subsectioned core samples. Specifically, ca. 30 mg of powdered dry sediment sample was employed for determination of total organic carbon (TOC) using a TOC - VCPH, model SSM - 5000A, SHIMADZU. This method has a detection limit of 4 $\mu\text{g kg}^{-1}$. The results are presented in percentage of organic carbon of dried sediment, and the relative standard deviation (% RSD) was less than 5 % for triplicate analyses. Particular size analysis was performed using standard sieve method (ASTM C136/C136M), and values are expressed as the percentage of fine sediment grains within the total sediment subsample.

Arsenic, iron and manganese were extracted from the sediment core samples following the EPA method 3050B (USEPA, 1996). Briefly, the extractions were conducted on 1 g dried and pulverized (*i.e.*, agate mortar and pestle) sediment samples that were initially digestion at $95 \pm 5^{\circ}\text{C}$ with 10 mL of 1:1 (v/v) ultrapure (OptimaTM grade) HNO₃ for 10 min. Subsequently, 5 mL of concentrated ultrapure (OptimaTM grade) HNO₃ (16N) was added to the slurry and allowed to react for 2 hours. The sediment slurry was further digested by addition of 5 mL of trace metal grade 30% H₂O₂ and heating for 2 hours. Subsequently, the digested materials were diluted up to 50 mL with ultrapure, Milli-Q H₂O (18.2 MΩ cm) and centrifuged at 3000 rpm for at least 10 min to separate the supernatant from any remaining particulate matter. The supernatant was then diluted by a factor of 1:10 using 2% HNO₃ (16N), and kept refrigerated (4° C) until analysis.

Total arsenic and manganese were analyzed by high resolution inductively coupled plasma mass spectrometry (ICP-MS) (Thermo Fisher Element 2) with a PC3 (ESI) spray chamber and FAST (ESI) auto sampler at Tulane University, using method discussed previously (Yang *et al.*, 2016). To each sample, a 1 µg L⁻¹ internal standard of scandium (High Purity Standards®) was added to monitor for instrument drift during analysis. The calibration curves were achieved by dilutions (0.1, 10, 100, 500, 1000 µg L⁻¹) from a standard multi-element solution (10 µg mL⁻¹) – Claritas PPT® Certified Reference Material. The detection limit for As and Mn for this approach was 0.02 µg kg⁻¹ and 0.01 µg kg⁻¹, respectively.

Due to high total Fe concentrations, the extracted solutions were diluted by a factor of 1:400 (v/v) and measured by UV/VIS spectrophotometry using a DR 2800 Spectrophotometer from Hach Company®, method 8008 – FerroVer® Method (HACH, 2007). For this method, a FerroVer Iron Reagent is added to 10 mL sample, where iron reacts with the 1,10 phenanthroline indicator in the reagent to form an orange color in proportion to the iron concentration (HACH, 2007). Absorption was measured at 510 nm, and the detection limit for Fe measurements was 0.02 mg kg⁻¹.

The accuracy and precision of analyses were ensured by the extraction and quantification of marine sediment reference material MESS-4 (National Research Council of Canada (NRCC)), where recoveries for arsenic and iron were in the 95% confidence limits for the CRM. For each batch of samples processed, a method blank was carried throughout the entire sample preparation and analytical process and the reported concentration for the sample were blank subtracted. Spiked duplicate samples were

processed on a routine basis (5% of each well), with relative standard deviation (RSD) less than 5%.

Results

Results of the analyses are presented below for the salt marsh cores followed by the cores collected from the shallow open water area at each of the three sites.

Salt marshes

Conductivity values of the sediment cores (Table 1) varied from 12.5 to 23.4 mS cm⁻¹ at location M1, which is exposed to long periods of saline water, to 1.9 to 8.6 mS cm⁻¹ at M3, which is predominantly dominated by freshwater (Fig. 1). Oxidation/reduction potential (Eh) varied from -61 to 211 mV for sediments from core M1, from -252 to -15 mV at site M2, and from -298 to -25 mV at site M3 (Table 1). Therefore, sediments can be characterized as belonging to oxic and suboxic zones (Masscheleyn *et al.*, 1991), with sediments from the freshwater site (M3) being the most reducing sediments (Table 1).

Marsh sediments from the M3 core also exhibit the highest percentage of fine grain sediments as well as the highest total organic carbon (TOC) content, reaching values from 3.4 to 87.2% and 0.2 to 12.9% respectively. For M2 sediments, TOC ranged from 0.2 to 5.1% and the fine grain sediment content varied between 14.4 and 61.2%. Marsh sediments from the M1 core had the lowest TOC content (0.2 to 1.9%) and the lowest fine grains content (3.3% to 25.5%). These results (Table 1) reflect the influence of the estuary hydrodynamics, whereby finer grain sediments and more organic matter accumulate in low energy regions of the estuary (*e.g.*, M3) compared higher energy regions near the outlet channel to the ocean (M1; Fig. 1). The larger sediment grain size and the higher pore water conductivity of sediments from the M1 core may also be responsible for the higher measured Eh. Specifically, the higher salinity that characterizes the M1 site leads to lower *Spartina* sp. biomass, which may contribute to the lower TOC contents of the sediments and hence, less respiration of reduced carbon (Pearcy and Ustin, 1984; Roman *et al.*, 1984).

Table 1 – Geochemical parameters for marsh sediments on fluvial domain – M locations. The upper numbers are the concentration range, and the mean \pm SD for the entire core is presented within parentheses.

Parameter	M1 Low estuary – Salt water	M2 Mid estuary – Brackish water	M3 High estuary – Freshwater
Conductivity (mS cm⁻¹)	<u>12.5 – 23.4</u> (14.8 \pm 2.5)	<u>8.2 – 21.7</u> (14.9 \pm 4.2)	<u>1.9 – 8.6</u> (5.7 \pm 2.2)
Eh (mV)	<u>-61.0 – 211.0</u> (63.5 \pm 64.5)	<u>-252.0 – -15.0</u> (-93.0 \pm 59.7)	<u>-298.0 – -25.0</u> (-152.5 \pm 88.9)
TOC (%)	<u>0.2 – 1.9</u> (0.7 \pm 0.3)	<u>0.2 – 5.1</u> (1.0 \pm 1.2)	<u>0.2 – 12.9</u> (2.6 \pm 3.4)
Fine grains (%)	<u>3.3 – 25.5</u> (14.7 \pm 4.5)	<u>14.4 – 61.2</u> (31.9 \pm 12.8)	<u>3.4 – 87.2</u> (16.9 \pm 18.8)
Fe (g kg⁻¹)	<u>11.9 – 29.3</u> (16.7 \pm 3.3)	<u>10.1 – 27.5</u> (17.1 \pm 4.3)	<u>12.1 – 27.3</u> (17.5 \pm 4.0)
Mn (mg kg⁻¹)	<u>39.2 – 382.0</u> (105.4 \pm 81.0)	<u>30.0 – 81.9</u> (54.2 \pm 14.5)	<u>48.7 – 178.6</u> (92.8 \pm 34.5)
As (mg kg⁻¹)	<u>2.1 – 7.0</u> (3.4 \pm 0.8)	<u>1.6 – 9.3</u> (3.7 \pm 1.5)	<u>3.0 – 7.9</u> (4.1 \pm 1.2)
Free sulfides (μmol L⁻¹)	<u>3.5 – 50.5</u> (22.8 \pm 14.6)	<u>4.9 – 57.2</u> (23.1 \pm 14.9)	<u>44.7 – 330.6</u> (110.5 \pm 86.2)
AVS (mg kg⁻¹)	<u>4.4 – 21.5</u> (8.5 \pm 5.3)	<u>28.6 – 206.2</u> (78.4 \pm 47.3)	<u>14.3 – 869.2</u> (186.8 \pm 280.1)
CRS (mg kg⁻¹)	<u>59.2 – 5306.0</u> (2173.3 \pm 1808.7)	<u>630.7 – 3899.8</u> (1707.4 \pm 1242.0)	<u>2057.8 – 8184.6</u> (4448.8 \pm 2097.1)

Sediments from the M1 site exhibit the highest Fe and Mn contents ($11.9 \text{ g kg}^{-1} \leq \text{Fe} \leq 29.3 \text{ g kg}^{-1}$; and $39.2 \text{ mg kg}^{-1} \leq \text{Mn} \leq 382.0 \text{ mg kg}^{-1}$), whereas sediments from the M2 core have the highest As contents ($1.6 \text{ mg kg}^{-1} \leq \text{As} \leq 9.3 \text{ mg kg}^{-1}$; Table 1). However, the mean $\pm 1\sigma$ values of the Fe and As contents of all three cores are not statistically different. Nevertheless, the mean $\pm 1\sigma$ value for Mn from the M2 core is statistically lower than the mean Mn contents of the M1 and M3 cores (Table 1). Positive correlation

between As and Fe exists in sediments from M3 core ($r^2 = 0.73$, $p < 0.05$, $n = 32$). Nevertheless, correlations are also observed between Fe and As in the other marsh sediment cores ($r^2 = 0.72$, $r^2 = 0.69$, $p < 0.05$, $n = 32$, for M1 and M2 correspondingly).

Variations in As, Fe and Mn contents exhibit similar trends with depth in each core, however, the trends are qualitatively more similar in cores M2 and M3, as can be seen in Fig. 2. Such similarity is less obvious in core M1, where Mn content with depth is more irregular (as described below). Each sediment core exhibits a mid-depth peak in As content, which occurs at 27 cm in M1, and 23 cm in cores M2 and M3 (Fig. 2). Arsenic concentrations subsequently decrease with greater depth to more or less nearly constant values at the bottom of each 60 – 66 cm deep core. We consider that the nearly constant As content at depth represents the average residual, or non-redox-sensitive, As content in these marsh sediments (e.g., Chaillou *et al.*, 2003). Iron contents of each marsh core exhibit variation with depth to As, with subsurface peaks at 27 cm (29.3 g kg^{-1}), 23 cm (27.5 g kg^{-1}), and 25 cm (27.3 g kg^{-1}) for M1, M2, and M3, respectively (Fig. 2). Manganese content with depth are more irregular, especially for core M1, where two subsurface peaks are observed at depths of 7 cm (382.0 mg kg^{-1}) and 27 cm (220.8 mg kg^{-1}). The subsurface Mn peak at 27 cm depth in the M1 core corresponds to the subsurface Fe and As peaks, however, the shallow subsurface Mn peak at 7 cm has no correspondence. As peak, and, at most, a small Fe peak (Fig. 2). The highest subsurface Mn concentration (81.9 mg kg^{-1}) in core M2 occurs at 21 cm depth, and for M3 the highest Mn peak (178.6 mg kg^{-1}) is at 25 cm depth, both of which correspond reasonably well to the subsurface As and Fe maxima in each core (Fig. 2).

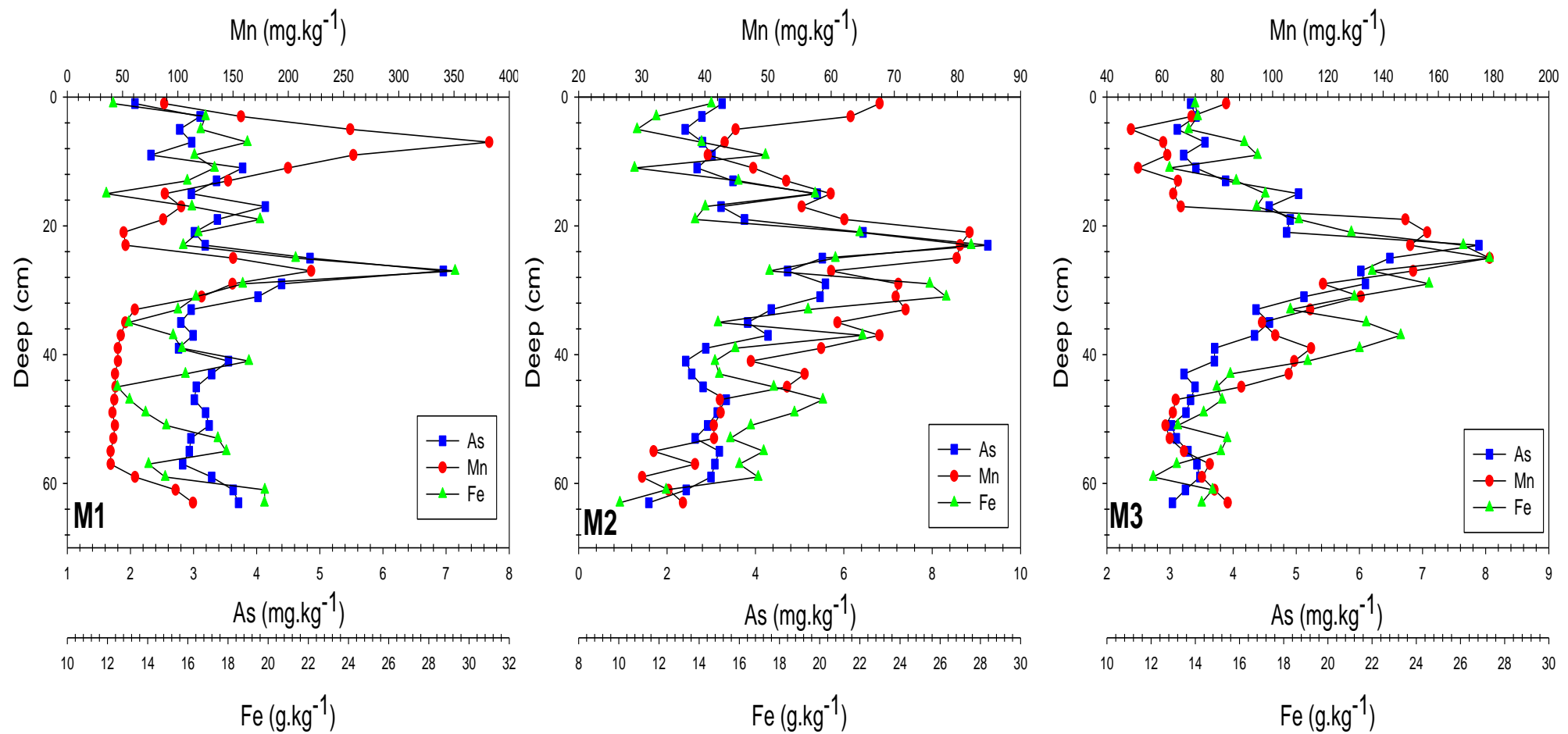


Figure 2 – Arsenic, manganese and iron vertical distribution for marshes areas (M1, M2 and M3).

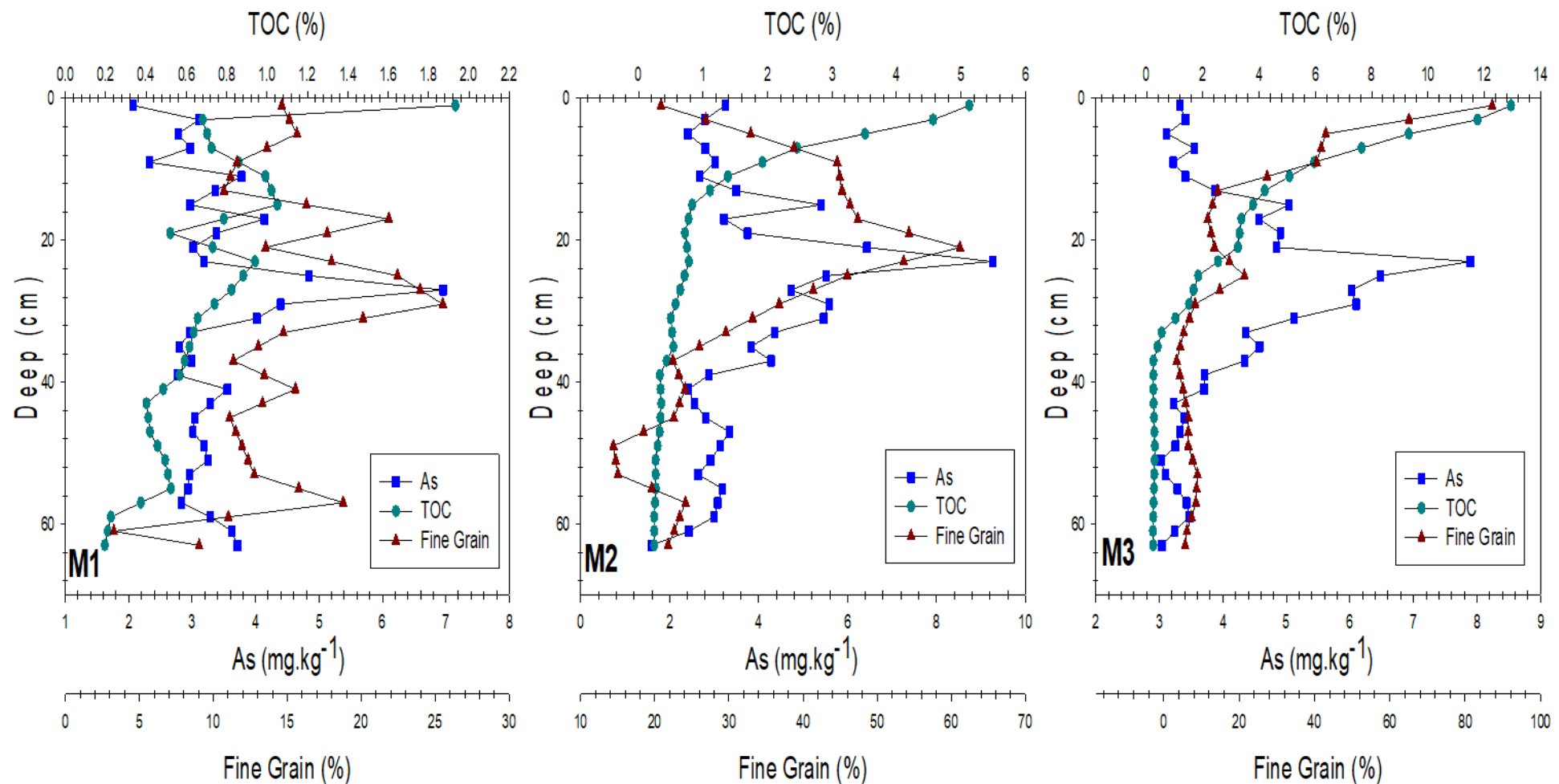


Figure 3 – Arsenic, total organic carbon and fine grains vertical distribution for marshes areas (M1, M2, and M3).

The highest concentrations for the free sulfides (*i.e.*, pore water dissolved sulfide), AVS, and CRS occur in sediments from core M3, where these parameters attain values of $330.6 \mu\text{mol L}^{-1}$, 869.2 mg kg^{-1} , and $8184.6 \text{ mg kg}^{-1}$, respectively (Table 1). Moreover, these measures of sulfide content also decrease in the order M3 > M2 > M1, and the same was observed for the AVS content (M3>M2>M1) (Table 1). Sediments from the freshwater marsh (M3) also present the highest CRS content (Table 1). These measures of sulfide contents in the marsh sediments are also consistent with the Eh measurements (Table 1). Nonetheless, the sediment core As contents do not correlate with these measures of sulfide content. Similarly, no correlation was found between As concentrations and the percentage of fine grain sediment ($r^2 = 0.28$, $r^2 = 0.35$, $r^2 = 0.03$, $p < 0.05$, $n = 32$, for M1, M2, and M3, respectively) or between As and total organic carbon ($r^2 = 0.01$, $r^2 = 0.02$, $r^2 = 0.02$, $p < 0.05$, $n = 32$, for M1, M2, and M3, respectively). Qualitative analysis of As contents, percentage of fine grain and TOC did not show any significant similarity with depth (Fig. 3).

Shallow open water areas

Geochemical parameters for sediment cores from the shallow open water sites from the low (saline water) estuary (Z1), mid (brackish water) estuary (Z2), and high (freshwater) estuary (Z3) are presented in Table 2. Expectedly, conductivity decreases for sediments collected further upstream from the ocean inlet ($Z1 > Z2 > Z3$). The mean redox potential of the sediment cores also decreased from $-116.4 \pm 49.5 \text{ mV}$ at Z1 to $-213.2 \pm 124.4 \text{ mV}$ at Z3. The average TOC content was the same at all three locations (0.5 %; Table 2). Grain size showed an irregular distribution throughout all the profiles, with the greatest variation for location Z1, where the amount of fine grains varied between 6.3 and 92.4%. The high variability of sediment grain size for core Z1 probably reflects the complex hydrodynamics that characterizes this high energy site (Marques *et al.*, 2009, 2010). For locations Z2 and Z3 the percentage of the sediment composed of fine grain sediment ranged from 12.4 to 54.4% and 7.6 to 70.2%, respectively (Table 2).

Although the content of fine grain sediment commonly correlates with sediment organic matter content of marine and estuarine sediments (*e.g.*, Mayer, 1994; Hedges and Keil, 1995), there are important variations, especially in estuaries, determined chiefly by local primary production, sedimentation rates, and the oxygen regime in the water column and sediments (Secrieru and Oaie, 2009). A positive correlation between TOC and the

fine grain sediment fraction was only found for cores Z2 and Z3 ($r^2 = 0.60$, $r^2 = 0.79$, $p < 0.05$, $n = 33$; respectively). The fine grain size fractions was also only weakly correlated with the As contents in the sediments from cores Z2 and Z3 ($r^2 = 0.38$, $r^2 = 0.37$, $p < 0.05$, $n = 33$; respectively). In addition, no correlation exists between the fine grain sediment content and the As content in sediments of core Z1 ($r^2 = 0.01$, $p < 0.05$, $n = 33$).

Table 2 – Geochemical parameters for shallow open water areas sediments on fluvial domain – Z locations. The upper numbers are the concentration range, and the mean \pm SD for the entire core is presented within parentheses

Parameter	Z1	Z2	Z3
	Low estuary – Salt water	Mid estuary – Brackish water	High estuary – Freshwater
Conductivity (mS cm⁻¹)	<u>28.3 – 57.4</u> (44.2 \pm 11.7)	<u>9.5 – 22.4</u> (15.9 \pm 4.3)	<u>2.7 – 17.7</u> (9.8 \pm 5.6)
Eh (mV)	<u>-188.0 - -25.0</u> (-116.4 \pm 49.5)	<u>-378.0 - -45.0</u> (-206.7 \pm 121.5)	<u>-367.0 – 118.0</u> (-213.2 \pm 124.4)
TOC (%)	<u>0.1 – 1.2</u> (0.5 \pm 0.3)	<u>0.3 – 1.1</u> (0.5 \pm 0.3)	<u>0.2 – 1.0</u> (0.5 \pm 0.3)
Fine grains (%)	<u>6.3 – 92.4</u> (49.4 \pm 25.4)	<u>12.4 – 54.4</u> (28.1 \pm 12.9)	<u>7.6 – 70.2</u> (36.6 \pm 20.3)
Fe (g kg⁻¹)	<u>7.9 – 31.9</u> (17.2 \pm 6.8)	<u>11.8 – 28.9</u> (19.0 \pm 5.1)	<u>7.7 – 31.5</u> (20.3 \pm 7.1)
Mn (mg kg⁻¹)	<u>20.4 – 255.7</u> (91.7 \pm 54.6)	<u>21.2 – 129.4</u> (65.6 \pm 31.2)	<u>45.93 – 346.67</u> (163.33 \pm 87.03)
As (mg kg⁻¹)	<u>1.4 – 5.4</u> (2.9 \pm 1.0)	<u>2.2 – 4.5</u> (3.1 \pm 0.7)	<u>2.0 – 5.0</u> (3.1 \pm 0.7)
Free sulfides (μmol L⁻¹)	<u>4.1 – 26.5</u> (11.0 \pm 6.7)	<u>10.6 – 755.5</u> (210.5 \pm 281.6)	<u>4.3 – 322.9</u> (73.4 \pm 111.5)
AVS (mg kg⁻¹)	<u>17.6 – 74.4</u> (38.1 \pm 19.2)	<u>3.6 – 299.6</u> (61.6 \pm 94.9)	<u>15.9 – 109.5</u> (43.1 \pm 27.9)
CRS (mg kg⁻¹)	<u>650.8 – 3940.8</u> (1925.2 \pm 1047.2)	<u>151.8 – 5474.0</u> (2032.3 \pm 1991.2)	<u>109.1 – 6745.2</u> (2301.0 \pm 2624.9)

The As, Fe, and Mn contents of all three shallow, open water sediment cores are similar and statistically indistinguishable (Table 2). For example, the mean \pm SD of the As contents for cores Z1, Z2, and Z3 are $2.9 \pm 1.0 \text{ mg kg}^{-1}$, $3.1 \pm 0.7 \text{ mg kg}^{-1}$, and $3.1 \pm 0.7 \text{ mg kg}^{-1}$, respectively. The mean \pm SD contents of As, Fe, and Mn of the shallow, open water cores are also similar to those of the marsh sediment cores (Tables 1, 2). Iron exhibits a positive correlation with As for all three open water sediment cores ($r^2 = 0.84$, $r^2 = 0.85$, $r^2 = 0.79$, $p < 0.05$, $n = 33$; for Z1, Z2, and Z3, respectively). Manganese and As also exhibit positive correlations for sediments from core Z1 and Z3 ($r^2 = 0.87$, $r^2 = 0.76$, $p < 0.05$, $n = 33$, for Z1 and Z3 respectively). In contrast, Mn is not correlated with As in sediment from core Z2 ($r^2 = 0.35$, $p < 0.05$, $n = 33$).

Distributions of As, Fe and Mn as a function of depth in each open water core are shown in Fig. 4. As with the marsh cores subsurface maxima also characterize As, Fe, and Mn in these shallow, open water cores. A major difference though is that subsurface maxima occur at greater depth in the open water cores compared to the marsh sediment cores (compare Fig. 4 with Fig. 2). More specifically, the highest As, Fe, and Mn content occurred at 40 cm depth in core Z1, 36 cm to 48 cm depth in core Z2, and 32 cm to 48 cm depth in core Z3 (Fig. 4). Qualitative analysis also suggests that As contents are highest within the fine-grained sediment layers (Fig. 5). Because the TOC content of these sediments also corresponds to higher amounts of fine grain sediment content in these cores, As contents also exhibit a qualitative association with sediment TOC contents (Fig. 5).

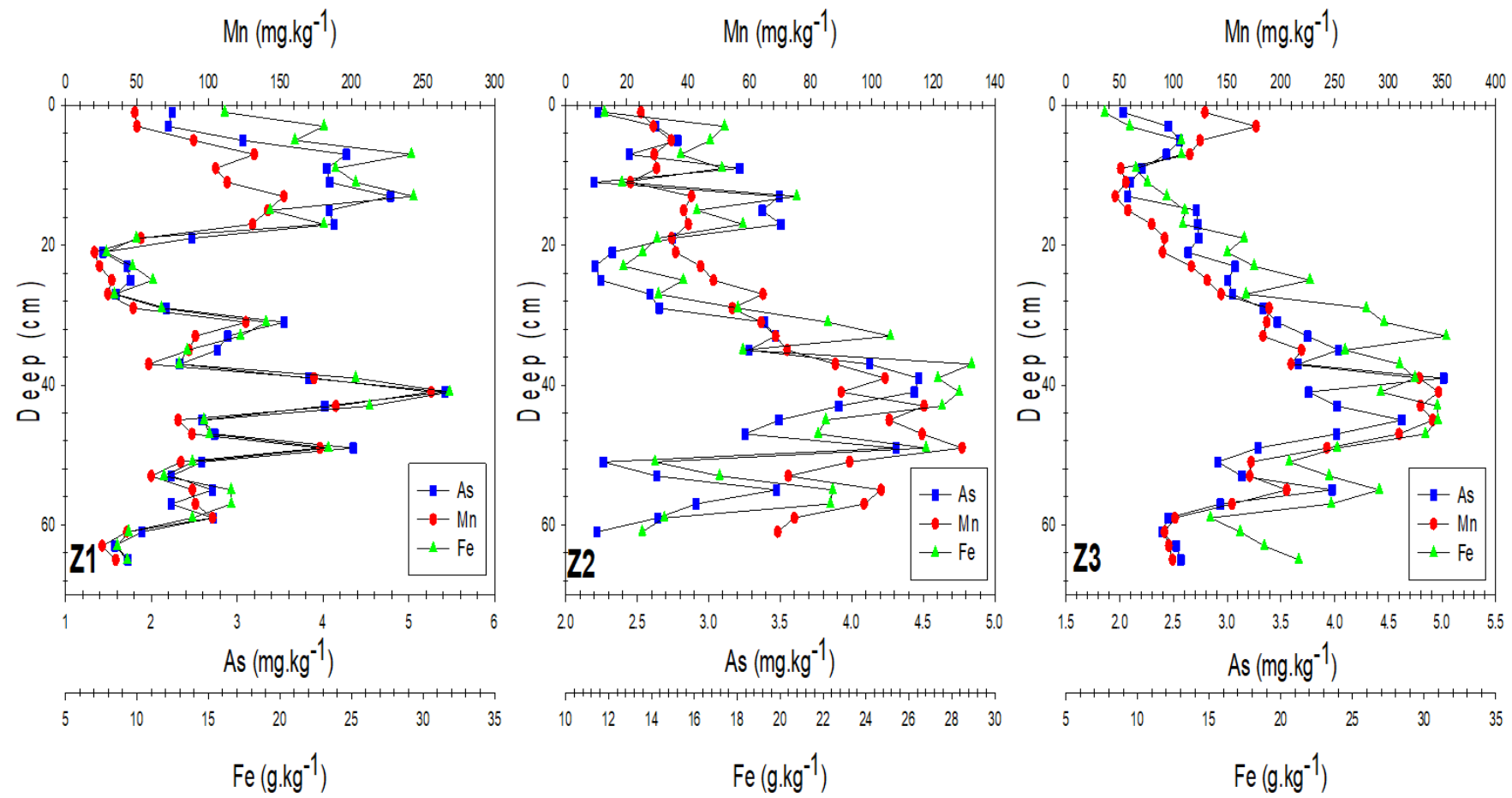


Figure 4 – Arsenic, manganese and iron vertical distribution for shallow open water areas (Z1, Z2, and Z3).

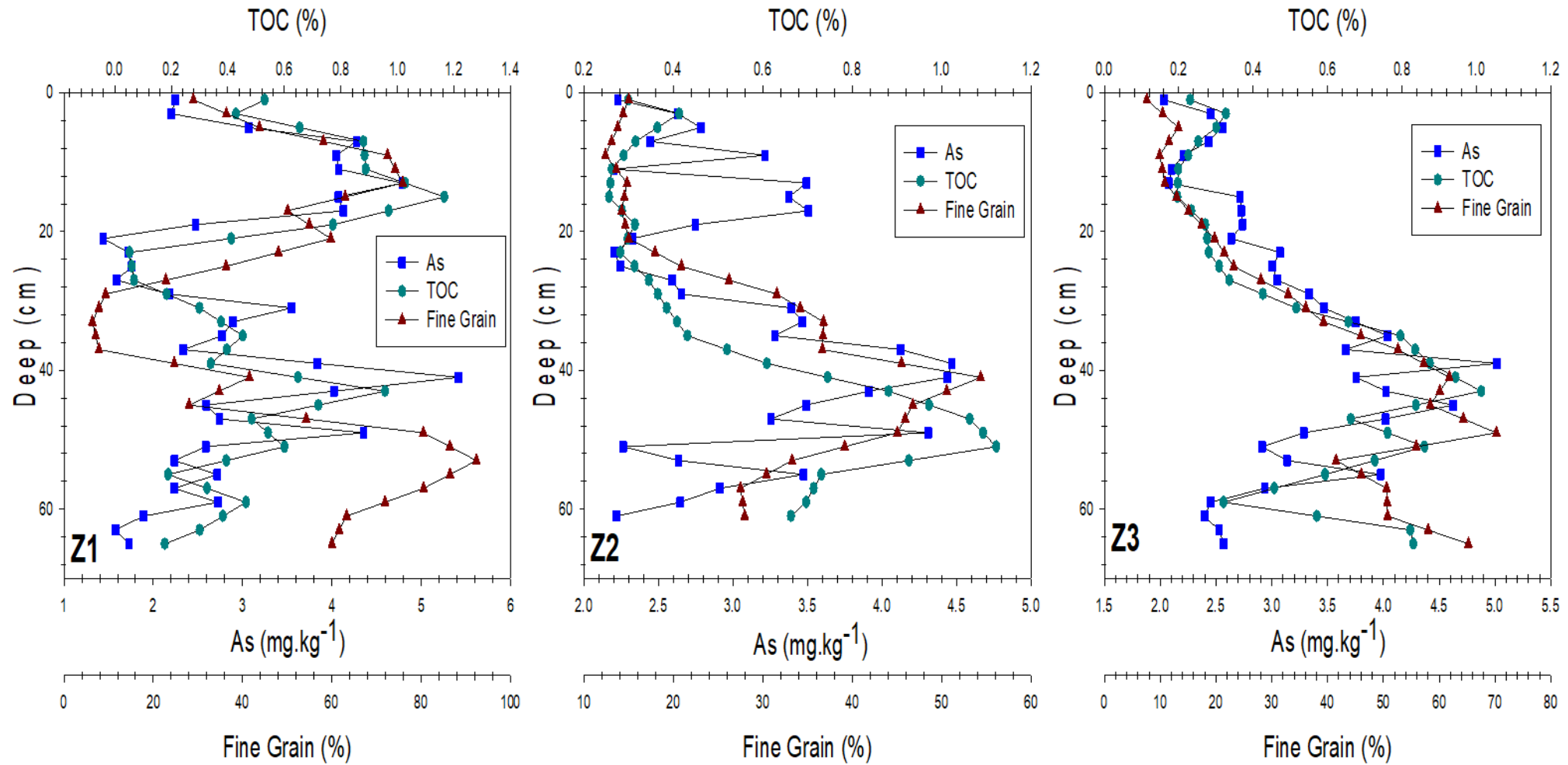


Figure 5 – Arsenic, total organic carbon and fine grains vertical distribution for shallow open areas (Z1, Z2, and Z3).

Vertical distributions of As, AVS, CRS, and free sulfides did not reveal significant statistical evidence of correlation between those parameters. In part, this reflects the fewer numbers of samples that we measured for these sulfide parameters compared to the samples quantified for As, Fe, and Mn in the sediments. Nonetheless, subsurface maxima for free sulfides in the pore waters coincide with those for As, Fe and Mn (Fig. 6). Concentrations of free sulfides are higher for Z2 sediments, reaching values from 10.6 to 755.5 $\mu\text{mol L}^{-1}$, but also exhibit high values, between 4.3 and 322.9 $\mu\text{mol L}^{-1}$, in sediments from the Z3 core. Inspection of Fig. 6 suggests that sediments from the Z2 and Z3 cores have broadly similar pore water free sulfide concentrations as a function of depth. We note that sediments from cores Z2 and Z3 also exhibit the lowest Eh values. Specifically, Eh values at depths of 40 cm were -188, -301 and -346 mV for the Z1, Z2, and Z3 cores, respectively. The free sulfide concentrations of pore water from core Z1 (4.1 to 26.5 $\mu\text{mol L}^{-1}$) were lower than at either cores Z2 or Z3, and showed an irregular distribution with depth (Fig. 6). The highest concentrations of Fe coincided with some of the lowest AVS contents in the cores (*e.g.*, 24.5, 22.1, 15.9 mg kg^{-1} , for Z1, Z2 and Z3, respectively). The CRS contents generally increased in each core with increasing depth, broadly consistent with the higher TOC and also the Fe, As, and Mn peaks.

Discussion

Salt marshes

The high As contents in the deeper horizons observed in all marsh cores likely reflect the continuous penetration of oxygen-rich surface water, which drives oxidation of upward diffusing Fe(II) and Mn(II) resulting in deposition of Fe(III)/Mn(IV) oxides/oxyhydroxides on the walls of the (*N. granulates*) crab burrows (Fig. 2). More specifically, the subsurface peaks in As content can be explained by adsorption onto and/or co-precipitation with Fe(III)/Mn(IV) oxides/oxyhydroxides as dissolved As comes into contact with these precipitating metal oxides/oxyhydroxides (Widerlund and Ingrı, 1995; Choi *et al.*, 2009). The biological disturbance of marsh sediments in the redox zone by *N. granulates* crabs leads to the penetration of oxygen via the crab burrow, which commonly reach depths of 20 cm to 30 cm below the marsh surface, corresponding to the subsurface maxima observed for As, Fe, and Mn in these sediments (Fig. 2). Others have observed similar trends with depth in salt marshes, where ferruginous incrustations and

nODULES ENRICHED WITH ARSENIC WERE REPORTED ALONG ROOTS AND CRAB CHANNELS THAT PROPAGATE TO DEPTHS OF OVER 35 CM (RIEDEL *ET AL.*, 1987; DOYLE AND OTTE, 1997; HYACINTHE *ET AL.*, 2001; CHAILLOU *ET AL.*, 2003; COSTA *ET AL.*, 2017).

Correlations between As and Fe contents with depth in the marsh sediments reflect similarities in their redox cycling, as well as the high sorptive capacity of Fe(III) oxides/oxyhydroxides for trace elements like As (Pierce and Moore, 1982; Moore *et al.*, 1988; Masscheleyn *et al.*, 1991; Rittle *et al.*, 1995; Harrington *et al.*, 1998; Smedley and Kinniburgh, 2002; Chaillou *et al.*, 2003; Dixit and Hering, 2003; Nóbrega *et al.*, 2013). Indeed, the close coupling of As and Fe redox cycling in both oxidizing and reducing environments is well documented (Welch *et al.*, 2000; Smedley and Kinniburgh, 2002; Fitz and Wenzel, 2003; Ravenscroft *et al.*, 2009). This close coupling includes Fe and As cycling in estuarine sediments (Widerlund and Ingri, 1995; Sullivan and Aller, 1996; Wang *et al.*, 2012)

Ferric iron, and to a lesser extent, Mn(IV) oxides/oxyhydroxides are known to be strong adsorbents of As under oxic conditions (Sullivan and Aller, 1996; Dixit and Hering, 2003; Choi *et al.*, 2009), and can persist, becoming the major geochemical carriers of arsenic under moderately reduced soil conditions (0 to -100 mV; Masscheleyn *et al.*, 1991). Such conditions are indeed characteristic at depths of 20 to 30 cm for all three salt marsh sediment cores studied here, where Eh reaches values as low as -100 mV (Table 1). Berner (1981) devised a simple classification scheme for oxic, suboxic, and anoxic systems, which we apply here to facilitate our conceptual model of As cycling in sediments of the Patos Lagoon estuary. Briefly, oxic environments can be characterized as having dissolved oxygen concentrations greater than 10 μM (Berner, 1981). When oxygen is depleted, metabolisms supporting nitrate reduction, Mn reduction, and Fe reduction dominate in the suboxic zone (Berner, 1981; Canfield and Thamdrup, 2009). These environments (*i.e.*, nitrogenous, manganeseous, and ferruginous zones of Canfield and Thamdrup, 2009) have dissolved oxygen concentrations that are commonly greater than 1 μM but less than 10 μM , and H_2S concentrations that are less than 10 μM (Berner, 1981). The anoxic zone is characterized by high H_2S concentrations (*i.e.*, greater than 10 μM) and supports sulfate reduction (Berner, 1981; Canfield and Thamdrup, 2009). Such environments are also referred to as anoxic and sulfidic, or simply sulfidic (Canfield and Thamdrup, 2009).

The lower contents of Fe and Mn below depths of ca. 30 cm in the marsh sediment cores suggest that oxygen is depleted and Mn and Fe reduction are occurring, promoting

dissolution of Fe(III)/Mn(IV) oxides/oxyhydroxides. Hence, we consider a depth of ca. 30 cm in the marsh sediments are marking the approximate boundary between oxic and suboxic conditions as defined by Berner (1981). The highest As contents are generally located just above this oxic/suboxic boundary in the sediment cores (at depths of 27 cm for M1 core, and at 23 cm for M2 and M3), which supports the notion that upward diffusing As is captured by adsorption onto and/or co-precipitation with authigenic Fe(III)/Mn(IV) oxides/oxyhydroxides at these depths (Chaillou *et al.*, 2003). Therefore, the data presented here are consistent with redox changes modifying As contents in Patos Lagoon sediments. Furthermore, redox conditions in the salt marsh sediments, in particular, are directly related to the depth of oxygen penetration into the sediment, which is controlled by the balance between downward transport of sediment and organic matter, and associated intensity of organic matter mineralization, the latter of which is strongly influenced by bioturbation/bioirrigation processes (Nóbrega *et al.*, 2013).

Similar accumulation of arsenic at the depth of the oxic/suboxic boundary in estuarine/marsh sediments is observed elsewhere (*e.g.*, La Force *et al.*, 2000; O'Day *et al.*, 2004). Compared to the depth of biologically facilitated O₂ penetration in the Patos Lagoon marsh sediments, the effect of salinity differences appears to be less significant in As cycling in the estuary. Although, the higher salinity at location M1 could be responsible for lower *Spartina sp.* biomass at M1, which in turn could translate to lower organic carbon contents and mineralization rates, and thus higher Eh values in these sediments, our data do not allow us to specifically test this hypothesis. Nevertheless, it is reasonable to postulate that the lower TOC and higher Eh of the M1 sediments may explain the differences in As retention in these sediments compared to those from the M2 and M3 cores.

Shallow open water areas

Most coastal and estuarine sediments possess only a thin (*i.e.*, few centimeters) oxidized surface layer, where As contents are commonly elevated (Widerlund and Ingrı, 1995; Bone *et al.*, 2006; Wang *et al.*, 2012). Redox potential (Eh) as measured by platinum electrode as a function of depth in the sediment cores for the shallow, open water cores demonstrate that moderately reduced conditions occur only for the first 10 cm, where Eh values are greater than -70 mV in each core. Consequently, high concentrations of As in these sediments should not be expected for depths greater than 10 cm, assuming that As enrichment in the sediments chiefly reflects scavenging by authigenic Fe/Mn

oxides/oxyhydroxides as discussed above (*e.g.*, Masscheleyn *et al.*, 1991). The As content of the surface sediments from these shallow, open water cores average about 3 mg kg⁻¹, and are in agreement with what is expected for unpolluted sediments (Presley *et al.*, 1992; Leoni and Sartori, 1996; Hatje *et al.*, 2010). Higher As contents were found deeper in the sediments from each open water core, which may indicate enrichment by another means such as precipitation with authigenic sulfide minerals (*e.g.*, O'Day *et al.*, 2004) under the anoxic and sulfidic conditions that characterizes depths greater than ca. 20 cm in these cores (Fig. 6).

In suboxic conditions, Fe(III) and Mn(IV) are reduced and solubilized to Fe(II) and Mn(II) species, which in part can diffuse upward until they are oxidized and reprecipitated as Fe(III) and Mn(IV) oxides/oxyhydroxides. Another portion of the solubilized Fe(II) and Mn(II) constituents can diffuse downwards and precipitate as iron monosulfides (such as mackinawite or amorphous FeS) or as meta-pyrite (Huerta-Diaz and Morse 1992). Reduced Mn(II) commonly is removed from solution in anoxic pore waters as rhodochrosite (MnCO₃; Lebron and Suarez, 2010). Our data demonstrate that iron sulfides precipitate at greater depths in the shallow, open water sediment cores compared to the marsh cores, which appears to chiefly reflect the formation of pyrite as indicated by the CRS contents (Fig. 6). The strong correlation observed between Eh, free sulfide concentration, and CRS for sediment cores Z2 and Z3 supports this concept.

The As contents for these sediment cores strongly suggest that As precipitates at the same depth in these open water sediments where pore water dissolved sulfide concentrations (*i.e.*, free sulfides) increase, which is also the same depth where the measured Eh values of the sediments are extremely low (below -300 mV). Therefore, we submit that these data and observations are consistent with pyrite precipitation being an important sink for As in the shallow, open water sediments of the Patos Lagoon. Huerta-Diaz and Morse (1992) found similar behavior for anoxic-sulfidic sediments, where an increase with depth of trace metals was associated with the pyrite phase, and a mirror-image relationship between the reactive- and pyrite-trace metal profiles.

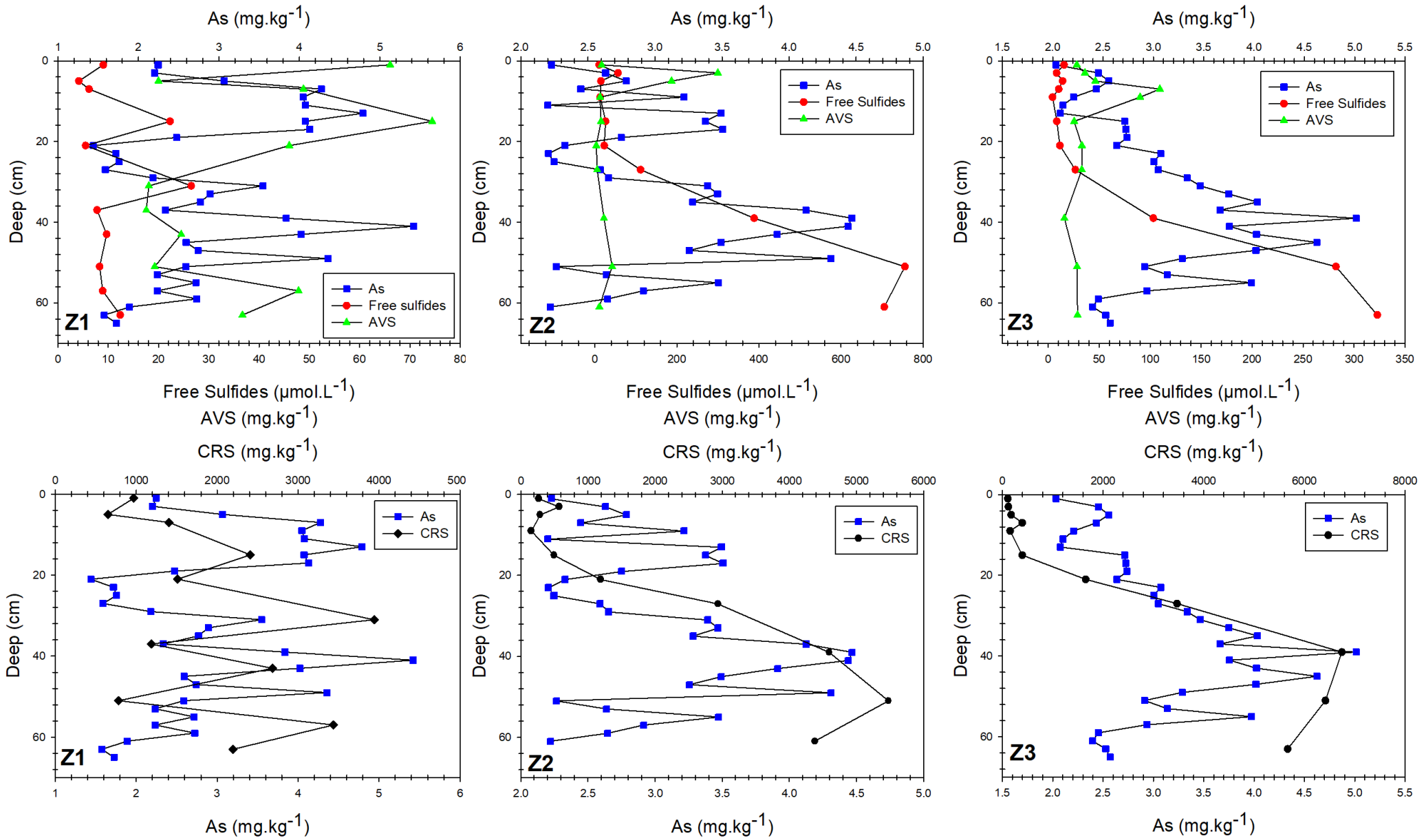


Figure 6 – Arsenic, free sulfides, AVS and CRS vertical distribution in shallow open water areas (Z1, Z2, and Z3).

During diagenesis free sulfides concentrations of the pore waters tend to be influenced by three main processes: 1) oxidation; 2) participation in the formation of metal sulfides; and 3) incorporation into organic compounds (Jørgensen and Kasten, 2006). Increasing free sulfide concentrations in the pore waters in conjunction with increasing CRS contents of sediments with depth for the Z2 and Z3 cores, as well as the low AVS contents, also suggest that pyrite is being formed by the “H₂S mechanism” in the Patos Lagoon sediments. Specifically, this mechanism hypothesizes that H₂S reacts directly with Fe(II) monosulfide minerals (*e.g.*, mackinawite, FeS) to form pyrite (Rickard and Morse, 2005; Rickard and Luther, 2007). In addition, the high concentrations of free sulfides may indicate two distinct factors: 1) the presence of high sulfate-reduction rates in these sediments; and/or 2) low availability of reactive iron to react with H₂S and remove it from solution (He *et al.*, 2010). In contrast, in the case of the Z1 sediments from the outlet channel of Patos Lagoon to the ocean, the absence of free sulfides in the pore waters and the higher Eh values (-180 mV) suggest this process (*i.e.*, sulfate reduction followed by meta-pyrite precipitation) is not occurring. The suboxic conditions established at depths of 40 cm in the Z1 core, characterized by the lower content of free sulfides, are a result of the greater abundance of coarser grain sediments, higher hydraulic energy, and lower TOC in the sediments.

In summary, authigenic sulfide mineral precipitation may explain the high As contents, and possibly Mn, at depths of 40 cm observed in sediments from core Z2 and Z3 (Fig. 6). Other researchers have reported that sedimentary pyrite is an important sink for As and is a moderately important sink for Co, Cu, Mn in marine and estuarine sediments (Huerta-Diaz and Morse, 1992; Huerta-Diaz *et al.*, 1998). The removal of these trace elements from anoxic pore waters likely occurs by coprecipitation (As and Mn) with FeS(s) and/or adsorption (As and Mn) onto FeS(s) (Huerta-Diaz and Morse, 1992; Huerta-Diaz *et al.*, 1998).

Conclusion

The geochemistry of arsenic in the Patos Lagoon estuary is strongly affected by iron and can also be affected by manganese (shallow water sediments). Arsenic in the estuary sediments is generally concentrated in the surface oxic layer of the sediment, which can reach depths as great as 20 cm below the sediment surface in the salt marshes, where it is associated with hydrous Fe and Mn oxide minerals. The dissolution of iron oxyhydroxides in the suboxic zone of these sediments would lead to the simultaneous

release of iron and arsenic to the corresponding pore waters. Dissolved As can then diffuse upwards and be fixed onto precipitating Fe/Mn oxide/oxyhydroxide particles by adsorption or co-precipitation in the oxic zone (*e.g.*, salt marshes) or can also migrate downwards to the zone of sulfate reduction and be precipitated with sulfide minerals (shallow water areas; Edenborn *et al.*, 1986; Chaillou *et al.*, 2003).

The proposed As cycle for Patos Lagoon sediments is supported by Fe, As, Mn contents of the sediments as well as the concentration of dissolved sulfide (*i.e.*, free sulfides) in pore waters from the estuarine sediments. The greater depth of the oxic Fe/Mn-rich zone in the marsh sediments (20 – 30 cm) where As is enriched compared to the shallow, open water sediment cores reflects bioturbation by *N. granulates* crabs that populate the marsh. Here, upwards diffusing As is fixed on the particulate Fe/Mn oxide/oxyhydroxide phase that precipitates near the redox boundary, which can be at 20 cm deep in these highly bioturbated sediments. Precipitation of As in anoxic and sulfidic conditions that characterize depths of 40 cm or more in the shallow, open water sediment cores can be attributed to uptake of As by precipitating, authigenic meta-pyrite in these sediments. The conclusions are supported by the high dissolved sulfide concentrations of pore waters from greater than 40 cm depth, and the increasing content of CRS, which is commonly attributed to pyrite.

The similarities in the distributions of As and Fe suggest that the diagenetic Fe cycle controls the particulate As-distribution and that Fe(III) oxides/oxyhydroxides are the principal As-carrier phase in the estuarine sediments, even though Mn can be an important carrier for As in shallow water locations. Fundamental questions still remain concerning the extent of sulfide interactions with trace metals, and consequently with As. For example, little is known about how trace elements are associated with sulfides (*i.e.* co-precipitated or adsorbed on Fe sulfides, or precipitated as discrete metal sulfides) (Otero and Macias, 2003; Nóbrega *et al.*, 2013). Parameters as the degree of pyritization (DOP) can be considered as a measure of the extent to which non-silicate iron (*i.e.*, reactive iron) has been transformed to pyrite and should be used to better understand how trace elements are associated with sedimentary sulfides. These combined approaches will provide improved understanding of the geochemical cycling and ultimate fate of As in estuarine environments.

Acknowledgments

This study was supported by grant from “Coordenação de Aperfeiçoamento de Pessoal de Nível Superior – Brasil” (CAPES) as well as funds made available by Michael and Mathilda Cochran through the Cochran Family Professorship at Tulane University.

References

- Beck, M. *et al.* (2008) ‘Cycling of trace metals (Mn, Fe, Mo, U, V, Cr) in deep pore waters of intertidal flat sediments’, *Geochimica et Cosmochimica Acta*. doi: 10.1016/j.gca.2008.04.013.
- Bednar, A. J. *et al.* (2005) ‘Effects of iron on arsenic speciation and redox chemistry in acid mine water’, *Journal of Geochemical Exploration*. doi: 10.1016/j.gexplo.2004.10.001.
- Berner, R. A. (1981) ‘A New Geochemical Classification of Sedimentary Environments’, *Journal of Sedimentary Petrology*. doi: 10.1306/212F7C7F-2B24-11D7-8648000102C1865D.
- Bhattacharyya, R. *et al.* (2003) ‘High arsenic groundwater: Mobilization, metabolism and mitigation - An overview in the Bengal Delta Plain’, *Molecular and Cellular Biochemistry*. doi: 10.1023/A:1026001024578.
- Bone, S. E., Gonnea, M. E. and Charette, M. A. (2006) ‘Geochemical cycling of arsenic in a coastal aquifer’, *Environmental Science and Technology*. doi: 10.1021/es052352h.
- Brannon, J. M. and Patrick, W. H. (1987) ‘Fixation, Transformation, and Mobilization of Arsenic in Sediments’, *Environmental Science and Technology*. doi: 10.1021/es00159a005.
- Brooks, Kenneth M. 2001. *An evaluation of the relationship between salmon farm biomass, organic inputs to sediments, physiochemical changes associated with those inputs and the infaunal response - with emphasis on total sediment sulfides, total volatile solids, and oxidation-reduction potential as surrogate endpoints for biological monitoring, final report*. Port Townsend, Wash: Kenneth M. Brooks.
- Burdige, D. J. (1993) ‘The biogeochemistry of manganese and iron reduction in marine sediments’, *Earth Science Reviews*. doi: 10.1016/0012-8252(93)90040-E.
- Canfield, D. E. and Thamdrup, B. (2009) ‘Towards a consistent classification scheme for geochemical environments, or, why we wish the term “suboxic” would go away: Editorial’, *Geobiology*. doi: 10.1111/j.1472-4669.2009.00214.x.

- Chaillou, G. *et al.* (2003) ‘The behaviour of arsenic in muddy sediments of the Bay of Biscay (France)’, *Geochimica et Cosmochimica Acta*. doi: 10.1016/S0016-7037(03)00204-7.
- Charette, M. A. and Sholkovitz, E. R. (2002) Oxidative precipitation of groundwater-derived ferrous iron in the subterranean estuary of a coastal bay. *Geophys. Res. Lett.* 29(10). <http://dx.doi.org/10.1029/2001GLO4512>
- Choi, S., O’Day, P. A. and Hering, J. G. (2009) ‘Natural attenuation of arsenic by sediment sorption and oxidation’, *Environmental Science and Technology*. doi: 10.1021/es802841x.
- Clark, M. W. *et al.* (1998) ‘Redox stratification and heavy metal partitioning in Avicennia-dominated mangrove sediments: a geochemical model’, *Chemical Geology*. doi: 10.1016/S0009-2541(98)00034-5.
- Costa, C. S. B., Marangoni, J. C. and Azevedo, A. M. G. (2003) ‘Plant zonation in irregularly flooded salt marshes: Relative importance of stress tolerance and biological interactions’, *Journal of Ecology*. doi: 10.1046/j.1365-2745.2003.00821.x.
- Costa, L., Mirlean, N. and Garcia, F. (2017) ‘Arsenic Environmental Threshold Surpass in Estuarine Sediments: Effects of Bioturbation’, *Bulletin of Environmental Contamination and Toxicology*, 98(4), pp. 521–524. doi: 10.1007/s00128-016-2024-z.
- D’Incao, F. *et al.* (1992) ‘Responses of Chasmagnathus granulata Dana (Decapoda: Grapsidae) to salt-marsh environmental variations’, *Journal of Experimental Marine Biology and Ecology*. doi: 10.1016/0022-0981(92)90095-R.
- Dixit, S. and Hering, J. G. (2003) ‘Comparison of arsenic(V) and arsenic(III) sorption onto iron oxide minerals: Implications for arsenic mobility’, *Environmental Science and Technology*. doi: 10.1021/es030309t.
- Doyle, M. O. and Otte, M. L. (1997) ‘Organism-induced accumulation of iron, zinc and arsenic in wetland soils’, *Environmental Pollution*. doi: 10.1016/S0269-7491(97)00014-6.
- Edenborn, H. M. *et al.* (1986) ‘Observations on the diagenetic behavior of arsenic in a deep coastal sediment’, *Biogeochemistry*. doi: 10.1007/BF02180326.
- Elderfield, H. and Hepworth, A. (1975) ‘Diagenesis, metals and pollution in estuaries’, *Marine Pollution Bulletin*. doi: 10.1016/0025-326X(75)90149-6.
- Fitz, W. J. and Wenzel, W. W. (2003) ‘Environmental Chemistry of Arsenic’, *Journal of*

- Environment Quality*. doi: 10.2134/jeq2003.1572a.
- Flora, S. J. S. (2015) *Handbook of Arsenic Toxicology, Handbook of Arsenic Toxicology*. doi: 10.1016/C2013-0-08322-3.
- Fossing, H. and Jørgensen, B. B. (1989) ‘Measurement of bacterial sulfate reduction in sediments: Evaluation of a single-step chromium reduction method’, *Biogeochemistry*. doi: 10.1007/BF00002889.
- Froelich, P. N., Klinkhammer, G. P., Bender, M. L., Luedtke, N. A., Heath, G. R., Cullen, D., and Dauphin, P. (1979) Early oxidation of organic matter in pelagic sediments of the eastern equatorial Atlantic: Suboxic diagenesis. *Geochim. Cosmochim. Acta* 43, 1075-1090.
- La Force, M. J., Hansel, C. M. and Fendorf, S. (2000) ‘Arsenic speciation, seasonal transformations and co-distribution with iron in a mine waste-influenced palustrine emergent wetland’, *Environmental Science and Technology*. doi: 10.1021/es0010150.
- Gaillard, J.-F., Pauwels, H. and Michard, G. (1989) ‘Chemical diagenesis in coastal marine sediments’, *Oceanologica Acta*.
- Garellick, H. et al. (2008) ‘Arsenic pollution sources’, *Reviews of Environmental Contamination and Toxicology*. doi: 10.1007/978-0-387-79284-2_2.
- HACH, C. (2007) ‘DR 2800 Spectrophotometer User Manual’, *Hach Company*. doi: 10.3928/01477447-20101221-06; 10.3928/01477447-20101221-06.
- Harrington, J. M. et al. (1998) ‘Phase associations and mobilization of iron and trace elements in Coeur d’Alene Lake, Idaho’, *Environmental Science and Technology*. doi: 10.12693/APhysPolA.133.447.
- Hatje, V. et al. (2010) ‘Inorganic As speciation and bioavailability in estuarine sediments of Todos os Santos Bay, BA, Brazil’, *Marine Pollution Bulletin*. doi: 10.1016/j.marpolbul.2010.08.014.
- He, Y. T. et al. (2010) ‘Geochemical processes controlling arsenic mobility in groundwater: A case study of arsenic mobilization and natural attenuation’, *Applied Geochemistry*. doi: 10.1016/j.apgeochem.2009.10.002.
- Hedges, J. I. and Keil, R. G. (1995) ‘Sedimentary organic matter preservation: an assessment and speculative synthesis’, *Marine Chemistry*. doi: 10.1016/0304-4203(95)00008-F.

- Helz G. R. and Tossell J. A. (2008) Thermodynamic model for arsenic speciation in sulfidic waters: a novel use of ab initio computations. *Geochim. Cosmochim. Acta* **72**, 4457-4468.
- Huerta-Diaz, M. A. and Morse, J. W. (1992) ‘Pyritization of trace metals in anoxic marine sediments’, *Geochimica et Cosmochimica Acta*. doi: 10.1016/0016-7037(92)90353-K.
- Huerta-Diaz, M. A., Tessier, A. and Carignan, R. (1998) ‘Geochemistry of trace metals associated with reduced sulfur in freshwater sediments’, *Applied Geochemistry*. doi: 10.1016/S0883-2927(97)00060-7.
- Hyacinthe, C. *et al.* (2001) ‘Early diagenetic processes in the muddy sediments of the bay of biscay’, *Marine Geology*. doi: 10.1016/S0025-3227(01)00127-X.
- Iribarne, O. *et al.* (2000) ‘The role of burrows of the SW Atlantic intertidal crab Chasmagnathus granulata in trapping debris’, *Marine Pollution Bulletin*. doi: 10.1016/S0025-326X(00)00058-8.
- Jørgensen, B. B. and Kasten, S. (2006) ‘Sulfur cycling and methane oxidation’, in *Marine Geochemistry*. doi: 10.1007/3-540-32144-6_8.
- Kjerfve, B. (1994) ‘Coastal Lagoons’, *Elsevier Oceanography Series*. doi: 10.1016/S0422-9894(08)70006-0.
- Kneebone, P. E. *et al.* (2002) ‘Deposition and fate of arsenic in iron- and arsenic-enriched reservoir sediments’, *Environmental Science and Technology*. doi: 10.1021/es010922h.
- Krantzberg, G. (1985) ‘The influence of bioturbation on physical, chemical and biological parameters in aquatic environments: A review’, *Environmental Pollution. Series A, Ecological and Biological*. doi: 10.1016/0143-1471(85)90009-1.
- Lebron, I. and Suarez, D. L. (2010) ‘Mechanisms and Precipitation Rate of Rhodochrosite at 25°C as Affected by PCO₂ and Organic Ligands’, *Soil Science Society of America Journal*. doi: 10.2136/sssaj1999.03615995006300030019x.
- Leoni, L. and Sartori, F. (1996) ‘Heavy metals and arsenic in sediments from the continental shelf of the Northern Tyrrhenian/Eastern Ligurian seas’, *Marine Environmental Research*. doi: 10.1016/0141-1136(94)00153-7.
- Machado, W. *et al.* (2008) ‘Relation of Reactive Sulfides with Organic Carbon, Iron, and Manganese in Anaerobic Mangrove Sediments: Implications for Sediment Suitability to Trap Trace Metals’, *Journal of Coastal Research*. doi: 10.2112/06-0736.1.

- Magalhães, M. C. F. (2007) ‘Arsenic. An environmental problem limited by solubility’, *Pure and Applied Chemistry*. doi: 10.1351/pac200274101843.
- Marangoni, J. C. and Costa, C. S. B. (2012) ‘Short- and Long-Term Vegetative Propagation of Two Spartina Species on a Salt Marsh in Southern Brazil’, *Estuaries and Coasts*. doi: 10.1007/s12237-011-9474-7.
- Marques, W. C. et al. (2009) ‘Numerical modeling of the Patos Lagoon coastal plume, Brazil’, *Continental Shelf Research*, 29(3), pp. 556–571. doi: 10.1016/j.csr.2008.09.022.
- Marques, W. C. et al. (2010) ‘Dynamics of the Patos Lagoon coastal plume and its contribution to the deposition pattern of the southern Brazilian inner shelf’, *Journal of Geophysical Research: Oceans*, 115(10). doi: 10.1029/2010JC006190.
- Masscheleyn, P. H., Delaune, R. D. and Patrick, W. H. (1991) ‘Effect of Redox Potential and pH on Arsenic Speciation and Solubility in a Contaminated Soil’, *Environmental Science and Technology*. doi: 10.1021/es00020a008.
- Masscheleyn, P. H., Delaune, R. D. and Patrick, W. H. (2010) ‘Arsenic and Selenium Chemistry as Affected by Sediment Redox Potential and pH’, *Journal of Environment Quality*. doi: 10.2134/jeq1991.00472425002000030004x.
- Mayer, L. M. (1994) ‘Relationships between mineral surfaces and organic carbon concentrations in soils and sediments’, *Chemical Geology*. doi: 10.1016/0009-2541(94)90063-9.
- Mermillod-Blondin, F. et al. (2004) ‘Influence of bioturbation by three benthic infaunal species on microbial communities and biogeochemical processes in marine sediment’, *Aquatic Microbial Ecology*. doi: 10.3354/ame036271.
- Mermillod-Blondin, F. (2011) ‘The functional significance of bioturbation and biodeposition on biogeochemical processes at the water–sediment interface in freshwater and marine ecosystems’, *Journal of the North American Benthological Society*. doi: 10.1899/10-121.1.
- Mirlean, N. et al. (2003) ‘Arsenic pollution in Patos Lagoon estuarine sediments, Brazil’, *Marine Pollution Bulletin*. doi: 10.1016/S0025-326X(03)00257-1.
- Mirlean, N. et al. (2012) ‘Arsenic enrichment in shelf and coastal sediment of the Brazilian subtropics’, *Continental Shelf Research*. doi: 10.1016/j.csr.2012.01.006.
- Mirlean, N. and Costa, C. S. B. (2017) ‘Geochemical factors promoting die-back gap formation in colonizing patches of Spartina densiflora in an irregularly flooded marsh’, *Estuarine, Coastal and Shelf Science*. doi: 10.1016/j.ecss.2017.03.006.

- Mladenov, N. *et al.* (2015) ‘Dissolved Organic Matter Quality in a Shallow Aquifer of Bangladesh: Implications for Arsenic Mobility’, *Environmental Science and Technology*. doi: 10.1021/acs.est.5b01962.
- Moller, O. O. *et al.* (1996) ‘The Patos Lagoon summertime circulation and dynamics’, *Continental Shelf Research*. doi: 10.1016/0278-4343(95)00014-R.
- Moller, O. O. *et al.* (2001) ‘The Influence of Local and Non-Local Forcing Effects on the Subtidal Circulation of Patos Lagoon’, *Estuaries*. doi: 10.2307/1352953.
- Moore, J. N., Ficklin, W. H. and Johns, C. (1988) ‘Partitioning of Arsenic and Metals in Reducing Sulfidic Sediments’, *Environmental Science and Technology*. doi: 10.1021/es00169a011.
- Nickson, R. T. *et al.* (2000) ‘Mechanism of arsenic release to groundwater, Bangladesh and West Bengal’, *Applied Geochemistry*. doi: 10.1016/S0883-2927(99)00086-4.
- Niencheski, L. F., Moore, W. S. and Windom, H. L. (2014) ‘History of human activity in coastal southern Brazil from sediment’, *Marine Pollution Bulletin*, 78(1–2), pp. 209–212. doi: 10.1016/j.marpolbul.2013.10.042.
- Niencheski, L. F., Windom, H. L. and Smith, R. (1994) ‘Distribution of particulate trace metal in Patos Lagoon estuary (Brazil)’, *Marine Pollution Bulletin*. doi: 10.1016/0025-326X(94)90545-2.
- Nóbrega, G. N. *et al.* (2013) ‘Iron and sulfur geochemistry in semi-arid mangrove soils (Ceará, Brazil) in relation to seasonal changes and shrimp farming effluents’, *Environmental Monitoring and Assessment*. doi: 10.1007/s10661-013-3108-4.
- Nordstrom, D. K. (2002) ‘Worldwide occurrences of arsenic in ground water’, in *Science compass*. doi: 10.1126/science.1072375.
- O’Day, P. A. *et al.* (2004) ‘The influence of sulfur and iron on dissolved arsenic concentrations in the shallow subsurface under changing redox conditions’, *Proceedings of the National Academy of Sciences*. doi: 10.1073/pnas.0402775101.
- Otero, X. L. and Macias, F. (2003) ‘Spatial variation in pyritization of trace metals in salt-marsh soils’, *Biogeochemistry*. doi: 10.1023/A:1021115211165.
- Pearcy, R. W. and Ustin, S. L. (1984) ‘Effects of salinity on growth and photosynthesis of three California tidal marsh species’, *Oecologia*. doi: 10.1007/BF00377375.
- Pierce, M. L. and Moore, C. B. (1982) ‘Adsorption of arsenite and arsenate on amorphous iron hydroxide’, *Water Research*. doi: 10.1016/0043-1354(82)90143-9.

- Planer-Friedrich B., London J., McCleskey R. B., Nordstrom D. K., and Wallschläger D. (2007) Thioarsenates in geothermal waters of Yellowstone National Park: Determination, preservation, and geochemical importance. *Environ. Sci. Technol.* **41**, 5245-5251.
- Presley, B. J., Taylor, R. J. and Boothe, P. N. (1992) 'Trace metal concentrations in sediments of the Eastern Mississippi Bight', *Marine Environmental Research*. doi: 10.1016/0141-1136(92)90142-9.
- Ravenscroft P., Brammer H., and Richards K. (2009) *Arsenic Pollution: A Global Synthesis*. John Wiley & Sons, Chichester, UK.
- Rickard, D. and Luther, G. W. (2007) 'Chemistry of iron sulfides', *Chemical Reviews*. doi: 10.1021/cr0503658.
- Rickard, D. and Morse, J. W. (2005) 'Acid volatile sulfide (AVS)', *Marine Chemistry*. doi: 10.1016/j.marchem.2005.08.004.
- Riedel, G. F., Sanders, J. G. and Osman, R. W. (1987) 'The effect of biological and physical disturbances on the transport of arsenic from contaminated estuarine sediments', *Estuarine, Coastal and Shelf Science*. doi: 10.1016/0272-7714(87)90016-3.
- Rittle, K. A., Drever, J. I. and Colberg, P. J. S. (1995) 'Precipitation of arsenic during bacterial sulfate reduction', *Geomicrobiology Journal*. doi: 10.1080/01490459509378000.
- Roman, C. T., Niering, W. A. and Warren, R. S. (1984) 'Salt marsh vegetation change in response to tidal restriction', *Environmental Management*. doi: 10.1007/BF01866935.
- Rosa, L. C. and Bemvenuti, C. E. (2005) 'Effects of the burrowing crab Chasmagnathus granulata (Dana) on meiofauna of estuarine intertidal habitats of Patos Lagoon, Southern Brazil', *Brazilian Archives of Biology and Technology*. doi: 10.1590/S1516-89132005000200014.
- Roy, M., Martin, J. B., Cherrier, J., Cable, J. E., and Smith, C. G. (2010) Influence of sea level rise on iron diagenesis in an east Florida subterranean estuary. *Geochim. Cosmochim. Acta* **74**, 5560-5573.
- Roy, M., Martin, J. B., Smith, C. G., and Cable, J. E. (2011) Reactive-transport modeling of iron diagenesis and associated organic matter mineralization in a Florida (USA) subterranean estuary. *Earth Planet Sci. Lett.* **304**, 191-201.
- Sá, F. *et al.* (2015) 'Arsenic fractionation in estuarine sediments: Does coastal

- eutrophication influence As behavior?', *Marine Pollution Bulletin*. doi: 10.1016/j.marpolbul.2015.04.037.
- Sailo, L. and Mahanta, C. (2014) 'Arsenic mobilization in the Brahmaputra plains of Assam: groundwater and sedimentary controls', *Environmental Monitoring and Assessment*. doi: 10.1007/s10661-014-3890-7.
- Secrieru, D. and Oaie, G. (2009) 'The relation between the grain size composition of the sediments from the NW Black Sea and their Total Organic Cabbon (ToC) content', *Geo-Eco-Marina*.
- Sharma, V. K. and Sohn, M. (2009) 'Aquatic arsenic: Toxicity, speciation, transformations, and remediation', *Environment International*. doi: 10.1016/j.envint.2009.01.005.
- Shimada, N. (1996) 'Geochemical conditions enhancing the solubilization of arsenic into groundwater in Japan', *Applied Organometallic Chemistry*. doi: 10.1002/(SICI)1099-0739(199611)10:9<667::AID-AOC545>3.0.CO;2-I.
- Smedley, P. L. and Kinniburgh, D. G. (2002) 'A review of the source, behaviour and distribution of arsenic in natural waters', *Applied Geochemistry*. doi: 10.1016/S0883-2927(02)00018-5.
- Smith, A. H., Lingas, E. O. and Rahman, M. (2000) 'Contamination of drinking-water by arsenic in Bangladesh: A public health emergency', *Bulletin of the World Health Organization*. doi: 10.1590/S0042-96862000000900005.
- Smith, E., Smith, J. and Naidu, R. (2006) 'Distribution and nature of arsenic along former railway corridors of South Australia', *Science of the Total Environment*. doi: 10.1016/j.scitotenv.2005.05.039.
- Stucker V. K., Silverman D. R., Williams K. H., Sharp J. O., and Ranville J. F. (2014) Thioarsenic species associated with increased arsenic release during biostimulated subsurface sulfate reduction. *Environ. Sci. Technol.* **48**, 13367-13375.
- Sullivan, K. A. and Aller, R. C. (1996) 'Diagenetic cycling of arsenic in Amazon shelf sediments', *Geochimica et Cosmochimica Acta*. doi: 10.1016/0016-7037(96)00040-3.
- Telfeyan, K. *et al.* (2017) 'Arsenic, vanadium, iron, and manganese biogeochemistry in a deltaic wetland, southern Louisiana, USA', *Marine Chemistry*. doi: 10.1016/j.marchem.2017.03.010.
- USEPA, U. S. E. P. A. (1991) *Draft analytical method for determination of acid volatile sulfide in sediment*. EPA-821-R-91-100, Washington, DC.

- USEPA, U. S. E. P. A. (1996) *Method 3050B - Acid digestion of sediments, sludges, and soils.*, 1996. doi: 10.11117/12.528651.
- Van Cappellen, P. and Wang, Y. (1996) Cycling of iron and manganese in surface sediments: A general theory for the coupled transport and reaction of carbon, nitrogen, sulfur, iron, and manganese. *Am. J. Sci.* 296, 197-243.
- Vidal-Durà, A. *et al.* (2018) ‘Reoxidation of estuarine sediments during simulated resuspension events: Effects on nutrient and trace metal mobilisation’, *Estuarine, Coastal and Shelf Science*. doi: 10.1016/j.ecss.2018.03.024.
- Wallner-Kersanach, M. *et al.* (2016) ‘Temporal evolution of the contamination in the southern area of the Patos Lagoon estuary, RS, Brazil’, *Revista de Gestão Costeira Integrada*, 16(3), pp. 263–279. doi: 10.5894/rgci596.
- Wang, S. *et al.* (2012) ‘Arsenic retention and remobilization in muddy sediments with high iron and sulfur contents from a heavily contaminated estuary in China’, *Chemical Geology*. doi: 10.1016/j.chemgeo.2012.05.005.
- Welch, A. H. *et al.* (2000) ‘Arsenic in ground water of the United States: Occurrence and geochemistry’, *Ground Water*. doi: 10.1111/j.1745-6584.2000.tb00251.x.
- Widerlund, A. and Ingri, J. (1995) ‘Early diagenesis of arsenic in sediments of the Kalix River estuary, northern Sweden’, *Chemical Geology*. doi: 10.1016/0009-2541(95)00073-U.
- Windom, H. L., Niencheski, L. F. and Smith, R. G. (1999) ‘Biogeochemistry of nutrients and trace metals in the estuarine region of the patos lagoon (Brazil)’, *Estuarine, Coastal and Shelf Science*. doi: 10.1006/ecss.1998.0410.
- Yang, N. *et al.* (2016) ‘High arsenic (As) concentrations in the shallow groundwaters of southern Louisiana: Evidence of microbial controls on As mobilization from sediments’, *Journal of Hydrology: Regional Studies*. doi: 10.1016/j.ejrh.2015.11.023.
- Ying, S. C., Kocar, B. D. and Fendorf, S. (2012) ‘Oxidation and competitive retention of arsenic between iron- and manganese oxides’, *Geochimica et Cosmochimica Acta*. doi: 10.1016/j.gca.2012.07.013.
- Yücel, M. *et al.* (2010) ‘Sulfur speciation in the upper Black Sea sediments’, *Chemical Geology*. doi: 10.1016/j.chemgeo.2009.10.010.

CAPÍTULO II: Effects of bioirrigation and salinity on arsenic distributions in ferruginous concretions from salt marsh sediment cores (southern Brazil)

Regional Studies in Marine Science

Em revisão

Abstract

Arsenic (As), iron (Fe) and manganese (Mn) contents in sediment nodules and associated pore waters obtained from sediment cores collected from a salt marsh on Polvora Island (southern Brazil) were measured. Sediment cores (ca. 30 cm) were obtained during a brackish water period at two different salt marsh environments: an unvegetated mudflat colonized by crabs (*Neohelice granulata*), and a low intertidal stand vegetated by *Spartina alterniflora*. Specifically, we determined the percentage of nodules in each depth interval of the cores, along with the redox potential, and As, Fe, and Mn contents of the nodules. The mineralogy of the nodules was investigated and, results showed that they are mainly composed by quartz, phyllosilicates, and amorphous Fe-Mn oxides/oxyhydroxides. Pore water results showed that bioturbation by local crabs supports oxygen penetration to depths of ca. 25 cm below the salt marsh surface, with lower Fe contents in pore water associated with the brackish period. However, *Spartina alterniflora* growth appears to have a greater impact on sediment geochemistry due to sulfate reduction and the associated decrease in pore water pH. Higher Fe concentrations were observed in the pore waters during the period of brackish water dominance, which also corresponded to the *S. alterniflora* growth season in the salt marsh. This study demonstrates clear differences in the geochemical conditions (*i.e.*, Fe content) for the different types of bioirrigation (*i.e.*, by crabs versus growth of *S. alterniflora*) in salt marshes sediments.

Key-words: Arsenic; Marshes; Bioturbation; Iron-Manganese oxides/oxyhydroxides.

Introduction

Arsenic (As) is a highly toxic metalloid that occurs naturally in the environment (Javed *et al.*, 2014). Accordingly, the As content of sediments depends on the type and abundance of adsorbing components within the sediment (*e.g.*, minerals, organic matter), the pH of the aqueous solution, and the redox potential of the system (Masscheleyn *et al.*,

1991; Buschmann *et al.*, 2006). Many studies have investigated the processes responsible for As mobilization from sediments to pore waters and/or groundwaters (Nickson *et al.*, 2000; Smedley and Kinniburgh, 2002; Bhattacharyya *et al.*, 2003; He *et al.*, 2010). The main processes are: (1) reductive dissolution of metal oxides followed by release of sorbed/co-precipitated As; (2) pH or alkali induced desorption; (3) sulfide mineral oxidation with increasing pH; and (4) geothermal processes (Ravenscroft *et al.*, 2009).

Because As is strongly adsorbed onto and coprecipitates with iron (Fe) and manganese (Mn) oxides/oxyhydroxides, the formation of these metal oxides/oxyhydroxides in sediments under oxidizing conditions is recognized as a major pathway of As fixation in sediments (Smith *et al.*, 1998; Nickson *et al.*, 2000; Wu *et al.*, 2015). Dissolved arsenic occurs in multiple oxidation states in natural waters, including As(-III), As(0), As(II), As(III), and As(V), although As(III) and As(V) are most common (Cullen and Reimer, 1989). In neutral to alkaline pH surface waters, which are almost always oxic, equilibrium thermodynamics using currently available data predicts that arsenate, As(V), will predominate as H_2AsO_4^- or HAsO_4^{2-} depending on pH, whereas under reducing conditions, arsenite, As(III), should dominate as $\text{H}_3\text{AsO}_3^{\circ}$ (Smedley and Kinniburgh, 2002; Chaillou *et al.*, 2003; Nordstrom and Archer, 2003; Nordstrom *et al.*, 2014). Nevertheless, the trivalent and pentavalent forms of As are highly susceptible to adsorption onto mineral surfaces, especially surfaces of Fe(III) oxides/oxyhydroxides (Pierce and Moore, 1982; Wilkie and Hering, 1996; Dixit and Hering, 2003). Amorphous forms of Fe(III) oxides/oxyhydroxides (*e.g.*, ferrihydrite) are generally considered as being more labile than crystalline forms like goethite and especially hematite, and hence more readily dissolved by reducing conditions (Sadiq, 1997; Smedley and Kinniburgh, 2002; Larios *et al.*, 2012). However, for strongly reducing conditions in the presence of dissolved sulfide ($\Sigma\text{S}^{\text{-II}}$), As may instead be sequestered with Fe sulfide minerals that precipitate under highly reducing conditions (Wilkin and Ford, 2006; Stucker *et al.*, 2014).

In general, for pore waters where Fe(II) exceeds dissolved sulfide concentrations, dissolved As concentrations are commonly suppressed owing to the formation and uptake by iron sulfide minerals, whereas where $\Sigma\text{S}^{\text{-II}}$ concentrations are high and exceed Fe(II) concentrations, As may be mobile in the form of dissolved thioarsenic species (Wilkin and Ford, 2006; Planer-Friedrich *et al.*, 2007; Stucker *et al.*, 2014). Seasonal variations in the redox conditions in sediment pore waters (*e.g.*, due to flooding conditions) may thus promote or hinder the ability of SO_4^{2-} reducing bacteria to produce dissolved sulfide,

shifting the iron/sulfide ion balance and affecting aqueous As mobility (Wilkin, 2001; Wilkin *et al.*, 2003). Whereas the influence of redox potential and pH on As partitioning is well known, our understanding of how variable salinity affects As behavior in pore waters is less clear, especially in complex ecosystems such as estuarine and coastal wetlands.

Various hydrological and salinity conditions influence biochemical processes in estuaries by changing nutrient and trace element speciation, which affects their mobility and bioavailability (Du Laing *et al.*, 2008; Bai *et al.*, 2012). Pore water salinity in salt marshes increases during flood tides, and can be decreased by submarine groundwater discharge (Northrup *et al.*, 2018). These processes can also alter the local redox potential of pore waters, which may be decreased by water inundation or increased if the rising water is well oxygenated (Gong *et al.*, 2007). Therefore, shifting salinity combined with the dynamics of changing redox potential are expected to affect the geochemical cycling of redox-sensitive elements such as As in salt marsh pore waters (Du Laing *et al.*, 2007; Northrup *et al.*, 2018), and have a major impact on their bioavailability (Du Laing *et al.*, 2002).

Bioturbation and/or bioirrigation contribute with the complexity of effects of salinity and redox conditions on trace element biogeochemical cycling in complex salt marsh environments (Caetano and Vale, 2002; Ferreira *et al.*, 2007). Bioturbation includes sediment mixing and reworking by benthic organisms (*e.g.*, burrowing) and plants (Mermillod-Blondin, 2011), whereas bioirrigation refers to the enhanced transport of solutes across the sediment-water interface induced by the activities of bottom-dwelling organisms (Volkenborn *et al.*, 2016). Nevertheless, little is known about how different biological activities and salinity affect the distribution and cycling of As in salt marshes. Northrup *et al.* (2018) reported that during extreme events, a distinct pulse of As was observed in pore waters with the highest salinity. In contrast, Wang *et al.* (2012) attributed their reported increase in As mobility within the Yangtze River estuary to the summer enhancement of anoxic conditions in the sediment pore waters owing to the growth of *Spartina alterniflora*. Here, oxygen released from *S. alterniflora* roots oxidizes sulfide minerals within the sediments releasing Fe and As to solution. Iron and As are subsequently transported towards the root by both diffusion and advective pore water flow associated with the root water uptake (*e.g.*, Caetano and Vale, 2002).

In this contribution, we investigate the effect of biological activity (*i.e.*, plants and macro fauna) and hydrological variations in salinity (fresh water and brackish period) on

the redox conditions of salt marsh sediments from Pólvora Island in southern Brazil, and how these processes modify redox-sensitive trace elements like Fe, Mn and As in the sediment and pore waters. More specifically, this study aims to better understand the processes that control the distribution of As in estuarine sediments and that lead to the appearance of metalloid high concentrations.

Study Area

The Patos Lagoon (Fig 1) is the largest (10,360 km²; Moller *et al.*, 1996) choked lagoon in the world, and is located on the Atlantic coast in southern Brazil (Kjerfve, 1994). The penetration of brackish water in the lagoon is generally restricted to the estuary area, which is classified as a microtidal system (< 0.5 m tidal range; Moller *et al.*, 1996; Marques *et al.*, 2010). Consequently, seasonal fresh water discharge and wind variations in the Patos Lagoon are such that high water levels and low salinities (0–5 psu) occur during the rainy winter/spring season and low water levels and high salinities (20–30 psu) characterize the summer/fall season (Moller *et al.*, 1996; Marques *et al.*, 2010).

The Patos Lagoon estuary has over 7,000 ha of salt marshes (Marangoni and Costa, 2012), including Pólvora Island, the location of this study (Fig 1). Along adjacent saltmarsh/mudflats in the region, *Neohelice granulata* is one of the most abundant crab species, with population densities as high as 60 individual m⁻² (D'Incao *et al.*, 1992; Gutiérrez *et al.*, 2006). *Neohelice granulata* plays an important role in nutrient recycling in the lagoon's salt marsh environments, excavating and maintaining semi-permanent open burrows (D'Incao *et al.*, 1992; Iribarne *et al.*, 2000; Rosa and Bemvenuti, 2005). *Spartina alterniflora* and *S. densiflora* are the dominant plant species in the Patos Lagoon estuary (Costa *et al.*, 2003; Marangoni and Costa, 2012; Mirlean and Costa, 2017). Previously, we demonstrated that ferruginous incrustations and nodules are common among *Spartina* sp. roots and within crab burrows in the Patos Lagoon estuary (Costa *et al.*, 2017).

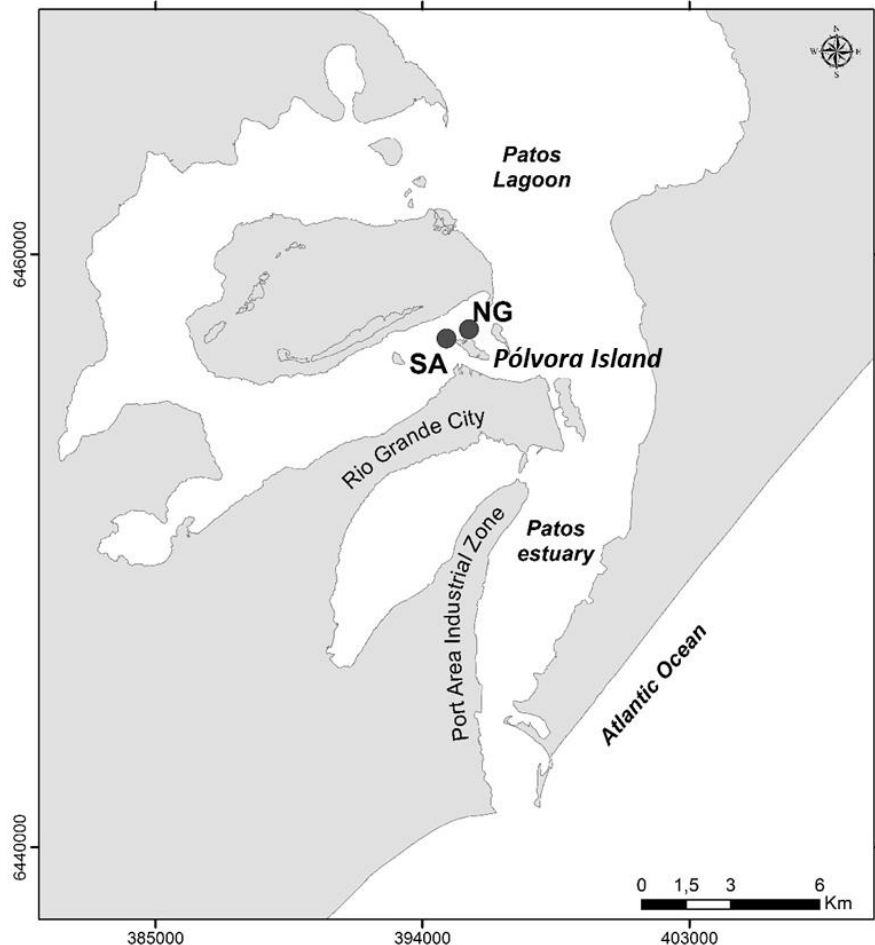


Figure 1 – Patos Lagoon estuary showing our sampling locations. Site labeled with “NG” represents location where the crab *Neohelice granulata* is chiefly responsible for bioturbation, whereas location labeled with “SA” shows the sampling site occupied by *Spartina alterniflora*.

Methods

Sampling approach

Sediment samples were collected in April and October 2018 when Pólvora Island was dominated, respectively, by the influence of marine water influx (*i.e.*, brackish period) and fluvial discharge (*i.e.*, fresh water period). Salinity conditions ranging between 20 and 30 prevailed at the study site for about a month before the brackish period sampling commenced. For the fresh water period, salinity conditions were below 3 psu for a month prior to sampling. Two zones/environments of the salt marsh were examined in both the brackish and fresh water periods based on different biological activities: a zone occupied by *S. alterniflora* (SA) and another by *N. granulata* (NG) (Fig 1). For the

brackish water period (April 2018), two sediments cores were collected at each site (SA and NG), one for pore water analysis and the other one for sediment analysis. However, for the fresh water period (October, 2018) only pore water samples were collected and analyzed. Therefore, only one sediment core was obtained at each sample location during the fresh water period.

Sediment sampling and analysis

Each sediment core was about 30 cm long (Fig 2) and was collected in PVC tubes (8 cm in inner diameter). Each core was hermetically sealed in the field and then transported vertically to the laboratory. Sediments treatment was performed immediately after sample collection and initially involved opening the cores longitudinally and splitting each in half. One half was immediately covered with polyethylene film to prevent sediment oxidation. Redox potential (Eh) were measured in subsamples of 2 cm depth each, using a combined Pt-electrode (Analion®). The Eh measurement in mV was recorded after the reading had stabilized. Pore water was obtained from the sediment subsamples by centrifugation at 3,000 rpm for 30 min. After centrifugation the supernatant was decanted and filtered through 0.45 µm membrane filters. The pH of the subsamples was measured in the interstitial pore water (intervals of 2 cm) with a pH meter (model pH6/00702-75; Oakton®).

The Fe/Mn-rich nodules (Fig 2) that characterize the local marsh sediments consist of hard, generally spherical-shaped, discrete bodies made of soil or sediment materials that have been cemented by Fe/Mn oxides/oxyhydroxides (Gasparatos *et al.*, 2005; Gasparatos *et al.*, 2019). Sediment nodules occurring within each 1 cm subsample of the cores were separated from the bulk sediment by wet sieving (45 µm sieve), washing repeatedly with deionized water, and then dried at 85° C.



Figure 2 – Sediment cores collected from the NG (A) and the SA (B) sites of the Pólvora Island salt marsh. Ferruginous nodules/concretions subsamples from 15 cm depth in each core are also shown.

Thereafter, nodules were collected visually, weighed, and stored in glass containers for future analysis. The other half of the sediment core was also sectioned into 1 cm subsamples that were dried at 45°C and weighed. These analyses were employed to compute the percentage of nodules in each core subsample according to equation 1:

$$\% \text{ Nodules} = \left(\frac{\text{dry nodule weight}}{\text{dry total subsample weight}} \right) \times 100 \% \quad (1)$$

The dried half of the sediment core mentioned above was used to measure the total organic carbon content (TOC), and the fine grain (clay and silt) percentage. Granulometric analysis was performed using standard sieve methods (ASTM C136/C136M), and values are expressed as the percentage of fine sediment grains within the total sediment subsample. For the determination of TOC, 30 mg of powdered sediment was analyzed in a TOC - VCPH, model SSM - 5000A, SHIMADZU, with a detection limit of 4 $\mu\text{g kg}^{-1}$. The relative standard deviation (%RSD) was less than 5% for triplicate analyses.

Furthermore, for each sampling location (SA and NG), nodules (*i.e.*, one each from the top, middle, and bottom of the respective cores) were chosen to further microscopic, mineralogical, and internal structure investigation. Nodules were fractured and the fresh broken surfaces then examined by scanning electron microscope (SEM) using a Hitachi 4800 high-resolution SEM with a 1.0 nm resolution at 15 kV. The SEM was equipped with energy-dispersive X-ray spectroscopy (EDS) system for qualitative elemental analysis. Energy dispersive X-ray analysis (XRD) of each nodule was performed with a 300-s count time. Analysis provided high-resolution images and qualitative elemental composition for the fresh nodule surfaces. The mineralogy of the nodules was further examined using an X-ray diffractometer (Scintag, XDS 2000, Cu K α , $\lambda = 0.154$ nm, U = 8.047 KeV, I = 38 mA) at a scanning rate of 1°/min. The XRD was equipped with a high-resolution solid-state detector and automated sample changer.

Aliquots of the sediment nodules were subsequently submitted to integral dissolution in hot acid digestion, following EPA method 3050B (USEPA, 1996) for As, Fe, and Mn analysis (Costa *et al.*, 2019), which is a very strong acid digestion that dissolves almost all elements that could become environmentally available (*i.e.* Fe/Mn oxides/oxyhydroxides). Briefly, the method involves digesting 0.5 g of dried and pulverized sediment sample at 95 ± 5 °C with 10 mL of 1:1 (v/v) ultrapure (Optima™ grade) HNO₃ for 10 min. Subsequently, 5 mL of concentrated ultrapure (Optima™ grade) HNO₃ (16N) was added to the slurry and allowed to react for 2 hours. Sedimentary organic matter is then, eliminated by adding 5 mL of trace metal grade 30% H₂O₂ to the sediment slurry and heating for 2 hours. The digested materials were then diluted to 50 mL with ultrapure, Milli-Q H₂O (18.2 MΩ cm) and centrifuged at 3000 rpm for at least 10 minutes. The supernatant was then diluted by a factor of 10 using 2% HNO₃ (16N) for As and Mn analyses, and kept refrigerated (4° C) until analysis.

Because we expected that the nodules had high Fe contents, aliquots of the supernatant were diluted by a factor of 400 (v/v) and measured by UV/VIS spectrophotometry using the FerroVer Iron Reagent method (HACH, 2007; Costa *et al.*, 2019). Absorption was measured at 510 nm using a DR 2800 Spectrophotometer (Hach Company®, method 8008; HACH, 2007), for which the detection limit is 0.02 mg kg⁻¹.

Arsenic and Mn were analyzed by high resolution inductively coupled plasma mass spectrometry (ICP-MS) (Thermo Fisher Element 2) with a PC3 (ESI) spray chamber and FAST (ESI) autosampler at Tulane University using methods described previously (Yang *et al.*, 2016; Costa *et al.*, 2019). The detection limit for As and Mn was 0.02 µg

kg^{-1} and $0.01 \mu\text{g kg}^{-1}$, respectively, for this approach. The analyses were calibrated using a standard 5-point calibration curve (*i.e.*, 0.1, 10, 100, 500, $1000 \mu\text{g L}^{-1}$) made using a standard multi-element solution ($10 \mu\text{g mL}^{-1}$; Claritas PPT® Certified Reference Material). Spiked duplicate samples were processed on a routine basis (5 % of each core), which indicated that the relative standard deviation (RSD) of all the analyses was less than 5 %. A marine sediment reference material MESS-4 (National Research Council of Canada; NRCC) was analyzed to ensure the accuracy and precision of the method. Recoveries for Fe, As and Mn for our analyses of MESS-4 were in the 95 % confidence limits for the CRM (Table 1). Reported concentration for the samples were blank subtracted. Results were studied statistically using regression analysis.

Table 1 - Analytical quality control data, average and standard deviation obtained for 3 replicates of the standard reference material MESS-4

CRM		As (mg kg^{-1})	Fe (g kg^{-1})	Mn (mg kg^{-1})
Mess-4	Certified Concentration	21.7 ± 2.8	37.9 ± 1.6	298 ± 14
	Measured	23.3 ± 3.2	35.2 ± 2.7	275.2 ± 21

Pore water analysis

Pore water samples were extracted from cores collected from the SA and NG sites for the seasonal periods dominated by fresh water and brackish water. Cores were opened longitudinally and handled within a glove box under an inert N_2 atmosphere to avoid any sample oxidation. Cores were sectioned in 3 cm slices from 5-11 cm depth and in 2 cm intervals from 11-20 cm depth, with top (0-5 cm) and bottom samples (20-25 and 25-30 cm) added to support a better understanding of the oxic/anoxic boundary in the marsh sediments. Subsamples were placed in 50 mL Falcon tubes and centrifuged at 3000 rpm for at least 30 min to separate the pore water from the sediment. The pore water acquired was then transferred to 10 mL Falcon tubes and diluted by a factor of 10 using 2% HNO_3 (16N). Thereafter, As, Fe and Mn were analyzed in the ICP-MS (Thermo Fisher Element 2) with a PC3 (ESI) spray chamber and FAST (ESI) autosampler at Tulane University, as described above. The detection limits for As, Mn and Fe were $0.02 \mu\text{g kg}^{-1}$, $0.01 \mu\text{g kg}^{-1}$ and $0.03 \mu\text{g kg}^{-1}$, respectively. Results were studied statistically using regression analysis.

Results

Sediment geochemistry

Redox potential (Eh) varied from -92.7 to 134.1 mV for sediments from core NG, and from -291.7 to 34.5 mV at site SA (Table 2; Fig 3). The mean Eh values for the NG site (25.2 mV), and SA site (-154.2 mV) indicate that sediments from the NG core can be characterized as being relatively oxic, on average, whereas sediments from the SA site are more reducing (*e.g.*, mainly characterized as being from the suboxic zone; Berner, 1981; Masscheleyn *et al.*, 1991). The percentage of fine grain sediment and TOC contents were similar for both salt marsh cores (Table 2; Fig 3); fine grain sediment varied from 20.8 to 61.2% for the NG core and from 32.0 to 60.4% for the SA core. The content of TOC ranged between 0.5 to 5.1 % for the NG core and from 0.5 to 4.3 % for the SA core. The TOC values are similar to others studies in the salt marshes of Pólvora Island (Mirlean and Costa, 2017; Costa *et al.*, 2019), and statistical correlations ($r^2 = 0.56$ and $r^2 = 0.60$, $p < 0.05$, $n = 16$; for NG and SA respectively) are found between the amount of fine grain and TOC, as it has been described elsewhere (Stein, 1991; Burone *et al.*, 2003). Statistical analysis did not show any correlation ($r^2 = 0.34$ and $r^2 = 0.21$, $p < 0.05$, $n = 16$; for NG and SA respectively) between TOC content, and Eh values in either the NG or SA cores. Furthermore, the depth variations of these parameters (*i.e.*, percent of fine grain sediment, TOC content, and Eh) were not obvious associated with geochemical processes that could explain the accumulation of As, Fe, and Mn in the sediment cores.

Marsh sediments from the SA core exhibit higher percentages of ferruginous nodules, reaching values as high as 8.5% by weight (Table 2), compared to the marsh sediments from the NG core, where the content of ferruginous nodules is always $\leq 5.8\%$ by weight (Table 2). There is no significant statistical correlation ($r^2 = 0.15$ and $r^2 = 0.22$, $p < 0.05$, $n = 16$; for NG and SA respectively) between Eh and the percentage of ferruginous nodules. The percentages of nodules peaked at a depth of 15 cm in the NG core, and at a depth of 16 cm in the SA core. These Fe-rich sediment nodules occurred from the top (0 cm depth) down to a depth of 21 cm in the NG core, but are only observed for the depth interval between 7 cm and 22 cm in the SA core.

Table 2 – Geochemical parameters for marsh nodules, salt water period. The upper numbers are the concentration range, and the mean \pm SD for the entire core is presented within parentheses.

Parameter	NG	SA
	Marsh occupied by <i>N. granulata</i>	Marsh occupied by <i>S. alterniflora</i>
Eh (mV)	<u>-92.7 – 134.1</u> (25.2 ± 68.0)	<u>- 291.5 – 34.5</u> (-154.2 ± 85.3)
Fine Grain (%)	<u>20.8 – 61.2</u> (42.1 ± 10.4)	<u>32.0 – 60.4</u> (46.1 ± 8.0)
TOC (%)	<u>0.5 – 5.1</u> (1.6 ± 1.5)	<u>0.5 – 4.3</u> (1.5 ± 1.1)
% Nodules	<u>0.0 – 5.8</u> (1.0 ± 1.5)	<u>0.0 – 8.5</u> (1.3 ± 2.2)
Fe (g kg ⁻¹)	<u>45.6 – 127.4</u> (84.2 ± 30.9)	<u>90.7 – 166.2</u> (138.6 ± 21.9)
Mn (mg kg ⁻¹)	<u>115.9 – 592.7</u> (342.4 ± 138.1)	<u>142.3 – 460.2</u> (257.2 ± 87.2)
As (mg kg ⁻¹)	<u>31.5 – 149.0</u> (67.9 ± 38.7)	<u>67.3 – 171.8</u> (119.0 ± 26.5)

Ferruginous nodules from the SA site exhibit the highest Fe and As contents ($90.7 \text{ g kg}^{-1} \leq \text{Fe} \leq 166.2 \text{ g kg}^{-1}$; and $67.3 \text{ mg kg}^{-1} \leq \text{As} \leq 171.8 \text{ mg kg}^{-1}$; Table 2), whereas nodules from the NG core have the highest Mn contents ($115.9 \text{ mg kg}^{-1} \leq \text{Mn} \leq 592.7 \text{ mg kg}^{-1}$; Table 2). A positive correlation exists between As and Fe in the ferruginous nodules from the NG core ($r^2 = 0.85$, $p < 0.05$, $n = 11$), whereas a weaker positive correlation exists between As and Mn in nodules from the SA core ($r^2 = 0.62$, $p < 0.05$, $n = 10$). Distributions of As, Fe, and Mn as a function of depth in each core are shown in Fig. 4. Each sediment core exhibits a subsurface peak in As and Fe content that occurs at 15 to 16 cm depth for both locations (Fig 4). The Mn content also peaked at 15 cm depth in the SA core, but occurred at a slightly shallower depth of 13 cm in the NG core.

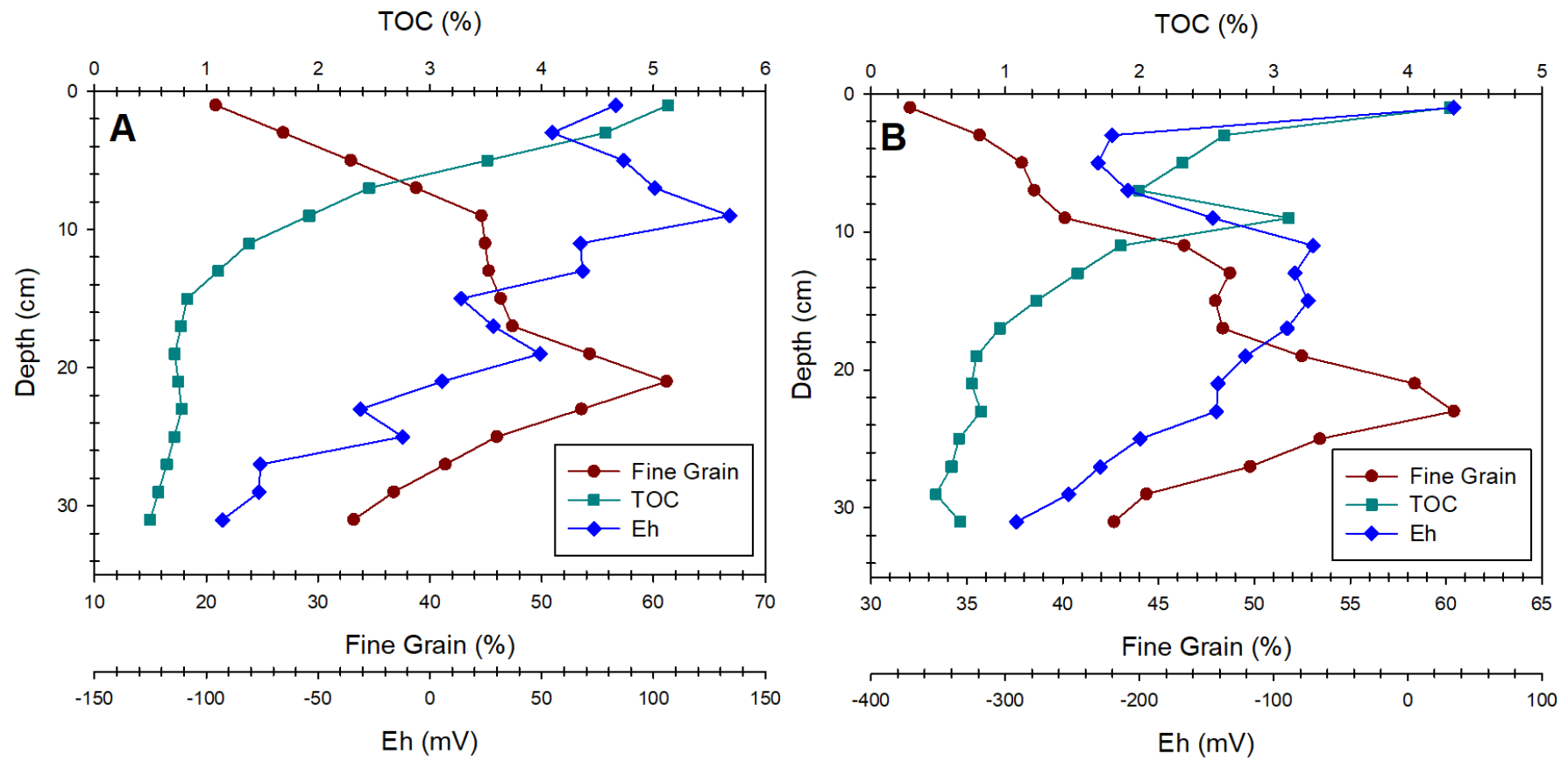


Figure 3 – Percentage of fine grain sediment, total organic carbon (TOC) content, and redox potential (Eh) as a function of depth for sediment cores collected from the NG (A) and SA (B) sites in the Pólvora Island salt marsh.

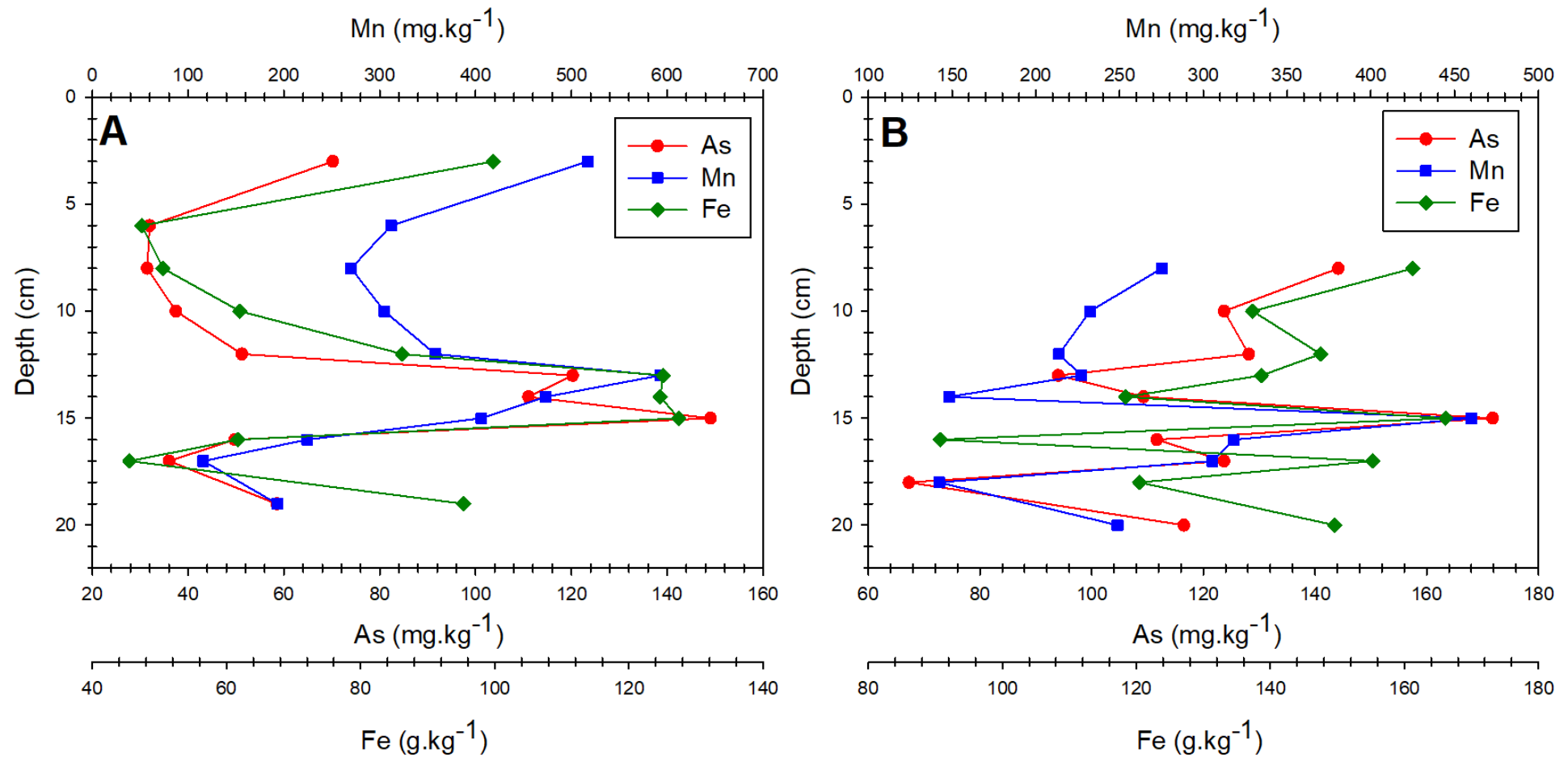


Figure 4 – Arsenic, manganese, and iron content in ferruginous sediment nodules as a function of depth for sediment cores collected from the NG (A) and SA (B) sites within the Pólvora Island salt marsh. See Figure 1 for locations of the cores.

Six nodules were examined closely by optical microscopy, scanning electron microscopy (SEM) with dispersive energy spectroscopy (EDS), and X-ray diffraction (XRD). Inspection by optical microscopy of the nodules surfaces showed a dense and heterogeneous surface coating of a brown, filmy material along with minor occluded quartz grains (Fig 5). Nodules from location NG were generally smaller in size (ca. 0.01 to 1 cm) and more spherical in shape when compared with nodules from the SA core (ca. 0.05 to 2 cm; Fig 5).

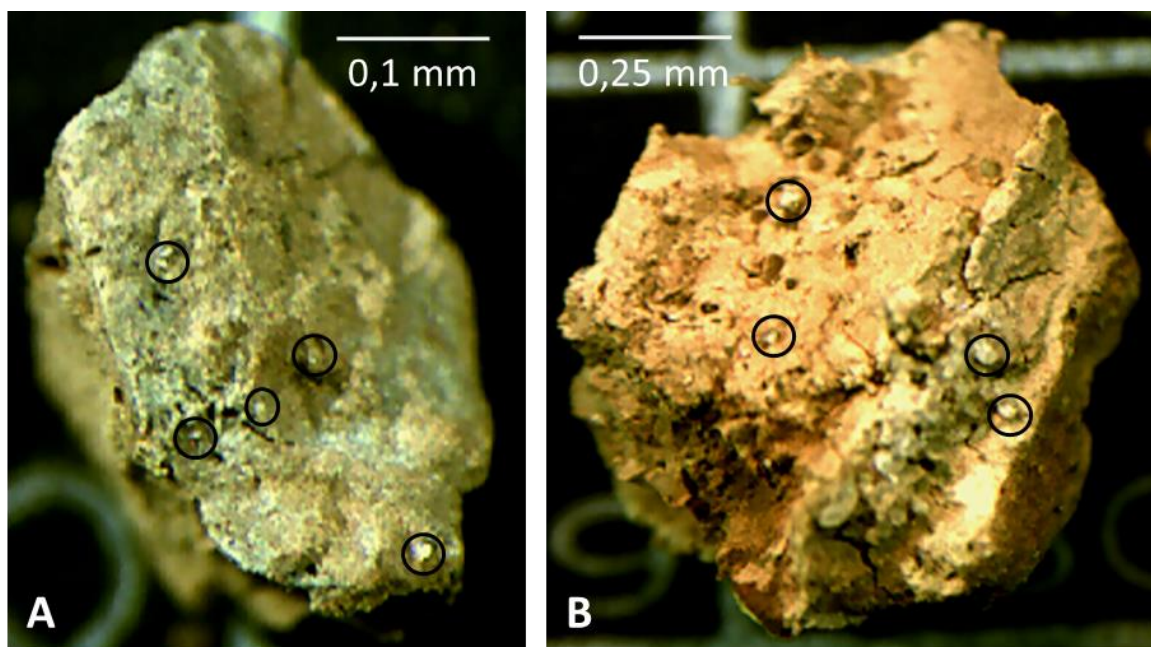


Figure 5 – Optical microscope images of the inner part of ferruginous nodules from the NG (A) and SA (B) cores, obtained from a depth of 17 cm. The nodules contain occluded quartz grains, examples of which are circled on each nodule sample. Magnification of 2.5x and 1.6x for NG and SA, respectively.

Examination by SEM clearly showed individual quartz grains occluded within what appears to be very fine-grained matrix with no obvious internal structure such as discrete layering (Fig 6A) as reported elsewhere (Gasparatos *et al.*, 2005). Energy dispersive spectroscopy of individual nodules reveals that they are largely composed of Fe, Si, Al, Ca, and Ti, with lesser amounts of Mg, K, and P (Fig 6B). Results from X-ray diffraction (Fig 6C) analyses indicate that the nodules are dominantly composed of quartz (SiO_2), along with minor amounts of muscovite ($\text{KAl}_2\text{Si}_3\text{AlO}_{10}(\text{OH})_2$), kaolinite ($\text{Al}_2\text{Si}_2\text{O}_5(\text{OH})_4$), and dickite ($\text{Al}_2\text{Si}_2\text{O}_5(\text{OH})_4$).

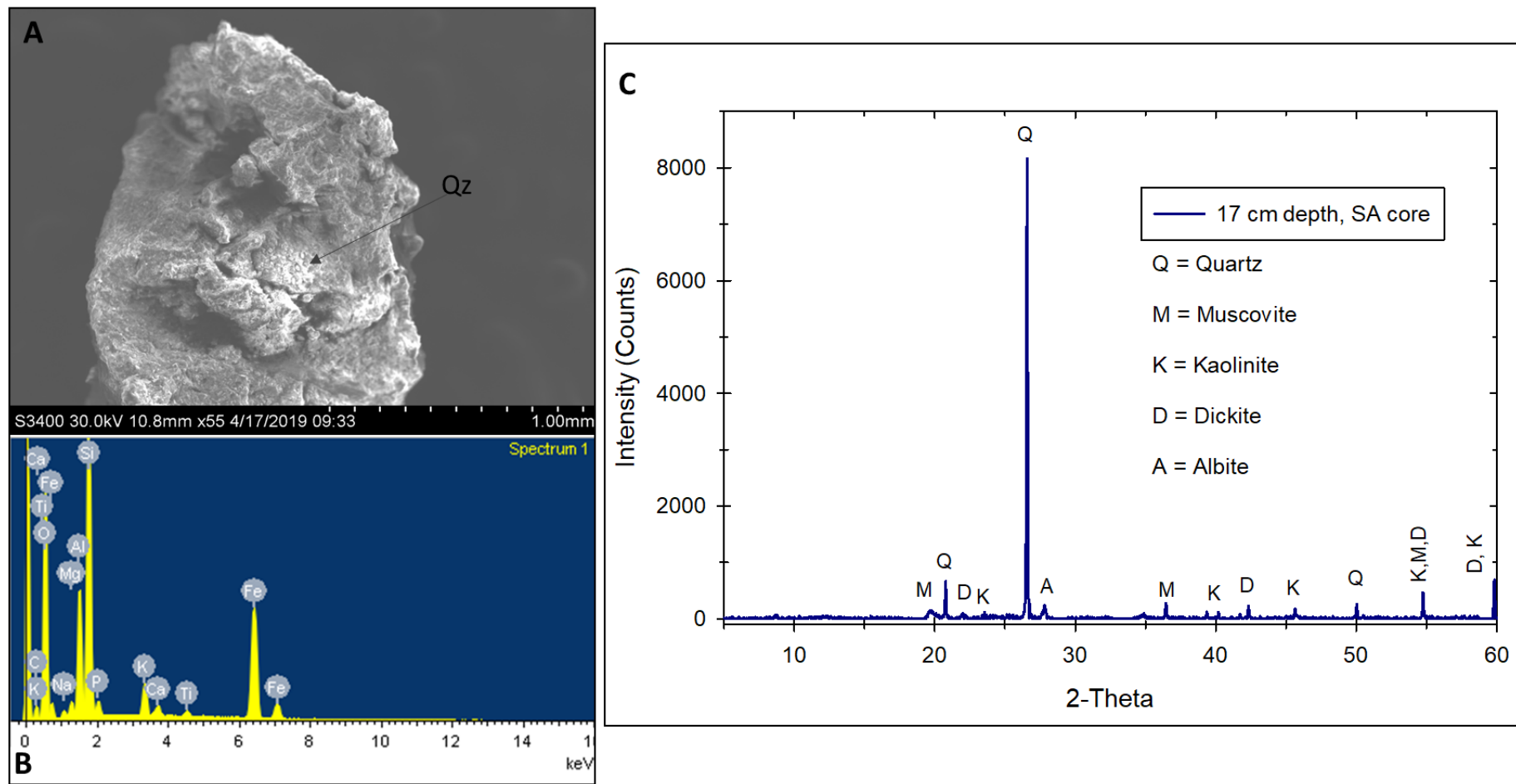


Figure 6 – Mineralogical characteristics of a nodule from 17 cm depth – SA location. A) SEM image shows no internal structure, Nevertheless, quartz grains (Qz) can be observed within the ferruginous nodule (arrow in panel A). B) EDS analysis shows high intensities of Fe, Si, Ca, Al, and Ti. C) X-ray diffraction analyses (XRD) indicate the presence of quartz, muscovite, kaolinite, dickite, and albite.

Nodules from the NG and SA core also contained albite ($(\text{Na}, \text{Ca})\text{Al}(\text{Si}, \text{Al})_3\text{O}_8$). Despite the abundance of Fe indicated by the SEM-EDS analysis, in conjunction with the brownish to orange color of the nodules, the XRD analysis did not reveal the presence of Fe(III)/Mn(IV) oxides/oxyhydroxides within the nodules. Because the XRD technique is commonly capable of detecting minerals that occur at abundances as low as 3 to 5% by weight, we interpret this result as indicating that Fe/Mn oxides/oxyhydroxides chiefly occur in these nodules as amorphous to poorly crystalline phases. The mineralogical composition as determined by XRD was similar for all nodules analyzed (*i.e.*, depths of 7, 12 and 17 cm) for both cores (NG and SA sites). Because the detection limit of the XRD method was on the order of ca. 4 wt. %, were also not able to detect or identify specific As mineral in the sediments. The mineral composition of ferruginous nodules from the NG and SA sediment cores are similar to what has been reported previously for similar nodules in salt marshes sediments (*e.g.*, Velde and Church, 1999; Velde and Barré, 2010).

Pore water chemistry

During the brackish water period, the pH of sediment pore water from the NG core varied from 7.2 to 8.0, whereas pH varied from 4.5 to 6.6 in pore waters from the SA core (Table 3; Fig 7). The mean pH values for the brackish water period for the NG site (7.6) and the SA site (5.6) indicates that pore water from the NG core is more alkaline than the pore waters from the SA core. In contrast, during the fresh water period the pH values of pore waters were similar at both locations, with a mean pH of 7.1 for the NG core was 7.1, and a mean pH of 7.2 for pore water from the SA core (Table 3; Fig 7). Arsenic concentrations were below detection (*i.e.*, $0.02 \mu\text{g kg}^{-1}$) in all of the pore water samples analyzed. Manganese exhibited similar concentrations in all of the pore waters analyzed (Table 3). For example, the mean \pm SD of Mn concentrations in the pore waters from the NG core for both the brackish and fresh water dominated periods was $0.2 \pm 0.2 \mu\text{g kg}^{-1}$ and $0.2 \pm 0.05 \mu\text{g kg}^{-1}$, respectively. The mean \pm SD Mn concentration for pore waters from the SA core was slightly higher; exhibiting a mean value for the period dominated by brackish waters of $0.6 \pm 0.2 \mu\text{g kg}^{-1}$.

Table 3 – Iron, manganese contents and pH for NG and SA pore water. The upper numbers are the concentration range, and the mean \pm SD for the entire core is presented within parentheses.

Parameter	NG		SA	
	Brackish water	Fresh Water	Brackish water	Fresh Water
pH	<u>7.2 – 8.0</u> (7.6 \pm 0.3)	<u>5.9 – 7.9</u> (7.1 \pm 0.5)	<u>4.5 – 6.6</u> (5.6 \pm 0.6)	<u>6.9 – 7.5</u> (7.2 \pm 0.2)
Fe ($\mu\text{g kg}^{-1}$)	<u>0.1 – 0.6</u> (0.3 \pm 0.1)	<u>2.4 – 49.9</u> (14.8 \pm 17.9)	<u>0.4 – 60.9</u> (41.1 \pm 14.8)	<u>1.1 – 11.3</u> (5.9 \pm 3.2)
Mn ($\mu\text{g kg}^{-1}$)	<u>0.02 – 0.7</u> (0.2 \pm 0.2)	<u>0.1 – 0.3</u> (0.2 \pm 0.05)	<u>0.2 – 0.9</u> (0.6 \pm 0.2)	<u>0.1 – 0.3</u> (0.2 \pm 0.04)
As ($\mu\text{g kg}^{-1}$)	<u>< 0.02</u>	<u>< 0.02</u>	<u>< 0.02</u>	<u>< 0.02</u>

An outstanding feature of the pore water Fe concentration data for the two sites is that the relative concentrations exhibited differential behavior. Specifically, the highest Fe concentrations for NG core pore waters were observed during the fresh water period, $49.9 \mu\text{g kg}^{-1}$, which was ca. 83-fold higher than the pore water Fe concentrations (*i.e.*, $0.6 \mu\text{g kg}^{-1}$) that occurred when brackish water dominated the estuary. In contrast, the highest Fe concentration in SA core pore water occurred during the brackish period, $60.9 \mu\text{g kg}^{-1}$, when Fe was ca. 5.4 times higher than during the fresh water period ($11.3 \mu\text{g kg}^{-1}$).

Pore water concentrations versus depth profiles for Fe, Mn, and pH for both the SA and NG site are presented in Fig. 7. Vertical distributions of pore water pH, Fe, and Mn concentrations are similar at the NG site for both periods (Fig 7). For each sampling period (*i.e.*, brackish and fresh water) the pore water pH, Fe, and Mn concentrations exhibit overall increases with depth in the NG sediments. The Fe and Mn concentrations are considerably lower for pore waters extracted from the sediments at the top of the core, revealing subsurface Fe and Mn minima for the top 5 cm that are observed for both sampling periods. Greater differences in Fe and Mn concentrations between the core top and bottom sediments also characterize the pore waters from the NG location.

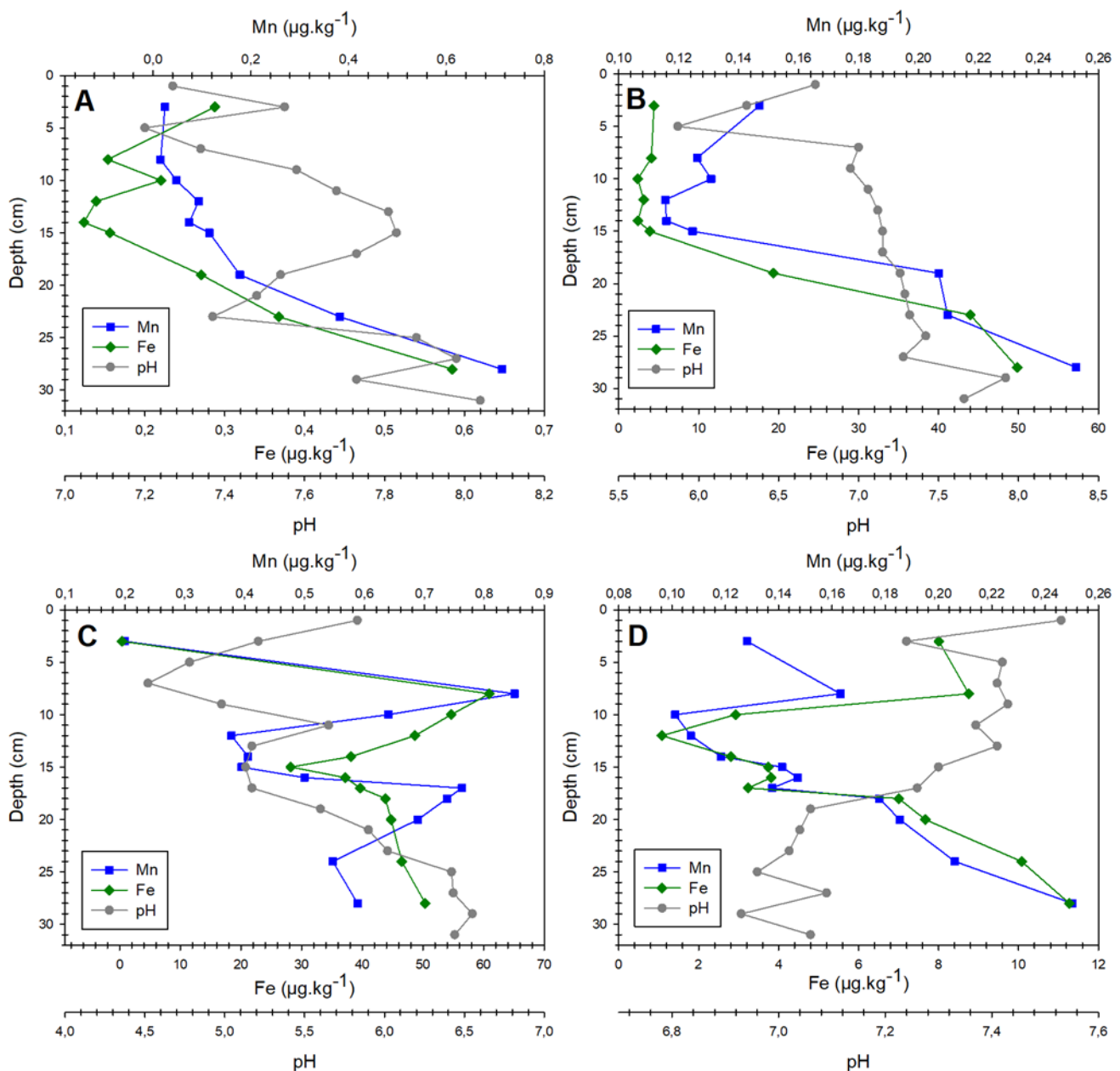


Figure 7 –pH, Mn, and Fe concentrations in pore water as a function of depth at sites for sediment cores collected in Pólvora Island. A: NG core collected during brackish water period. B: NG core collected during fresh water period. C: SA core collected during brackish water period. D: SA core collected during fresh water period.

Although, Fe and Mn concentration initially decrease or remain relatively constant between 5 and 15 cm in NG pore waters, both subsequently increase dramatically at depths greater than 20 cm (Fig 7). For core SA similarities are less notable, as both brackish and fresh water cores exhibit concentration peaks in Mn and Fe content at a depth of 8 cm (Fig 7), where pH decreases, especially for the brackish water period.

Lower pore water Mn and Fe concentrations occur at depths of ca. 12-15 cm in the SA core. Pore water concentrations of both Fe and Mn exhibit substantial increases at depths below 18 cm in the SA core when fresh water dominates the estuary (Fig 7).

Discussion

Controls on As distribution in salt marshes sediments

The relatively high Eh values that characterize sediments from the NG core (*i.e.*, positive values) are consistent with the activity and presence of the *N. granulata* crabs species, whereby their burrow structures enlarge the area of oxic interfaces within the saltmarsh sediments by 20 to 60%, or more (Gribsholt *et al.*, 2003). Taylor and Allanson (1993) showed that *N. granulata* burrows generally extend from 3 to 25 cm into the sediment, which is in agreement with observations at our study site (Costa *et al.*, 2019). Again, the Fe (III) oxide/oxyhydroxide nodules rich sediment at the NG core location occur at depths between 0 and 21 cm, and thus within the depth range of the abundant *N. granulata* burrows. For the SA core the measured Eh values were generally lower (*i.e.*, $Eh < 0$ mV), indicating a more reducing sediment environment. We suggest that the lower Eh values of the SA core reflects the presence of living *S. alterniflora* roots and the associated rhizomes that supply organic matter to the sediment through root excretion of dissolved organic carbon, as well as fermentation products from anaerobic root metabolism where sulfate reducers, create a reduced environment (Hikes *et al.*, 1999).

The lower percentages of ferruginous sediment nodules at the NG core location (up to 8.5% for SA core samples compared to at most 5.8% for NG core samples) can be explained by the burrow excavation by *N. granulata*. Moreover, material from the oxic surface sediment layers (including nodules) can be transferred via gravitational settling into the deeper, more reducing zones within the sediments by the activity of these burrowing crabs (Krantzberg, 1985; Montague, 2013). That is, gravitational settling of the Fe (III) oxide/oxyhydroxide-rich nodules via burrows and/or active crab burrowing can subsequently promote the dissolution of the nodules in the deeper, sediment suboxic zone.

High arsenic contents were previously reported in salt marsh sediments where iron-rich nodules are common, especially around plant roots (Sanders and Osman, 1985; Vale *et al.*, 1990; Caetano and Vale, 2002; Costa *et al.*, 2017). Vale *et al.*, (1990)

demonstrated that salt marsh sediments of the Tagus Estuary are enriched in metals, and in particular Fe (110 g kg^{-1}) and Mn ($1496 \mu\text{g g}^{-1}$). Indeed, Gasparatos (2013) and Kalyvas (2018) showed that similar Fe-rich nodules can be enriched 30–60 times in Mn with respect to the host sediment, and moderately enriched in Fe. In addition to Fe, our analyses reveal that Mn is also an important component of the nodules we collected from both locations in Pólvora Island ($116 \text{ mg kg}^{-1} \leq \text{Mn} \leq 593 \text{ mg kg}^{-1}$ for the NG site, and $142 \text{ mg kg}^{-1} \leq \text{Mn} \leq 460 \text{ mg kg}^{-1}$ for the SA location). Moreover, high As and Fe contents (up to 172 mg kg^{-1} for As, and up to 162 g kg^{-1} for Fe) characterize the sediments from the SA core, which can be explained by oxygen released from *S. alterniflora* roots, which has been reported to lose significant amounts of oxygen to its rhizosphere with potentially important effects on salt marsh biogeochemical cycling (Mendelssohn *et al.*, 1981; Howes and Teal, 1994).

The aerenchyma tissue in the *S. alterniflora* conveys sufficient oxygen to roots and rhizomes, for predominately aerobic respiration, in moderately reduced substrates (Mendelssohn *et al.*, 1981). Researchers have shown that oxygen transport to *S. alterniflora* roots through the lacunae commonly exceeds respiratory demands, whereby the "excess" O_2 can exit the root system, thereby oxidizing the rhizosphere (Howes and Teal, 1994). The O_2 that leaves the root system subsequently oxidizes Fe minerals within the sediments, thereby releasing Fe and As into the pore waters. Consequently, if Fe (III) precipitates as oxides/oxyhydroxides in the micro oxic zone around the roots of *S. alterniflora*, it can retain As by sorption and/or coprecipitation in the sediments.

The positive correlation reported herein between the As and Fe contents of the NG core nodules is consistent with results from previous studies of salt marsh geochemistry (*e.g.*, Y. Wang *et al.*, 2012; Costa *et al.*, 2017). More specifically, the close coupling of As and Fe reflects similarities in their redox cycling (Moore *et al.*, 1988; Masschelein *et al.*, 1991; Chaillou *et al.*, 2003; Dixit and Hering, 2003). In contrast, we did not observe a positive correlation between As and Fe in ferruginous nodules collected from the SA sediment core. We suggest that the lack of correlation between As and Fe in the ferruginous nodules from the *S. alterniflora* sediment core (SA site) reflects the fact that the redox cycle of Fe is controlled not only by sediment oxidation but also by sulfate reduction in these sediments (Kostka and Luther, 1995). Iron and S redox cycling can have differential effects on As because oxidation of Fe(II) followed by precipitation of Fe(III) oxides/oxyhydroxides will favor removal of As from solution via adsorption and/or coprecipitation, whereas sulfate reduction may enhance As mobility in solution by

formation of thioarsenic species (Dixit and Hering, 2003; Planer-Friedrich *et al.*, 2007; Stucker *et al.*, 2014). Additionally, for salt marshes occupied by *S. alterniflora* it is commonly observed that the majority of solid Fe is cycled rapidly and completely between oxidized reactive Fe and reduced Fe as pyrite, which may also confound relationships between As and Fe in salt marsh sediments (Kostka and Luther, 1995).

Our study shows that the highest As, Fe, and Mn content of Pólvora Island sediments occur at a depth of ca. 15 cm for both sampling sites (Fig 4). We note that similar accumulations of As in marsh/estuarine sediments to depths of ca. 20 cm have been observed elsewhere (*e.g.*, Caetano and Vale, 2002; O'Day *et al.*, 2004; Costa *et al.*, 2017). Kostka and Luther (1995) reported that the zone where reactive Fe (III) is available in the sediments from a salt marsh in Delaware (USA) extended to a depth of at least 20–25 cm. Because Fe is an important, redox-active component in geochemical process (*e.g.*, Luther *et al.*, 1992), we propose that normalizing the As content by the sediment Fe content provides a tool for evaluating the relative As distribution with depth in such sediments. The increase in the percentage of Fe-rich nodules in the NG and SA cores is plotted versus the normalized As/Fe ratio in Fig. 8. Both parameters exhibit local maxima at a depth of ca. 15 cm (Fig 8), suggesting that pore water As is captured by adsorption onto and/or coprecipitation with authigenic Fe(III) oxides/oxyhydroxides at this depth in the Pólvora Island salt marsh sediments (Chaillou *et al.*, 2003).

Unlike the NG core sediments where nodules occur at the core top, nodules in the SA core are not found above a depth of 8 cm in the sediments. This observation likely reflects strong acidification of pore water at the SA site (Table 3; Fig 7). Previously, we showed that water-soluble sulfide concentrations increase between depths of 0 to 8 cm at the SA site when brackish water dominates the Patos Lagoon marshes occupied by *Spartina* species (Mirlean and Costa, 2017). Kostka and Luther (1995) argued that for salt marshes occupied by *S. alterniflora*, the precipitation of amorphous Fe (III) oxides/oxyhydroxides is hindered in surface sediments and for depths greater than 25 cm. In the salt marsh on Pólvora Island, occupied by *N. granulata*, there is no *S. alterniflora*, and consequently there is no redox cycling driven by *S. alterniflora* and its associated roots and rhizosphere. Hence, pore water composition commonly reflects the conditions at the surface of the NG sites, which means that during the brackish period, sediment Eh is expected to be higher (*i.e.*, positive values at location NG; Table 2), and pH should be ca. 6 for the NG marsh location (Fig 7A,B; Mirlean and Costa, 2017).

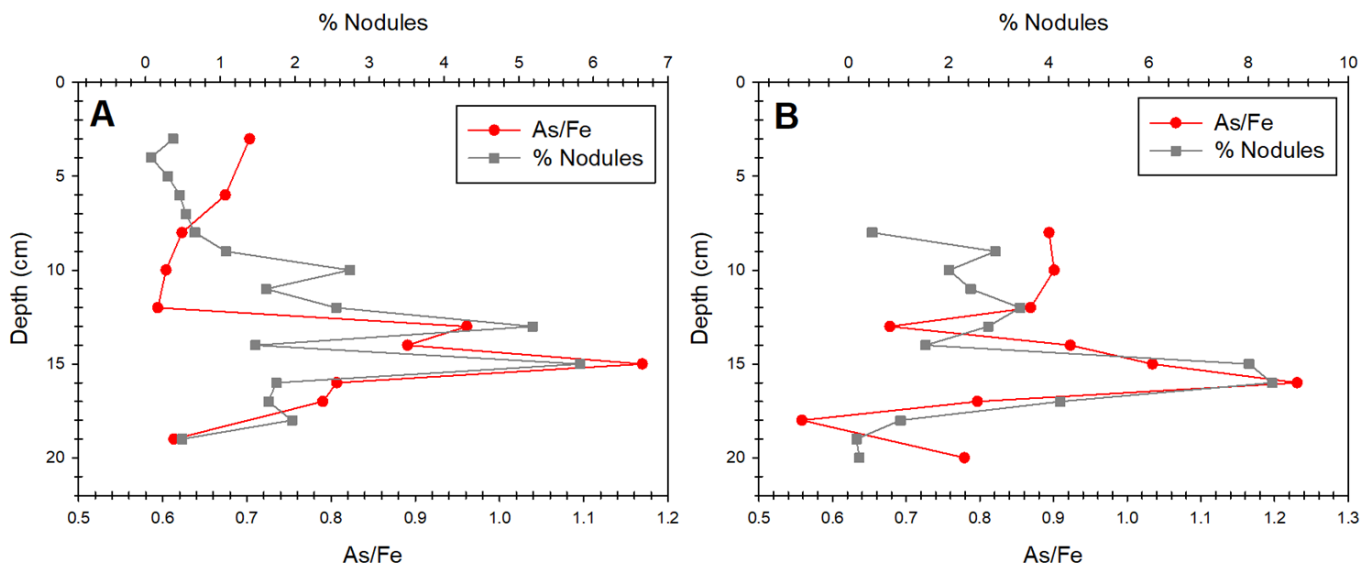


Figure 8 –Arsenic content in sediment nodules normalized by iron content and the percentage of nodules as functions of depth for sites NG (A) and SA (B).

Furthermore, XRD analysis performed on nodules supported our results that Fe is released by dissolution of amorphous Fe(III) oxides/oxyhydroxides. The presence of amorphous Fe(III) oxides/oxyhydroxides suggests rapid redox cycling of Fe in response to changes in pore water Eh and pH (Kostka and Luther, 1995). The absence of any obvious internal structure for all the ferruginous nodules examined herein by SEM (Fig 6) is in agreement with the study from Norman *et al.* (1996), where it was suggested that irregularly shaped nodules lacked well-developed banding of Fe and Mn. The absence of Fe and Mn banding within the ferruginous nodules collected from the Pólvora Island cores also supports the notion of a rapid Fe (and Mn) redox cycle, which is consistent with constant exposure of the sediments to a supply of organic carbon produced by plants roots, and oxygen provided by the atmosphere (*i.e.*, crabs borrows) and tidal waters (Luther *et al.*, 1992; Kostka and Luther, 1995).

The mineralogy of the ferruginous nodules collected from Pólvora Island salt marsh sediments (*i.e.*, chiefly quartz, phyllosilicates, and feldspars) is similar to Fe–Mn nodules studied by Szymański *et al.* (2014), which revealed the predominance of silicate minerals. The similar mineral composition of the Fe–Mn nodules (shown in Fig 6) and bulk sediment material from the Pólvora Island salt marsh sediments and other marshes within the Patos Lagoon estuarine system (Mirlean *et al.*, 2003) indicates that the nodules

were formed in situ owing to redox cycling of Fe- and Mn-oxides/oxyhydroxides (Szymański *et al.*, 2014).

Pore water redox cycling

Because the burrow structures of the *N. granulata* crab increase the surface area of oxic interfaces within the saltmarsh sediments to depths of ca. 25 cm, high Fe concentrations in the associated pore waters are not expected. As such the pore waters from the NG sediment cores (*i.e.*, for both the brackish water and fresh water periods) exhibit low Fe and Mn concentrations in the upper part of the cores, but increase below a depth of 17 cm, attaining the highest concentrations at 27 cm depth (Fig 7). These results are in agreement with the As contents that can be explained by upward diffusion that is subsequently captured by adsorption onto and/or coprecipitation with authigenic Fe(III)/Mn(IV) oxides/oxyhydroxides that form at, or just above, the oxic/suboxic boundary (15 cm depth) in these sediments. Higher concentrations of Fe and Mn in the pore water are, therefore, associated with a suboxic environment in the sediments.

Our study also reveals that lower Fe concentrations occur in the pore waters from the NG location when brackish water predominates in the estuary. These relatively lower pore water Fe concentrations likely reflect the continuous penetration of oxygen-rich surface waters that occurs when seawater inundates the estuary during the summer and fall (brackish period; Moller *et al.*, 1996; Marques *et al.*, 2010). In other words, the flooding of the estuary with seawater helps to maintain oxic conditions within the sediments. Costa *et al.* (2003) reported Eh values between +46 and +371 mV in this saltmarsh in the brackish period, in agreement with the Eh results of this study (Table 2). In contrast, when the Patos Lagoon estuary is flushed with high levels of fresh water (0–5) with lower dissolved oxygen concentrations during the fresh water period, sediment pore waters commonly exhibit negative Eh values and higher Fe concentrations (Costa *et al.*, 2003).

Gribsholt *et al.* (2003) reported that bioturbated, unvegetated salt marsh sediments, such as those from the NG location, had pore waters with relatively constant pH values as a function of depth. The pore water pH for unvegetated salt marsh should be similar to the pH range of the overlying, surface estuarine waters ($6.5 \leq \text{pH} \leq 8.5$; Gribsholt *et al.*, 2003), which is in agreement with the pH values we measured in pore waters from the NG location during both periods (Table 3, Fig 7). Costa *et al.* (2003) reported that the pH of pore waters from the same salt marsh ranged between 5.4 and 7.4

during the period when brackish water dominated the estuary, and between 6.1 and 8.5 when fresh water was predominant. Gribsholt *et al.* (2003) have also pointed out that low sulfate-reduction rates occurred adjacent to the walls of burrow constructed by the *N. granulata* crabs, and therefore pore water acidification is not expected and pH values for both periods should be similar. Thus, the Fe concentrations in pore waters extracted from the NG cores reflect variations in redox conditions in the sediments, driven by shifting between brackish and fresh water periods that characterizes this choked estuary.

However, during the active growing season, *S. alterniflora* appears to have a greater impact on sediment and pore water geochemistry than the variable hydrologic regime. For example, Kostka and Luther (1995) pointed that during active growth of *S. alterniflora* (during spring and summer), sulfate reduction was stimulated and the underlying sediments were supplied with sufficient oxidants to cause the rapid turnover of sulfide. Furthermore, these vegetated sediments released Fe(II) into the upper pore waters, which corresponded to a large decrease in pore water pH at the beginning of the *S. alterniflora* growth season, providing further evidence of sulfide oxidation (Clarke 1978; Kostka and Luther, 1995). Hines *et al.* (1989) also showed that sulfate reduction rates respond quickly to changes in salt marsh plant physiology.

The period when brackish water dominates (summer and beginning of fall) at Pólvora Island also corresponds to the *S. alterniflora* growth season (Marangoni and Costa, 2012). Our results show lower pH values of pore waters during the brackish water period (Table 3), where the lowest values are found at depths of 5 and 7 cm where pH values are 4.78 and 4.52, respectively. Moreover, Mirlean and Costa (2017) demonstrated that pH was substantially lower (< 4) in pore waters from salt marsh sediments vegetated by *S. densiflora* during the brackish water period. Such low pH values may, in part, be responsible for the dissolution of Fe(III) oxides/oxyhydroxides, which is consistent with the higher pore water Fe concentrations measured during the brackish water period. The dissolution of Fe(III) oxides/oxyhydroxides may also be responsible for the release of As that subsequently could migrate down to a depth of 15 cm where it undergoes adsorption onto Fe oxides/oxyhydroxides nodules that are enriched in As at this depth (Fig 8). Iron contents peak at 7 cm depth for the brackish period for core SA (Fig 7), are in agreement with what was reported by Kostka and Luther (1995), whereby Fe(II) displayed a seasonal average in vegetated pore waters to 12.5 cm depth, and higher concentrations were associated with sulfide oxidation at shallower depths. Gribsholt *et al.* (2003) also reported

that pore water pH can be as low as 5.4 in the rhizosphere zone of vegetated marsh sediments.

Hence, lower pore water pH values in the rhizosphere zone may be responsible for the local high Fe and Mn concentrations in pore water from the SA core during both periods (*i.e.*, brackish and fresh water dominant periods), whereas the slightly higher Fe concentrations of pore waters collected during the brackish water period could be a response to sediment acidification. The lower Mn and Fe concentrations measured at depths of ca. 12-15 cm in pore waters from the SA core likely reflect precipitation of authigenic Fe(III)/Mn(IV) oxides/oxyhydroxides that occurs at a depth of 15 cm. Furthermore, the increase in Fe and Mn content at depths greater than 23 cm are the result of the more reduced environment at the base of the sediment core, where Fe is likely retained in sulfide minerals like amorphous pyrite, and Mn may be sequestered in carbonates (Dellwig *et al.*, 2019).

Conclusion

The geochemistry of As in salt marshes of Pólvora Island is strongly affected by the Fe redox cycle in sediments with abundant populations of the crab, *N. granulata*, and it is also influenced by Mn redox cycling in locations occupied by *S. alterniflora*. Nodules in the salt marsh sediments are generally concentrated in the surface oxic layer of the sediment, which can reach depths as great as 20 cm below the sediment surface. These sediment nodules are largely composed of Fe and Mn oxides/oxyhydroxides and are the chief reservoir of As in the marsh sediments. Nearly all of the Fe-Mn oxides/oxyhydroxides extracted from the Pólvora Island sediments appear to be amorphous, which is consistent with the fast response of the Fe-Mn oxides/oxyhydroxides to geochemical changes within the estuary.

We present evidence that the redox cycle of Fe in the pore water is controlled by sediment oxidation-reduction reactions, but may also be driven in part by changes in pH. The Fe cycle also responds differently to seasonal changes in salt marshes occupied by *N. granulata* (crab) compared to salt marshes dominated by *S. alterniflora*. More specifically, Fe cycling exhibits a greater response to salinity variations in salt marshes occupied by *N. granulata*, whereas changes in pore water pH plays a greater role in the Fe cycling in salt marshes occupied by *S. alterniflora*. Therefore, the physiology of *Spartina* sp. has an important effect on the Fe cycle compared to changes in salinity.

Acknowledgments

This study was supported by grant from “Coordenação de Aperfeiçoamento de Pessoal de Nível Superior – Brasil” (CAPES), as well as funds made available by Michael and Mathilda Cochran through the Cochran Family Professorship at Tulane University. We are also grateful to Dr. Deborah Grimm with the Coordinated Instrumentation Facility at Tulane University for assistance with the ICP-MS analyses.

References

- Bai, J. *et al.* (2012) ‘Arsenic and heavy metal pollution in wetland soils from tidal freshwater and salt marshes before and after the flow-sediment regulation regime in the Yellow River Delta, China’, *Journal of Hydrology*. doi: 10.1016/j.jhydrol.2012.05.006.
- Berner, R. A. (1981) ‘A New Geochemical Classification of Sedimentary Environments’, *Journal of Sedimentary Petrology*. doi: 10.1306/212F7C7F-2B24-11D7-8648000102C1865D.
- Bhattacharyya, R. *et al.* (2003) ‘High arsenic groundwater: Mobilization, metabolism and mitigation - An overview in the Bengal Delta Plain’, *Molecular and Cellular Biochemistry*. doi: 10.1023/A:1026001024578.
- Burone, L., Muniz, P., Pires-Vanin, A. M. S., Rodrigues, M.. (2003) 'Spatial distribution of organic matter in the surface sediments of Ubatuba Bay (Southeastern - Brazil)'. *Anais da Academia Brasileira de Ciências*, 75(1), 77-80. doi:10.1590/S0001-37652003000100009
- Buschmann, J. *et al.* (2006) ‘Arsenite and arsenate binding to dissolved humic acids: Influence of pH, type of humic acid, and aluminum’, *Environmental Science and Technology*. doi: 10.1021/es061057+.
- Caetano, M. and Vale, C. (2002) ‘Retention of arsenic and phosphorus in iron-rich concretions of Tagus salt marshes’, *Marine Chemistry*. doi: 10.1016/S0304-4203(02)00068-3.
- Chaillou, G. *et al.* (2003) ‘The behaviour of arsenic in muddy sediments of the Bay of Biscay (France)’, *Geochimica et Cosmochimica Acta*. doi: 10.1016/S0016-7037(03)00204-7.
- Costa, C. S. B., Marangoni, J. C. and Azevedo, A. M. G. (2003) ‘Plant zonation in irregularly flooded salt marshes: Relative importance of stress tolerance and biological interactions’, *Journal of Ecology*. doi: 10.1046/j.1365-

2745.2003.00821.x.

- Costa, L., Mirlean, N. and Garcia, F. (2017) ‘Arsenic Environmental Threshold Surpass in Estuarine Sediments: Effects of Bioturbation’, *Bulletin of Environmental Contamination and Toxicology*, 98(4), pp. 521–524. doi: 10.1007/s00128-016-2024-z.
- Cullen W. R. and Reimer K. J. (1989) Arsenic speciation in the environment. *Chem. Rev.* **89**, 713-764.
- Dellwig O., Wegwerth A., Schnetger B., Schulz H., and Arz H. W. (2019) Dissimilar behaviors of the geochemical twins W and Mo in hypoxic-euxinic marine basins. *Earth-Sci. Rev.* **193**, 1-23.
- D’Incao, F. *et al.* (1992) ‘Responses of Chasmagnathus granulata Dana (Decapoda: Grapsidae) to salt-marsh environmental variations’, *Journal of Experimental Marine Biology and Ecology*. doi: 10.1016/0022-0981(92)90095-R.
- Dixit, S. and Hering, J. G. (2003) ‘Comparison of arsenic(V) and arsenic(III) sorption onto iron oxide minerals: Implications for arsenic mobility’, *Environmental Science and Technology*. doi: 10.1021/es030309t.
- Ferreira, T. O. *et al.* (2007) ‘Effects of bioturbation by root and crab activity on iron and sulfur biogeochemistry in mangrove substrate’, *Geoderma*. doi: 10.1016/j.geoderma.2007.07.010.
- Gasparatos, D. *et al.* (2005) ‘Microscopic structure of soil Fe-Mn nodules: Environmental implication’, *Environmental Chemistry Letters*. doi: 10.1007/s10311-004-0092-5.
- Gasparatos, D. (2013) ‘Sequestration of heavy metals from soil with Fe-Mn concretions and nodules’, *Environ. Chemistry Letters*. doi: 10.1007/s10311-012-0386-y.
- Gasparatos, D., Massas, I. and Godelitsas, A. (2019) ‘Fe-Mn concretions and nodules formation in redoximorphic soils and their role on soil phosphorus dynamics: Current knowledge and gaps’, *Catena*. doi: 10.1016/j.catena.2019.104106.
- Gong, W., Shen, J. and Reay, W. G. (2007) ‘The hydrodynamic response of the York River estuary to Tropical Cyclone Isabel, 2003’, *Estuarine, Coastal and Shelf Science*. doi: 10.1016/j.ecss.2007.03.012.
- Gribsholt, B., Kostka, J. E. and Kristensen, E. (2003) ‘Impact of fiddler crabs and plant roots on sediment biogeochemistry in a Georgia saltmarsh’, *Marine Ecology Progress Series*. doi: 10.3354/meps259237.
- Gutiérrez, J. L. *et al.* (2006) ‘The contribution of crab burrow excavation to carbon

- availability in surficial salt-marsh sediments', *Ecosystems*. doi: 10.1007/s10021-006-0135-9.
- HACH, C. (2007) 'DR 2800 Spectrophotometer User Manual', *Hach Company*. doi: 10.3928/01477447-20101221-06; 10.3928/01477447-20101221-06.
- He, Y. T. *et al.* (2010) 'Geochemical processes controlling arsenic mobility in groundwater: A case study of arsenic mobilization and natural attenuation', *Applied Geochemistry*. doi: 10.1016/j.apgeochem.2009.10.002.
- Hikes, M. E. *et al.* (1999) 'Molecular phylogenetic and biogeochemical studies of sulfate-reducing bacteria in the rhizosphere of *Spartina alterniflora*', *Applied and Environmental Microbiology*.
- Hines, M. E., Knollmeyer, S. L. and Tugel, J. B. (1989) 'Sulfate reduction and other sedimentary biogeochemistry in a northern New England salt marsh', *Limnology and Oceanography*. doi: 10.4319/lo.1989.34.3.0578.
- Howes, B. L. and Teal, J. M. (1994) 'Oxygen loss from *Spartina alterniflora* and its relationship to salt marsh oxygen balance', *Oecologia*. doi: 10.1007/BF00325879
- Iribarne, O. *et al.* (2000) 'The role of burrows of the SW Atlantic intertidal crab *Chasmagnathus granulata* in trapping debris', *Marine Pollution Bulletin*. doi: 10.1016/S0025-326X(00)00058-8.
- Javed, M. B., Kachanowski, G. and Siddique, T. (2014) 'Arsenic fractionation and mineralogical characterization of sediments in the Cold Lake area of Alberta, Canada', *Science of the Total Environment*. doi: 10.1016/j.scitotenv.2014.08.083.
- Kalyvas, G., Gasparatos, D. and Massas, I. (2018) 'A critical assessment on arsenic partitioning in mine-affected soils by using two sequential extraction protocols', *Archives of Agronomy and Soil Science*. doi: 10.1080/03650340.2018.1443443.
- Kjerfve, B. (1994) 'Coastal Lagoons', *Elsevier Oceanography Series*. doi: 10.1016/S0422-9894(08)70006-0.
- Kostka, J. E. and Luther, G. W. (1995) 'Seasonal cycling of Fe in saltmarsh sediments', *Biogeochemistry*. doi: 10.1007/BF00000230.
- Krantzberg, G. (1985) 'The influence of bioturbation on physical, chemical and biological parameters in aquatic environments: A review', *Environmental Pollution. Series A, Ecological and Biological*. doi: 10.1016/0143-1471(85)90009-1.
- Du Laing, G. *et al.* (2002) 'Heavy metal contents (Cd, Cu, Zn) in spiders (*Pirata piraticus*) living in intertidal sediments of the river Scheldt estuary (Belgium) as affected by substrate characteristics', *Science of the Total Environment*. doi: 10.1016/S0048-

9697(01)01025-7.

- Du Laing, G. *et al.* (2007) ‘Factors affecting metal concentrations in the upper sediment layer of intertidal reedbeds along the river Scheldt’, *Journal of Environmental Monitoring*. doi: 10.1039/b618772b.
- Du Laing, G. *et al.* (2008) ‘Effect of salinity on heavy metal mobility and availability in intertidal sediments of the Scheldt estuary’, *Estuarine, Coastal and Shelf Science*. doi: 10.1016/j.ecss.2007.10.017.
- Larios, R., Fernández-Martínez, R. and Rucandio, I. (2012) ‘Comparison of three sequential extraction procedures for fractionation of arsenic from highly polluted mining sediments’, *Analytical and Bioanalytical Chemistry*. doi: 10.1007/s00216-012-5730-3.
- Luther, G. W. *et al.* (1992) ‘Seasonal iron cycling in the salt-marsh sedimentary environment: the importance of ligand complexes with Fe(II) and Fe(III) in the dissolution of Fe(III) minerals and pyrite, respectively’, *Marine Chemistry*. doi: 10.1016/0304-4203(92)90049-G.
- Marangoni, J. C. and Costa, C. S. B. (2012) ‘Short- and Long-Term Vegetative Propagation of Two Spartina Species on a Salt Marsh in Southern Brazil’, *Estuaries and Coasts*. doi: 10.1007/s12237-011-9474-7.
- Marques, W. C. *et al.* (2010) ‘Dynamics of the Patos Lagoon coastal plume and its contribution to the deposition pattern of the southern Brazilian inner shelf’, *Journal of Geophysical Research: Oceans*, 115(10). doi: 10.1029/2010JC006190.
- Masscheleyn, P. H., Delaune, R. D. and Patrick, W. H. (1991) ‘Effect of Redox Potential and pH on Arsenic Speciation and Solubility in a Contaminated Soil’, *Environmental Science and Technology*. doi: 10.1021/es00020a008.
- Mendelssohn, I. A., McKee, K. L. and Patrick, W. H. (1981) ‘Oxygen deficiency in *Spartina alterniflora* roots: Metabolic adaptation to anoxia’, *Science*. doi: 10.1126/science.214.4519.439.
- Mermilliod-Blondin, F. (2011) ‘The functional significance of bioturbation and biodeposition on biogeochemical processes at the water–sediment interface in freshwater and marine ecosystems’, *Journal of the North American Benthological Society*. doi: 10.1899/10-121.1.
- Mirlean, N. *et al.* (2003) ‘Arsenic pollution in Patos Lagoon estuarine sediments, Brazil’, *Marine Pollution Bulletin*. doi: 10.1016/S0025-326X(03)00257-1
- Mirlean, N. and Costa, C. S. B. (2017) ‘Geochemical factors promoting die-back gap

- formation in colonizing patches of *Spartina densiflora* in an irregularly flooded marsh', *Estuarine, Coastal and Shelf Science*. doi: 10.1016/j.ecss.2017.03.006.
- Moller, O. O. *et al.* (1996) 'The Patos Lagoon summertime circulation and dynamics', *Continental Shelf Research*. doi: 10.1016/0278-4343(95)00014-R.
- Montague, C. L. (2013) 'The influence of fiddler crab burrows and burrowing on metabolic processes in salt marsh sediments', in *Estuarine Comparisons*. doi: 10.1016/b978-0-12-404070-0.50023-5.
- Moore, J. N., Ficklin, W. H. and Johns, C. (1988) 'Partitioning of Arsenic and Metals in Reducing Sulfidic Sediments', *Environmental Science and Technology*. doi: 10.1021/es00169a011.
- Nickson, R. T. *et al.* (2000) 'Mechanism of arsenic release to groundwater, Bangladesh and West Bengal', *Applied Geochemistry*. doi: 10.1016/S0883-2927(99)00086-4.
- Nordstrom D. K. and Archer D. G. (2003) Arsenic thermodynamic data and environmental geochemistry. In: Welch, A. H., Stollenwerk, K. G. (eds.) *Arsenic in Ground Water: Geochemistry and Occurrence*. Kluwer Academic Press, Boston, pp. 1-25.
- Nordstrom D. K., Majzlan J., and Königsberger E. (2014) Thermodynamic properties of arsenic minerals and aqueous species. *Rev. Mineral. Geochem.* **79**, 217-255.
- Norman White, G. and Dixon, J. B. (1996) 'Iron and manganese distribution in nodules from a young Texas vertisol', *Soil Science Society of America Journal*. doi: 10.2136/sssaj1996.03615995006000040042x
- Northrup, K., Capooci, M. and Seyfferth, A. L. (2018) 'Effects of Extreme Events on Arsenic Cycling in Salt Marshes', *Journal of Geophysical Research: Biogeosciences*. doi: 10.1002/2017JG004259.
- O'Day, P. A. *et al.* (2004) 'The influence of sulfur and iron on dissolved arsenic concentrations in the shallow subsurface under changing redox conditions', *Proceedings of the National Academy of Sciences*. doi: 10.1073/pnas.0402775101.
- Pierce M. L. and Moore C. B. (1982) Adsorption of arsenite and arsenate on amorphous iron hydroxide. *Water Res.* **16**, 1247-1253.
- Planer-Friedrich, B. *et al.* (2007) 'Thioarsenates in geothermal waters of yellowstone National Park: Determination, preservation, and geochemical importance', *Environmental Science and Technology*. doi: 10.1021/es070273v.
- Ravenscroft, P., Brammer, H. and Richards, K. (2009) *Arsenic Pollution: A Global Synthesis*, *Arsenic Pollution: A Global Synthesis*. doi: 10.1002/9781444308785.

- Rosa, L. C. and Bemvenuti, C. E. (2005) 'Effects of the burrowing crab *Chasmagnathus granulata* (Dana) on meiofauna of estuarine intertidal habitats of Patos Lagoon, Southern Brazil', *Brazilian Archives of Biology and Technology*. doi: 10.1590/S1516-89132005000200014.
- Sadiq, M. (1997) 'Arsenic chemistry in soils: An overview of thermodynamic predictions and field observations', *Water, Air, and Soil Pollution*. doi: 10.1023/A:1022135909197.
- Sanders, J. G. and Osman, R. W. (1985) 'Arsenic incorporation in a salt marsh ecosystem', *Estuarine, Coastal and Shelf Science*. doi: 10.1016/0272-7714(85)90083-6.
- Smedley, P. L. and Kinniburgh, D. G. (2002) 'A review of the source, behaviour and distribution of arsenic in natural waters', *Applied Geochemistry*. doi: 10.1016/S0883-2927(02)00018-5.
- Smith, E., Naidu, R. and Alston, A. M. (1998) 'Arsenic in the Soil Environment: A Review', in *Advances in Agronomy*. doi: 10.1016/S0065-2113(08)60504-0.
- Stein R. (1991) 'Accumulation of organic carbon in marine sediments. Results from the Deep Sea Drilling Project/Ocean Drilling Program'. *Lecture Notes in Earth Sciences*, vol. 34. Berlin: Springer-Verlag. 217p
- Stucker, V. K. et al. (2014) 'Thioarsenic species associated with increased arsenic release during biostimulated subsurface sulfate reduction', *Environmental Science and Technology*. doi: 10.1021/es5035206.
- Szymański, W., Skiba, M. and Błachowski, A. (2014) 'Mineralogy of fe-mn nodules in albeluvisols in the carpathian foothills, poland', *Geoderma*. doi: 10.1016/j.geoderma.2013.11.008
- Taylor, D. I. and Allanson, B. R. (1993) 'Impacts of dense crab populations on carbon exchanges across the surface of a salt marsh', *Marine Ecology Progress Series*.
- USEPA, U. S. E. P. A. (1996) *Method 3050B - Acid digestion of sediments, sludges, and soils.*, 1996. doi: 10.11117/12.528651.
- Vale, C. et al. (1990) 'Presence of metal-rich rhizoconcretions on the roots of *Spartina maritima* from the salt marshes of the Tagus Estuary, Portugal', *Science of the Total Environment, The*. doi: 10.1016/0048-9697(90)90265-V.
- Velde, B. and Barré, P. (2010) *Soils, plants and clay minerals: Mineral and biologic interactions, Soils, Plants and Clay Minerals: Mineral and Biologic Interactions*. doi: 10.1007/978-3-642-03499-2.

- Velde, B. and Church, T. (1999) 'Rapid clay transformations in Delaware salt marshes', *Applied Geochemistry*. doi: 10.1016/S0883-2927(98)00092-4.
- Volkenborn, N. *et al.* (2016) *Bioirrigation in Marine Sediments, Reference Module in Earth Systems and Environmental Sciences*. doi: 10.1016/B978-0-12-409548-9.09525-7.
- Wang, Y. *et al.* (2012) 'Dynamics of arsenic in salt marsh sediments from Dongtan wetland of the Yangtze River estuary, China', *Journal of Environmental Sciences (China)*. doi: 10.1016/S1001-0742(11)61048-6.
- Wilkie J. A. and Hering J. G. (1996) Adsorption of arsenic onto hydrous ferric oxide: effect of adsorbate/adsorbent ratios and co-occurring solutes. *Coll. Surf. A* **107**, 97-110.
- Wilkin, R. (2001) 'Iron Sulfide-Arsenite Interactions: Adsorption Behavior onto Iron Monosulfides and Controls on Arsenic Accumulation in Pyrite', *USGS Workshop on Arsenic in the Environment*.
- Wilkin, R. T. and Ford, R. G. (2006) 'Arsenic solid-phase partitioning in reducing sediments of a contaminated wetland', *Chemical Geology*. doi: 10.1016/j.chemgeo.2005.11.022.
- Wilkin, R. T., Wallschläger, D. and Ford, R. G. (2003) 'Speciation of arsenic in sulfidic waters', *Geochemical Transactions*. doi: 10.1039/b211188h.
- Wu, Y., Li, W. and Sparks, D. L. (2015) 'Effect of Iron(II) on Arsenic Sequestration by δ -MnO₂: Desorption Studies Using Stirred-Flow Experiments and X-Ray Absorption Fine-Structure Spectroscopy', *Environmental Science and Technology*. doi: 10.1021/acs.est.5b04087.
- Yang, N. *et al.* (2016) 'High arsenic (As) concentrations in the shallow groundwaters of southern Louisiana: Evidence of microbial controls on As mobilization from sediments', *Journal of Hydrology: Regional Studies*. doi: 10.1016/j.ejrh.2015.11.023.

CAPÍTULO III: Arsenic environmental threshold surpass in estuarine sediments: effects of bioturbation

Bull Environ Contam Toxicol (2017) 98: 521-524

DOI 10.1007/s00128-016-2024-z

Abstract

We investigate the distributions of the metalloid arsenic (As) and metals iron (Fe) and manganese (Mn) in the sediments of two pristine areas of a biological reserve in the Patos Lagoon Estuary. This area is occupied by *Spartina alterniflora* and by *Neohelice granulata* crab colonies and low concentrations of As are expected. The bioturbation/bioirrigation of sediments by crabs and the roots of plants lead to the penetration of oxygen below the oxic/suboxic division and the subsequent precipitation of Fe-Mn hydroxides. Ferruginous incrustations and nodules along roots and crab channels propagate to depths of over 35 cm and sediment contains up to 33 mg kg^{-1} of As. The metalloid distribution in sediments is strongly correlated with that of Fe but not with Mn. This study revealed that areas with biologically disturbed sediments could demonstrate high concentrations in As, which is not anthropogenic in origin.

Keywords: Arsenic; Sediments; Bioturbation; Contamination

Introduction

Arsenic (As) is a toxic metalloid and elevated As concentrations in sediments threaten aquatic biota and has subsequently attracted worldwide attention in studies of aquatic environments (Mirlean *et al.*, 2003; Pérez-López *et al.*, 2011). Different countries have established As concentration limits in sediments for the protection of aquatic life. The Brazilian environmental act on marine sediment quality criteria established a legislative threshold for marine sediments Threshold Effect Level (TEL) of 19 mg kg^{-1} (CONAMA 2012). TEL represents the concentration above which adverse biological effects are expected to occur.

Sediment quality monitoring requires knowledge of the local background values of tested components. Typically, background-level sampling stations are selected in neighboring zones (frequently in biological reserves) that are free of anthropogenic

impacts and where low concentrations of tested components are expected. Sediment quality monitoring in the Patos estuary of Southern Brazil detected high concentrations of As (greater than the TEL value) at the background station (Santos *et al.*, 2009). This result complicated the implementation of the monitoring program by creating an erroneous depiction of sediment toxicity which prevented identification of reference and polluted sediment areas within the survey.

It is generally accepted that Fe (III) oxides are efficient scavengers of arsenic in aquatic environments (Sadiq, 1992). A common opinion is also that As diagenesis is strongly coupled to Fe cycling and redox conditions that are determined by organic matter remineralization (Widerlund and Ingri, 1995). Remobilization of As due to the reduction and dissolution of Fe (III)- and/or Mn-oxides during early diagenesis is also well-documented in shelf sediments (Chaillou *et al.*, 2003; Bone *et al.*, 2006). These processes of As remobilization and adsorption/coprecipitation with Fe (III) hydroxides are observed on a microscale in iron-rich concretions that form in salt marshes (Caetano and Vale, 2002).

Normally a major fraction of the remobilized As is trapped in the oxidized surface layer, which forms a sediment zone (0–2 cm) that is relatively rich in this metalloid (Chaillou *et al.*, 2003). The 0 to 30 cm layer is collected when performing routine surface sediment sampling using a Van-Veen grab. Thus, the As level in the oxidized horizon is drastically diluted in the sediment sample and therefore results of metalloid measurements may be relatively low in comparison to typical background levels. However, in certain background areas sediment As content can reach relatively high levels throughout the upper one-meter depth interval due the reburial of As associated with Fe (III)-oxides (Mirlean *et al.*, 2012). In some cases, such enrichment may also be promoted by the activity of aquatic organisms known as bioturbation and/or bioirrigation. In this process, oxygen-rich water is usually pumped into the sediment and water containing less oxygen is pumped out. As a result the precipitation of Fe (III)-oxides enriched by As may occur inside the sediment column.

The presence of crabs can strongly contribute to bioturbation and/or bioirrigation. It was reported that crabs *Neohelice granulata* inhabit estuarine and protected coastal areas in neighboring temperate regions of Argentina, constructing vertical burrows of up to 10 cm of diameter that can reach up to 1 m depth in vegetated marshes (Angeletti & Cervellini, 2015). In Patos Lagoon estuary and other marshes in the southwestern Atlantic

the number of crab burrows is ca. 60 per m² (Alberti *et al.*, 2007; Freitas *et al.*, 2015; Freitas *et al.*, 2016; Martinetto *et al.*, 2016).

The Patos and Mirim Lagoons constitute the largest lagoonal system in South America (more than 14,000 km²). In the outlet of the Patos Lagoon to the Atlantic Ocean an estuary of 900 km² is formed. The Patos estuary is exposed to significant anthropogenic effects from a local port and both the industrial and dwelling areas of the Rio Grande City. The As pollution in Patos estuarine sediment was reported by Mirlean *et al.* (2003); however, there are no studies recording the effect of bioturbation/bioirrigation on As redistribution and accumulation in these estuarine sediments, which is the main purpose of this article. Therefore, this paper presents its results as a way to contribute to the investigation of contaminations levels by avoiding an erroneous description of the As distribution.

Methods and Materials

The study area, a shallow part of Patos estuary (32°01'18'' S and 52°06'08'' N), is situated upstream from industrial and port areas and is not subject to the direct effects of domestic and industrial effluents (Fig. 1). The water depth at the sampling station varies from tens of centimeters to one meter. Shallow (< 0.2 m) areas (SA) are occupied by *Spartina alterniflora*, and *Neohelice granulata* crabs populate the deeper (0.2–1.0 m) areas (DA). Sediments in the sampling areas are silty-argilous enriched by organic material.

The two sediments blocks (35 × 35 × 35 cm) the size of the Van Veen Grab were sampled from both the SA and DA using a quadrangular stainless box core, and were immediately transported to the laboratory. The grid sampling was performed on the freshly exposed surface of sediment blocks representing both the oxic and suboxic zones of the sediment. A plastic cochlear was used to sample approximately 5 g of sediment material at each point, and subsamples were immediately frozen for later treatment. A total of 21 and 36 samples were collected for the SA and DA sediment blocks, respectively. The Redox potential (Eh) was measured on the freshly exposed surface of sediment blocks in sampling points using naked Pt-electrode Analion®. Total elemental contents were determined according to the United States Environmental Protection Agency - USEPA - method 3051 (EPA, 2012). Sediment subsamples (200 mg wet weight) were also extracted for 24 h at ambient temperature using 25 mL of an ascorbate solution (50 g of NaHCO₃, 50 g of Na-citrate, 20 g of ascorbic acid per 1 L of solution; buffered

at pH 8) as described in Chaillou *et al.* (2003). This procedure removes the most reactive Fe (III) phases and their associated trace metals (Hyacinthe *et al.*, 2001). A separate extraction was carried out using 25 mL 1N HCl to determine the acid-soluble Mn and Fe and the associated As content.

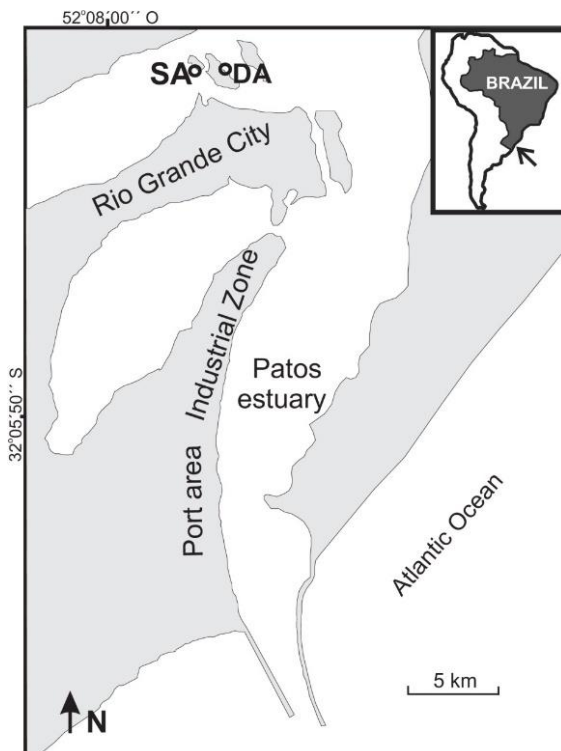


Figure 1 - Study area. Sampling points: DA- area populated by *Neohelice granulata* crabs; SA- area occupied by *Spartina alterniflora*.

The As content was determined by electrothermal atomic absorption spectrometry using a Perkin-Elmer 800 instrument equipped with a Zeeman background corrector with pyrolytically coated tubes with a platform. The Mn and Fe levels were determined using flame (acetylene –air) atomic-absorption spectrometry. The lower detection limit of analyzed elements As, Mn and Fe were 0.04 mg kg^{-1} , 20 mg kg^{-1} and 40 mg kg^{-1} , respectively. Each sediment sample was analyzed in triplicate. The precision determined as the relative standard deviation (% RSD) was less than 6.0%, 3.6%, and 4.5% for As, Mn, and Fe, respectively. Reference material (PACS-2, National Research Council of Canada) was analyzed together with each set of samples for accuracy control purposes.

Results and Discussion

The oxidation/reduction potential (Eh), measured at 58 points on the freshly exposed surfaces of sediment blocks, demonstrated high variation for both sites. In sampling points ($N = 36$) from the DA site Eh varied from -20 to 187 mV (mean 116 ± 43 mV), while in the SA site ($N = 22$) it varied from -35 to 126 mV (mean 65 ± 48 mV). In most marine sediments oxygen penetration is small relative to the depth of oxidized iron minerals. The reducing sediment below the suboxic zone has an Eh below 0 to 100 mV and down to -300 mV, and may be black or gray in color due to different forms of iron sulfide minerals.

According to the above mentioned definitions our sediments, due to variations of Eh, belong to oxic and suboxic zones. In distinction from undisturbed areas the studied sediments do not display well-marked vertical allocation of oxic and suboxic zones. The distribution of oxic and suboxic spots along the transverse section of sediment blocks is uniform and complies with spreading of crab burrows or root channels. The sediments from the DA site are more oxic than sediments from the SA site because of the larger diameter of crab burrows and more intense water irrigation compared with root channels.

All analyzed elements demonstrated a consistent distribution order in the extracted fractions of sediments from both sampling sites: total > acid soluble > reactive (Tab. 1). The concentration of the redox-susceptible metals Fe and Mn and the metalloid As exhibited a high variability for all analyzed fractions, which showed a tenfold variation for Fe and As and up to a one hundredfold variation for Mn. The sediments from the DA site demonstrated about two-times higher mean concentration of total As than sediments from the SA site. The mean value of total Fe was also higher in sediments from the DA site, while the sediments from the SA site were richer in total Mn.

The sediments from both sampling sites had similar mean concentrations of acid-soluble Fe and a twofold difference in mean acid-soluble Mn concentrations; whereas, the mean concentrations of acid-soluble As at the sampled sites differed threefold. At both sites sediments displayed similar mean concentrations of reactive Fe and Mn, whereas the mean concentration of reactive As was about two-times higher in the DA site. The highest detected concentration of As in the DA site was approximately two-times greater than the TEL value (19 mg kg^{-1}) for this element. In the neighboring SA site, the acid-soluble and highest total As concentrations were also greater than the TEL value.

Table 1 - Concentrations of elements in different extractions from sediments in crab (DA) and spartina (SA) areas. The concentration range is shown as the numerator, and the mean \pm SD is presented as the denominator.

Sampling site	DA			SA		
	Fractions	Total	Acid solub.	Reactive	Total	Acid solub.
Fe (%)	<u>0.8-10.6</u> 3.3 \pm 2.6	<u>0.3-8.1</u> 2.2 \pm 2.1	<u>0.01-2.5</u> 0.6 \pm 0.7	<u>0.9-8.4</u> 2.7 \pm 1.4	<u>0.2-6.7</u> 2.2 \pm 1.7	<u>0.1-1.0</u> 0.5 \pm 0.2
As (mg kg ⁻¹)	<u>0.4-33.4</u> 9.5 \pm 7.5	<u>0.2-31.7</u> 9.2 \pm 6.0	<u>0.1-7.6</u> 1.6 \pm 1.1	<u>0.3-24.2</u> 4.9 \pm 3.9	<u>0.1-22.7</u> 3.4 \pm 2.6	<u>0.1-2.6</u> 0.9 \pm 0.5
Mn (mg kg ⁻¹)	<u>57.0-1073.2</u> 354.6 \pm 124.6	<u>7.7-903.4</u> 226.4 \pm 178.4	<u>6.8-404.0</u> 52.7 \pm 78.9	<u>97.3-2398.4</u> 426.3 \pm 210.5	<u>23.3-517.8</u> 119.4 \pm 68.2	<u>0.01-472.8</u> 48.2 \pm 27.1

The highest positive correlation between studied elements was detected for the total fractions of Fe and As ($r^2 = 0.85$, $p < 0.01$, $n = 58$). Other fractions of these elements also demonstrated high correlations ($r^2 = 0.79$ and $r^2 = 0.76$; $p < 0.01$, $n = 58$) between the acid-soluble and reactive fractions, correspondingly. Contrary to Fe, Mn exhibited a low correlation with As in all fractions, and a poor correlation was most notable for the total fractions ($r^2 = 0.3$, $p < 0.01$, $n = 58$). Certain authors reported the adsorption of As onto Mn oxides, whereas others identified a weak relationship between these elements in oxidized surface sediment layers (Hyacinthe *et al.*, 2001). The poor correlation between Mn and As reported by Caetano and Vale (2002) reinforces the lesser importance of Mn-oxides on the post-mobilization of As in salt marsh environments. This weak adsorption effect is most likely related to the negative charge of Mn oxides in neutral or low-alkaline estuarine waters, which does not favor the sorption of negatively charged As species (Mirlean *et al.*, 2011).

The parallelism of As and Fe concentration distributions in both sediments reflects the relationship of their chemistries in these redox transition environments, including control by coprecipitation of the host iron phases, and demonstrating a strong connection between As and Fe distributions. The presence of high concentrations of As in an acid-soluble fraction confirms the process of metalloid fixation with labile and freshly deposited species of Fe.

In various areas, marine sediments naturally contain high levels of As (*e.g.*, in Bothnian Bay where surficial sediments often contain As in range of 30 to 320 mg kg⁻¹ (Leivuori and Niemistij, 1993)). However, in the majority of cases, high concentrations of As in marine sediments are recorded in the uppermost layers with a decrease to background values at depths below two centimeters (Widerlund and Ingri, 1995). In the case presented here, the formation of As-rich sediment zones in the deeper horizons is related to the continuous penetration of oxygen-rich surface water and the resulting Fe (III) deposition on the walls of crab burrows or precipitation along root channels due to oxygen released from roots. The oxidation of deeper parts of the sediment column visually differs in its intensity (*i.e.*, the brown-colored Fe (III) spots in crab burrows are more intense and consolidated due to the continuous flushing of channels during crab movement). Moreover, the Fe (III) concretions were detected by drilling to a depth of 1.0 m in crab-dominated areas, whereas the Fe (III) oxides were not observed deeper than 0.4 m at the *Spartina* (SA) sites.

We conclude that the biological disturbance of sediments in the redox zone leads to the penetration of oxygen via roots and crab channels. The deposition of Fe oxyhydroxides on the channel walls leads to As enrichment in the sediment. Because the monitoring of surface sediments is typically based on sampling over depth intervals that are subject to the activity of aquatic organisms, information on As distributions obtained from areas with biologically disturbed sediments may have a significant influence on environmental impact assessments and decision making in estuarine sediments that lack anthropogenic impacts.

Acknowledgements

The research was funded by the Brazilian National Research Council (CNPq, grant 470541/2010-5).

References

- Alberti J, Daleo P, Iribarne O, Silliman BR, Bertness M (2007) Local and geographic variation in grazing intensity by herbivorous crabs in SW Atlantic salt marshes. *Marine Ecology and Progress Series* 349:235-243.
- Angeletti S, Cervellini PM (2015) Population structure of the burrowing crab *Neohelice granulata* (Brachyura, Varunidae) in a southwestern Atlantic salt marsh. *Lat. Am. J. Aquat. Res.*, 43(3): 539-547.

- Bone SE, Gonnea ME, Charette MA (2006) Geochemical cycling of arsenic in a coastal aquifer. *Environmental Science and Technology*, 40:3273-3278.
- Caetano M, Vale C (2002) Retention of arsenic and phosphorus in iron-rich concretions of Tagus salt marshes. *Marine Chemistry*, 79:261-271.
- Chaillou G, Schafer J, Anschutz P et al (2003) The behaviour of arsenic in muddy sediments of The Bay of Biscay (France). *Geochimica et Cosmochimica Acta*, 67: 2993–3003.
- CONAMA Ministério do Meio Ambiente, Conselho Nacional do Meio Ambiente. Resolução nº 454, de 01 de novembro de 2012 (in Portuguese).
- EPA Method – 3051. www.caslab.com/EPA-Method-3051/ Accessed 21 March 2012.
- Freitas RF, Schrack EC, He Q, Silliman BR, Furlong EB, Telles AC, Costa CSB (2016) Consumer control of the establishment of marsh foundation plants in intertidal mudflats. *Marine Ecology and Progress Series* 547: 79-89.
- Freitas RF, Schrack EC, Sieg RD, Silliman BR, Costa CSB (2015) Grazing scar characteristics impact degree of fungal facilitation in *Spartina alterniflora* leaves in a South American salt marsh. *Braz. Arch. Biol. Technol.* 58: 103–108.
- Hyacinthe C, Anschutz P, Jouanneau JM, Jorissen FJ (2001) Early diagenesis processes in the muddy sediment of the Bay of Biscay. *Marine Geology*, 177:111–128.
- Leivuori M, Niemistii L (1993) Trace metals in the sediments of the Gulf of Bothnia. *Aqua Fennica*, 23:89-100.
- Martinetto P, Montemayor DI, Alberti J, Costa CSB, Iribarne O (2016) Crab bioturbation and herbivory may account for variability in carbon sequestration and stocks in south west Atlantic salt marshes. *Frontiers of Marine Sciences* 3, 122.
- Mirlean N, Andrus VE, Baisch, P et al (2003) Arsenic pollution in Patos Lagoon estuarine sediments, Brazil. *Marine Pollution Bulletin*, 46:1480-1484.
- Mirlean, N, Baisch P, Travassos MP, Nassar C (2011) Calcareous algae bioclast contribution to sediment enrichment by arsenic on the Brazilian subtropical coast. *Geo-Marine Letters*, 31:65-73.
- Mirlean N, Medeanic S, Garcia FA et al (2012) Arsenic enrichment in shelf and coastal sediment of the Brazilian subtropics. *Continental Shelf Research*, 35:129 –136.
- Pérez-López R, Nieto JM, López-Casajosa MJ et al (2011) Evaluation of heavy metals and arsenic speciation discharged by the industrial activity on the Tinto-Odiel estuary, SW Spain. *Marine Pollution Bulletin*, 62:405-411.

Sadiq, M (1992) Toxic Metal Chemistry in Marine Environments. Marcel Dekker, New York.

Santos CG, Garcia F, Baisch P, Mirlean N (2009) Relação entre fração fina e total no monitoramento de sedimentos contaminados por metais pesados na região portuária estuarina de Rio Grande. In Farg (Ed), Portos e dragagem, 23-25, Ceará: Farg (in Portuguese).

Widerlund A, Ingri J (1995) Early diagenesis of arsenic in sediments of the Kalix River estuary, northern Sweden. *Chemical Geology*, 125:185-196.

6. Considerações Finais e Conclusão

A diagênese do As para os sedimentos do estuário da Lagoa de Patos, é correlacionada com o conteúdo de Fe e secundariamente com o conteúdo de Mn dos sedimentos. Destaca-se ainda a influência da concentração de sulfeto dissolvido nas águas intersticiais dos sedimentos estuarinos na distribuição do metaloide. Altas concentrações de As em profundidades abaixo de 40 cm encontram-se em sedimentos de águas rasas caracterizados por condições anóxicas. Destaca-se ainda que essas altas concentrações do As podem ser atribuídas à captação dele por formação de pirita nesses sedimentos. Estas conclusões são corroboradas pelas altas concentrações de sulfeto dissolvido nas águas intersticiais com mais de 40 cm de profundidade e pelo aumento do conteúdo de CRS, que é comumente atribuído à meta-pirita.

Nas marismas do estuário, o As é geralmente concentrado na camada óxica dos sedimentos. Em maiores profundidades (20-30 cm), a distribuição vertical da concentração de As está relacionada com uma zona rica em Fe e Mn nesses sedimentos. Estes resultados refletem a bioturbação/biorrigação pelos caranguejos *Neohelice granulata* e por *Spartina alterniflora*, que povoam as marismas da região, e que levam à penetração de oxigênio abaixo da fronteira óxica/subóxica. Neste caso, a dissolução dos óxidos/óxi-hidróxidos de Fe na zona subóxica desses sedimentos levaria à liberação simultânea de Fe e As nas águas intersticiais. O As dissolvido difunde para cima e fixa nas partículas de óxidos/óxi-hidróxidos de Fe-Mn por adsorção próximo ao limite das fronteiras óxica e subóxica, que pode ter até 30 cm de profundidade nesses sedimentos altamente bioturbados. As semelhanças nas distribuições de As e Fe sugerem que a redistribuição do Fe nos sedimentos do estuário durante a diagênese precoce controla também a de As. Em locais de águas rasas e em locais ocupados por *S. alterniflora*, o Mn também atua como um controlador importante para a fixação do As em sedimentos.

Os nódulos dos sedimentos de marismas estão geralmente concentrados na camada óxica do sedimento, que pode atingir profundidades de até 35 cm abaixo da superfície do sedimento. Todos os óxidos/óxi-hidróxidos de Fe-Mn extraídos dos sedimentos do estuário da Lagoa de Patos são amorfos, o que é consistente com a resposta rápida dos óxidos/óxi-hidróxidos de Fe-Mn às mudanças hidroquímicas no estuário.

Apresentamos evidências que o comportamento do Fe durante a diagênese é controlado pelas variações de oxidação/redução do sedimento, mas pode ser

impulsionado em parte por alterações no pH. O comportamento do Fe também é diferentemente durante às mudanças sazonais nas marismas ocupadas por *N. granulata* em comparação com as marismas dominadas por *S. alterniflora*. Mais especificamente, o Fe exibe uma resposta maior às variações de salinidade nas marismas ocupadas pelo caranguejo *N. granulata*, enquanto as alterações no pH da água intersticial desempenham um papel maior nas concentrações de Fe nas marismas ocupadas por *S. alterniflora*. Portanto, a fisiologia da *Spartina* tem um efeito dominante nas transformações geoquímicas do Fe em comparação com mudanças na salinidade. Destaca-se ainda o papel da *S. alterniflora* em relação à criação de microambientes redox, que favoreceu a oxigenação dos sedimentos que circundam as suas raízes. Entretanto, durante o período de crescimento da *S. alterniflora* ocorreram ambientes redutores, devido à excreção de matéria orgânica dissolvida e produtos de fermentação anaeróbica pelas raízes.

As incrustações e nódulos ferruginosos ao longo dos canais de caranguejos e de raízes se propagam a profundidades superiores ao limite da camada óxica e podem conter até 172 mg kg⁻¹ de As. Nossa estudo revelou que áreas com sedimentos biologicamente perturbados podem superar valores estipulados pela norma CONAMA (CONAMA, 2012), que é de 19 mg kg⁻¹ (Nível 1) para sedimentos de águas salgadas. A formação de anomalias de arsênio em sedimentos do estuário Patos em zonas ao leste do canal de navegação é resultado da redistribuição diagenética do metaloide, e não tem caráter antropogênico. Sendo assim, é necessária a sensibilização das autoridades competentes para criar linhas de pesquisa específicas para subsidiar estudos que visem a propor valores de *background* geoquímico para elementos-traço importantes. Na medida em que estudos envolvendo essa temática forem desenvolvidos, para os mais variados sistemas naturais, maiores informações e guias para estudos futuros serão gerados.

Por fim, destaca-se que são necessárias mais informações para entender melhor o papel da sulfato-redução no ciclo do Fe no estuário da Lagoa de Patos, especialmente em locais com vegetação de *S. alterniflora*, onde a capacidade das bactérias redutoras de SO₄²⁻ de produzir sulfeto pode ser aprimorada. As taxas de sulfato-redução e o conteúdo de pirita forneceriam uma melhor compreensão sobre a geoquímica e o destino final do Fe e, consequentemente do As, em ambientes de marisma, como o estuário da Lagoa de Patos.

Permanecem questões fundamentais sobre a extensão das interações de sulfetos com metais traço e, consequentemente, com o As. Por exemplo, pouco se sabe sobre como os metais traço estão associados aos sulfetos (isto é, co-precipitados ou adsorvidos em

sulfetos de Fe) Parâmetros como o grau de piritização (DOP) podem ser considerados como uma medida da extensão em que o ferro reativo foi transformado em pirita, e deve ser usado para melhor entender como o As está associado aos sulfetos sedimentares.

7. Referências Bibliográficas

- ABNT. (1984). Solo – ‘Análise Granulométrica’. Método de Ensaio. *NBR 7181*.
- Ahmad, S.A *et al.* (1997) ‘Arsenic contamination in ground water and arsenicosis in Bangladesh.’ *International Journal of Environmental Health Research*, 7: 271-276.
- ATSDR. (2007) ‘Agency for Toxic Substances and Disease Registry.’ *Toxicological Profile for Arsenic*. Atlanta, GA.
- Baeyens, W., Mirlean, N., Bundschuh, J., de Winter, N., Baisch, P., da Silva Júnior, F.M.R., Gao, Y. (2009) ‘Arsenic enrichment in sediments and beaches of Brazilian coastal waters: A review’. *Science of the Total Environment* 681 (2019) 143–154
- Baisch, P., Niencheski, F., Lacerda, L. (1988) ‘Trace Metals Distribution in sediments of the Patos Lagoon Estuary, Brasil’. *Metals in coast Environments of Latin America*. (Seeliger U., de Lacerda L. et Patchinerlam S.R., eds.). Springer- Verlag. Berlin. p. 59-64.
- Baisch, P. (1994) ‘Les oligo-éléments métalliques du Système Fluvio-lagunaire dos Patos (Brésil) - Flux et Devenir’. *Thèse de Doctorat*. Université de Bordeaux I. n° 1136. 345p.
- Barra, C.M. *et al.* (2000) ‘Especiação de Arsênio – Uma revisão.’ *Química Nova*. 23(1): 58-70.
- Basílio, M.S., Friese K., Lena J.C., Júnior H.A.N., Roeser, H.M.P. (2005) ‘Adsorção de As, Cu, Pb e Cr na avaliação da capacidade de fixação de metais por resíduo de mineradores de ferro.’ *Química Nova*. 28 (5): 822-828.
- Beck, M. *et al.* (2008) ‘Cycling of trace metals (Mn, Fe, Mo, U, V, Cr) in deep pore waters of intertidal flat sediments’, *Geochimica et Cosmochimica Acta*. doi: 10.1016/j.gca.2008.04.013.
- Bento, D.M., Mirlean, N, Baisch, P. (2013) ‘Metal speciation in urban-industrial effluents: impact assessment for an estuary in southern Brazil’. *Fresenius Environmental Bulletin*. 22 (4a), p. 1-8.

- Bednar, A. J. *et al.* (2005) 'Effects of iron on arsenic speciation and redox chemistry in acid mine water', *Journal of Geochemical Exploration*. doi: 10.1016/j.gexplo.2004.10.001.
- Berner, R. A. (1981) 'A New Geochemical Classification of Sedimentary Environments', *Journal of Sedimentary Petrology*. doi: 10.1306/212F7C7F-2B24-11D7-8648000102C1865D.
- Bhattacharyya, R. *et al.* (2003) 'High arsenic groundwater: Mobilization, metabolism and mitigation - An overview in the Bengal Delta Plain', *Molecular and Cellular Biochemistry*. doi: 10.1023/A:1026001024578.
- Biswas, B.K *et al.* (1999). 'Groundwater arsenic contamination and sufferings of people in Bangladesh, a report up to January 1999.' Paper presented at the *International Conference, Arsenic in Bangladesh Ground Water: World's Greatest Arsenic Calamity*, Staten Island, New York, USA, 27-28.
- Bone, S. E., Gonnea, M. E., Charette, M. A. (2006) 'Geochemical cycling of arsenic in a coastal aquifer', *Environmental Science and Technology*. doi: 10.1021/es052352h.
- Bowell, R. J. (1994) 'Sorption of arsenic by iron oxides and oxyhydroxides in soils', *Applied Geochemistry*. doi: 10.1016/0883-2927(94)90038-8.
- Brannon J. M., Patrick, W. H. (1987) 'Fixation, Transformation, and Mobilization of Arsenic in Sediments', *Environmental Science and Technology*. doi: 10.1021/es00159a005.
- Brooks, K.M. (2001) 'Materials and Methods - free sulfide analysis'. In: Brooks, K.M. (Prod.). An evaluation of the relationship between salmon farm biomass, organic inputs to sediments, physicochemical changes associated with those inputs and the infaunal response - with emphasis on total sediment sulfides, total volatile solids, and oxidation-reduction potential as surrogate endpoints for biological monitoring. 172 pp. *Aquatic Environmental Science*, Washington, USA, pp 43-44.
- Caetano, M., Vale, C. (2002) 'Retention of arsenic and phosphorus in iron-rich concretions of Tagus salt marshes', *Marine Chemistry*. doi: 10.1016/S0304-4203(02)00068-3.
- Calliari, L.J. (1998) 'O ambiente e a biota da Lagoa dos Patos. Características Geológicas'. In: *Os Ecossistemas Costeiros e Marinhos do Extremo Sul do Brasil*. Editora Ecoscientia. 341p.

- Canfield, D. E., Thamdrup, B. (2009) 'Towards a consistent classification scheme for geochemical environments, or, why we wish the term "suboxic" would go away: Editorial', *Geobiology*. doi: 10.1111/j.1472-4669.2009.00214.x.
- Castello, J.P. (1985). 'La ecología de los consumidores del estuario de la Lagoa dos Patos.' In: YAÑEZ-ARANCIBIA, A (ed.). *Fish Community Ecology in Estuaries and Coastal Lagoons: Towards an Ecosystem Integration*. DR (R) UNAM Press, Mexico, Chap., p. 386-406.
- Chaillou, G. *et al.* (2003) 'The behaviour of arsenic in muddy sediments of the Bay of Biscay (France)', *Geochimica et Cosmochimica Acta*. doi: 10.1016/S0016-7037(03)00204-7.
- Choi, S., O'Day, P. A., Hering, J. G. (2009) 'Natural attenuation of arsenic by sediment sorption and oxidation', *Environmental Science and Technology*. doi: 10.1021/es802841x.
- Clark, M. W. *et al.* (1998) 'Redox stratification and heavy metal partitioning in Avicennia-dominated mangrove sediments: a geochemical model', *Chemical Geology*. doi: 10.1016/S0009-2541(98)00034-5.
- CONAMA (2005) – Ministério do Meio Ambiente, Conselho Nacional do Meio Ambiente. Resolução n° 357, de 17 de março de 2005.
- CONAMA (2008) - Ministério do Meio Ambiente, Conselho Nacional do Meio Ambiente. Resolução n° 396, de 3 de abril de 2008.
- CONAMA (2012) – Ministério do Meio Ambiente, Conselho Nacional do Meio Ambiente. Resolução n° 454, de 01 de novembro de 2012.
- Copertino, M., Costa, C.S.B., Seelinger, U. (1997). 'Dinâmica populacional de *Spatina alterniflora* em pântanos salgados do estuário da Lagoa dos Patos - Rio Grande, RS.' *Anais do VIII Seminário Regional de Ecologia*. 8: 295-312.
- Costa, C. S. B., Marangoni, J. C., Azevedo, A. M. G. (2003) 'Plant zonation in irregularly flooded salt marshes: Relative importance of stress tolerance and biological interactions', *Journal of Ecology*. doi: 10.1046/j.1365-2745.2003.00821.x.
- Costa, L., Mirlean, N., Garcia, F. (2017) 'Arsenic Environmental Threshold Surpass in Estuarine Sediments: Effects of Bioturbation', *Bulletin of Environmental Contamination and Toxicology*, 98(4), pp. 521–524. doi: 10.1007/s00128-016-2024-z.
- Costa, L., Mirlean, N., Quintana, G. *et al.* (2019) 'Distribution and Geochemistry of Arsenic in Sediments of the World's Largest Choked Estuary : the Patos Lagoon

- , Brazil'. *Estuaries and Coasts*. <https://doi.org/10.1007/s12237-019-00596-0>
- Cullen, W.R., Reimer, K.J. (1989) 'Arsenic speciation in the environment.' *Chemical Reviews* 89: 713-764.
- Das D., et al. (1996) 'Arsenic in groundwater in six districts of West Bengal, India.' *Environmental Geochemistry and Health*, 18: 5-15.
- Davis, A.M., Holland, H.D., Turekian, K.K. (2003) 'Treatise on Geochemistry'. Amsterdam, Pergamon Press, 5155 p.
- Dhar, R.K et al. (1997) 'Groundwater arsenic calamity in Bangladesh.' *Current Science*, 73: 48-59.
- Dixit, S., Hering, J. G. (2003) 'Comparison of arsenic(V) and arsenic(III) sorption onto iron oxide minerals: Implications for arsenic mobility', *Environmental Science and Technology*. doi: 10.1021/es030309t.
- Doyle, M. O., Otte, M. L. (1997) 'Organism-induced accumulation of iron, zinc and arsenic in wetland soils', *Environmental Pollution*. doi: 10.1016/S0269-7491(97)00014-6.
- Edenborn, H. M. et al. (1986) 'Observations on the diagenetic behavior of arsenic in a deep coastal sediment', *Biogeochemistry*. doi: 10.1007/BF02180326.
- Edmonds, J.S., Francesconi, K.A. (1987) 'Trimethylarsine oxide in estuary catfish (*Cnidoglanis macrocephalus*) and school whiting (*Sillago bassensis*) after oral administration of sodium arsenate; and as a natural component of estuary catfish. *Science of the total environment* 64: 317-323.
- Fagnani, E., Guimarães, J.R. (2011) 'Sulfetos Volatilizáveis por acidificação e metas extraídos simultaneamente na avaliação de sedimentos de água doce'. *Química Nova*, 34, 9, p. 1618-1628.
- Farias, J.S. (2011) 'Especiação química de Arsênio inorgânico no estuário da Lagoa dos Patos – RS'. *Dissertação* (Mestrado em Química Tecnológica e Ambiental) Universidade Federal do Rio Grande – Rio Grande, RS.
- Feldmann J., Krupp E.M. (2011) 'Critical review or scientific opinion paper: Arsenosugars—a class of benign arsenic species or justification for developing partly speciated arsenic fractionation in foodstuffs?' *Analytical and bioanalytical chemistry* 399: 1735-1741.
- Fernandes, E.H.L., Dyer, K.R., Möller, O.O. (2003). 'Morphological influence on the formation of spatial gradients in the southern Patos Lagoon'. In: *Proceedings of*

- the 3rd IAHR Symposium on River, Coastal and Estuarine Morphodynamics.*
Barcelona, Espanha, p. 504-515.
- Fernandes, E. H. L. *et al.* (2004) 'The attenuation of tidal and subtidal oscillations in the Patos Lagoon estuary', in *Ocean Dynamics*. doi: 10.1007/s10236-004-0090-y.
- Filgueras, A.S. (2009). 'Condições Oceanográficas e as assembléias ictioplanctônicas no estuário da Lagoa dos Patos.' **Dissertação** (Apresentada ao PPG em Oceanografia Biológica, Universidade Federal do Rio Grande), 72 pp.
- Fitz, W. J., Wenzel, W. W. (2003) 'Environmental Chemistry of Arsenic', *Journal of Environment Quality*. doi: 10.2134/jeq2003.1572a.
- Flora, S. J. S. (2015) '*Handbook of Arsenic Toxicology, Handbook of Arsenic Toxicology.*' doi: 10.1016/C2013-0-08322-3.
- Fossing, H., Jørgensen, B. B. (1989) 'Measurement of bacterial sulfate reduction in sediments: Evaluation of a single-step chromium reduction method', *Biogeochemistry*. doi: 10.1007/BF00002889.
- La Force, M. J., Hansel, C. M., Fendorf, S. (2000) 'Arsenic speciation, seasonal transformations and co-distribution with iron in a mine waste-influenced palustrine emergent wetland', *Environmental Science and Technology*. doi: 10.1021/es0010150.
- Förstner, U. (1987) 'Sediment-associated contaminants - an overview of scientific bases for developing remedial options', *Hydrobiologia*. doi: 10.1007/BF00048663.
- Gasparatos, D. *et al.* (2005) 'Microscopic structure of soil Fe-Mn nodules: Environmental implication', *Environmental Chemistry Letters*. doi: 10.1007/s10311-004-0092-5.
- Gasparatos, D. (2013) 'Sequestration of heavy metals from soil with Fe-Mn concretions and nodules', *Environmental Chemistry Letters*. doi: 10.1007/s10311-012-0386-y.
- Gough, L.P. (1993) 'Understanding Our Fragile Environment; Lessons from Geochemical studies. Denver, U. S. Geological Survey Circular, 1105, 34 p
- Gregati, R. A., Negreiros-Franozo, M. L. (2009) 'Population biology of the burrowing crab *Neohelice granulata*, (Crustacea: Decapoda: Varunidae) from a tropical mangrove in Brazil', *Zoologia*. doi: 10.1590/S1984-46702009000100006.
- Gribsholt, B., Kostka, J. E., Kristensen, E. (2003) 'Impact of fiddler crabs and plant roots on sediment biogeochemistry in a Georgia saltmarsh', *Marine Ecology Progress Series*. doi: 10.3354/meps259237.
- HACH, C. (2007) 'DR 2800 Spectrophotometer User Manual', *Hach Company*. doi:

- 10.3928/01477447-20101221-06; 10.3928/01477447-20101221-06.
- Harrington, J. M. *et al.* (1998) 'Phase associations and mobilization of iron and trace elements in Coeur d'Alene Lake, Idaho', *Environmental Science and Technology*. doi: 10.12693/APhysPolA.133.447.
- Hartmann, C. (1988). 'Utilização de dados digitais do mapeador temático para obtenção dos padrões de distribuição do material em suspensão na desembocadura da Laguna dos Patos, RS.' MSc., INPE -SP, 190p.
- Hartmann, C., Calliari, L. (1996). 'Composição e qualidade do material em suspensão durante alta turbidez na extremidade sul da Laguna dos Patos, RS, Brasil.' *Pesquisas em Geociências*, 22: 74-83.
- Hatje, V. *et al.* (2010) 'Inorganic As speciation and bioavailability in estuarine sediments of Todos os Santos Bay, BA, Brazil', *Marine Pollution Bulletin*. doi: 10.1016/j.marpolbul.2010.08.014.
- He, Y. T. *et al.* (2010) 'Geochemical processes controlling arsenic mobility in groundwater: A case study of arsenic mobilization and natural attenuation', *Applied Geochemistry*. doi: 10.1016/j.apgeochem.2009.10.002.
- Hedges, J. I., Keil, R. G. (1995) 'Sedimentary organic matter preservation: an assessment and speculative synthesis', *Marine Chemistry*. doi: 10.1016/0304-4203(95)00008-F.
- Helz, G. R., Tossell, J. A. (2008) 'Thermodynamic model for arsenic speciation in sulfidic waters: A novel use of ab initio computations', *Geochimica et Cosmochimica Acta*. doi: 10.1016/j.gca.2008.06.018.
- Huerta-Diaz, M. A., Morse, J. W. (1992) 'Pyritization of trace metals in anoxic marine sediments', *Geochimica et Cosmochimica Acta*. doi: 10.1016/0016-7037(92)90353-K.
- Huerta-Diaz, M. A., Tessier, A., Carignan, R. (1998) 'Geochemistry of trace metals associated with reduced sulfur in freshwater sediments', *Applied Geochemistry*. doi: 10.1016/S0883-2927(97)00060-7.
- Hyacinthe, C. *et al.* (2001) 'Early diagenetic processes in the muddy sediments of the bay of biscay', *Marine Geology*. doi: 10.1016/S0025-3227(01)00127-X.
- Iribarne, O. *et al.* (2000) 'The role of burrows of the SW Atlantic intertidal crab Chasmagnathus granulata in trapping debris', *Marine Pollution Bulletin*. doi: 10.1016/S0025-326X(00)00058-8.
- Jesus, H.C., Costa, E.A., Mendonça, A.S.F., Zandonade, E. (2004) 'Distribuição de metais

- pesados em sedimentos do sistema estuarino da Ilha de Vitória-ES'. *Química Nova*, 27:378- 386.
- Jorgensen, B. B., Kasten, S. (2006) 'Sulfur cycling and methane oxidation', in *Marine Geochemistry*. doi: 10.1007/3-540-32144-6_8.
- Kendall, R.J., Bens, C.M., Cobb III, G.P. (2003) 'Ecotoxicology.' In: Gagnon, F., Lampron-Goulet, É., Normandin, L., Langlois, M.F., 2016. Measurements of Arsenic in the Urine and Nails of Individuals Exposed to Low Concentrations of Arsenic in Drinking Water From Private Wells in a Rural Region of Québec, Canada. *Journal of environmental health* 78: 76-83.
- Kenneth, M. (2001) 'An evaluation of the relationship between salmon farm biomass, organic inputs to sediments, physicochemical changes associated with those inputs and the infaunal response — with emphasis on total sediment sulfides, total volatile solids, and oxidation-reduction potential as surrogate endpoints for biological monitoring'. Final report to the Technical Advisory Group, British Columbia Ministry of Environment. 644, Washington 98368: *Aquatic Environmental Sciences*. p. 78.
- Khan, A.W *et al.* (1997) 'Arsenic contamination in groundwater and its effect on human health with particular reference to Bangladesh.' *Journal of Preventive and Social Medicine*, 16 (1): 65-73.
- Khan, N.I., Owens, G., Bruce, D., Naidu, R. (2010) 'Human arsenic exposure and risk assessment at the landscape level: a review. *Environmental geochemistry and health* 31: 143-166.
- Kjerfve, B. (1994) 'Coastal Lagoons', *Elsevier Oceanography Series*. doi: 10.1016/S0422-9894(08)70006-0.
- Kneebone, P. E. *et al.* (2002) 'Deposition and fate of arsenic in iron- and arsenic-enriched reservoir sediments', *Environmental Science and Technology*. doi: 10.1021/es010922h.
- Leoni, L. and Sartori, F. (1996) 'Heavy metals and arsenic in sediments from the continental shelf of the Northern Tyrrhenian/Eastern Ligurian seas', *Marine Environmental Research*. doi: 10.1016/0141-1136(94)00153-7.
- Lima, E. A. M. (2008) 'Avaliação da qualidade dos sedimentos e prognóstico geoquímico ambiental da zona estuarina do Rio Botafogo, Pernambuco.' Tese (Doutorado). Universidade Federal de Pernambuco, 172p.
- Luther, G. W. *et al.* (1992) 'Seasonal iron cycling in the salt-marsh sedimentary

- environment: the importance of ligand complexes with Fe(II) and Fe(III) in the dissolution of Fe(III) minerals and pyrite, respectively', *Marine Chemistry*. doi: 10.1016/0304-4203(92)90049-G.
- Mabuchi K., Lilienfeld A.M., Snell L.M., (1980) 'Cancer and occupational exposure to arsenic: a study of pesticide workers.' *Preventive Medicine* 9: 51- 77.
- Machado, W. *et al.* (2008) 'Relation of Reactive Sulfides with Organic Carbon, Iron, and Manganese in Anaerobic Mangrove Sediments: Implications for Sediment Suitability to Trap Trace Metals', *Journal of Coastal Research*. doi: 10.2112/06-0736.1.
- Magalhães, M. C. F. (2007) 'Arsenic. An environmental problem limited by solubility', *Pure and Applied Chemistry*. doi: 10.1351/pac200274101843.
- Marangoni, J. C. and Costa, C. S. B. (2012) 'Short- and Long-Term Vegetative Propagation of Two Spartina Species on a Salt Marsh in Southern Brazil', *Estuaries and Coasts*. doi: 10.1007/s12237-011-9474-7.
- Marques, W. C. *et al.* (2009) 'Numerical modeling of the Patos Lagoon coastal plume, Brazil', *Continental Shelf Research*, 29(3), pp. 556–571. doi: 10.1016/j.csr.2008.09.022.
- Marques, W. C. *et al.* (2010) 'Dynamics of the Patos Lagoon coastal plume and its contribution to the deposition pattern of the southern Brazilian inner shelf', *Journal of Geophysical Research: Oceans*, 115(10). doi: 10.1029/2010JC006190.
- Masscheleyn, P. H., Delaune, R. D., Patrick, W. H. (1991) 'Effect of Redox Potential and pH on Arsenic Speciation and Solubility in a Contaminated Soil', *Environmental Science and Technology*. doi: 10.1021/es00020a008.
- Masscheleyn, P. H., Delaune, R. D., Patrick, W. H. (2010) 'Arsenic and Selenium Chemistry as Affected by Sediment Redox Potential and pH', *Journal of Environment Quality*. doi: 10.2134/jeq1991.00472425002000030004x.
- Mayer, L. M. (1994) 'Relationships between mineral surfaces and organic carbon concentrations in soils and sediments', *Chemical Geology*. doi: 10.1016/0009-2541(94)90063-9.
- Medeiros, P.M., Bicego, M.C., Castelao, R.M., Del Rosso, C., Fillmann, G., Zamboni, A.J. (2005) 'Natural and anthropogenic hydrocarbon inputs to sediments of Patos Lagoon Estuary, Brazil.' *Environment International*, 31, 77-87.
- Melamed, D. (2005) 'Monitoring arsenic in the environment: a review of science and technologies with the potential for field measurements.' *Analytical Chemical Acta*,

532: 1-13.

- Melo, G. A. S. (1996) 'Manual de identificação dos Brachyura (caranguejos e siris) do litoral brasileiro.' Plêiade, São Paulo. 604p.
- Mirlean, N. *et al.* (2003) 'Arsenic pollution in Patos Lagoon estuarine sediments, Brazil', *Marine Pollution Bulletin*. doi: 10.1016/S0025-326X(03)00257-1.
- Mirlean, N., Baisch P., Travassos M.P., Nassar C. (2011) 'Calcareous algae bioclast contribution to sediment enrichment by arsenic on the Brazilian subtropical coast.' *Geo-Marine Letters*, 31:65-73
- Mirlean, N. *et al.* (2012) 'Arsenic enrichment in shelf and coastal sediment of the Brazilian subtropics', *Continental Shelf Research*. doi: 10.1016/j.csr.2012.01.006.
- Mirlean, N., Garcia, F., Baisch, P., Quintana, G.C., Agnes, F. (2013) 'Sandy beaches contamination by arsenic, a result of nearshore sediment diagenesis and transport (Brazilian coastline.)' *Estuarine, Coastal and Shelf Science*, 135, p. 241-247.
- Mirlean, N., Baisch, P., Diniz, D., (2014) 'Arsenic in groundwater of the Paraiba do Sul delta, Brazil: an atmospheric source?' *Sci. Tot. Environ.* 482–483, 148–156
- Mirlean, N., Costa, C. S. B. (2017) 'Geochemical factors promoting die-back gap formation in colonizing patches of Spartina densiflora in an irregularly flooded marsh', *Estuarine, Coastal and Shelf Science*. doi: 10.1016/j.ecss.2017.03.006.
- Moller, O. O. *et al.* (1996) 'The Patos Lagoon summertime circulation and dynamics', *Continental Shelf Research*. doi: 10.1016/0278-4343(95)00014-R.
- Möller, O.O., Castaing, P. (1999) 'Hydrological characteristics of the estuarine area of Patos Lagoon (30°S, Brazil)'. In: Perillo, G.M.E., MC Piccolo. (Eds.), *Estuaries of South America (their Geomorphology and Dynamics)*. Environmental Science. Springer, Berlin, p. 83 - 100.
- Moller, O. O. *et al.* (2001) 'The Influence of Local and Non-Local Forcing Effects on the Subtidal Circulation of Patos Lagoon', *Estuaries*. doi: 10.2307/1352953.
- Moore, J. N., Ficklin, W. H., Johns, C. (1988) 'Partitioning of Arsenic and Metals in Reducing Sulfidic Sediments', *Environmental Science and Technology*. doi: 10.1021/es00169a011.
- Nickson, R. T. *et al.* (2000) 'Mechanism of arsenic release to groundwater, Bangladesh and West Bengal', *Applied Geochemistry*. doi: 10.1016/S0883-2927(99)00086-4.
- Niencheski, L. F. H., Baumgarten, M. G., Fillman, G. & Windom, H. L. (1994) 'Nutrient and suspended matter behavior in the Patos Lagoon Estuary, Brazil'. *Estuaries of South America*. Ed. G. Perillo, Am. Geophys. Union.

- Nóbrega, G. N. *et al.* (2013) 'Iron and sulfur geochemistry in semi-arid mangrove soils (Ceará, Brazil) in relation to seasonal changes and shrimp farming effluents', *Environmental Monitoring and Assessment*. doi: 10.1007/s10661-013-3108-4.
- O'Day, P. A. *et al.* (2004) 'The influence of sulfur and iron on dissolved arsenic concentrations in the shallow subsurface under changing redox conditions', *Proceedings of the National Academy of Sciences*. doi: 10.1073/pnas.0402775101.
- Otero, X. L., Macias, F. (2003) 'Spatial variation in pyritization of trace metals in salt-marsh soils', *Biogeochemistry*. doi: 10.1023/A:1021115211165.
- Pierce, M. L., Moore, C. B. (1982) 'Adsorption of arsenite and arsenate on amorphous iron hydroxide', *Water Research*. doi: 10.1016/0043-1354(82)90143-9.
- Planer-Friedrich, B. *et al.* (2007) 'Thioarsenates in geothermal waters of yellowstone National Park: Determination, preservation, and geochemical importance', *Environmental Science and Technology*. doi: 10.1021/es070273v.
- Portz, L.C. (2005). 'Avaliação da contaminação por hidrocarbonetos em amostras ambientais do estuário da Lagoa dos Patos, RS, Brasil'. *Monografia* (Graduação em Oceanologia), Universidade Federal do Rio Grande (FURG), 88p.
- Rabelo, S.C. (1994) 'Modelo ecológico das marismas de *Spaprtina alterniflora Loisel.* (*Poaceae*) do estuário da Lagoa dos Patos, RS. **Dissertação** (Mestrado, Universidade Federal do Rio Grande, RS). 105 pp.
- Rahman, M.M., Dong, Z., Naidu, R. (2015) 'Concentrations of arsenic and other elements in groundwater of Bangladesh and West Bengal, India: potential cancer risk.' *Chemosphere*, 139: 54-64.
- Ravenscroft, P., Brammer, H. and Richards, K. (2009) *Arsenic Pollution: A Global Synthesis*, *Arsenic Pollution: A Global Synthesis*. doi: 10.1002/9781444308785.
- Riedel, G. F., Sanders, J. G. and Osman, R. W. (1987) 'The effect of biological and physical disturbances on the transport of arsenic from contaminated estuarine sediments', *Estuarine, Coastal and Shelf Science*. doi: 10.1016/0272-7714(87)90016-3.
- Rohde, G.M. (2004) 'Geoquímica Ambiental e Estudos de Impacto.' São Paulo, Signus Editora, 157 p. (2^a ed.).
- Sá, F. *et al.* (2015) 'Arsenic fractionation in estuarine sediments: Does coastal eutrophication influence As behavior?', *Marine Pollution Bulletin*. doi: 10.1016/j.marpolbul.2015.04.037.

- Sailo, L., Mahanta, C. (2014) 'Arsenic mobilization in the Brahmaputra plains of Assam: groundwater and sedimentary controls', *Environmental Monitoring and Assessment*. doi: 10.1007/s10661-014-3890-7.
- Salomons, W., Forstner, U., Salomons, W and Forstner, U. (1984) 'Metals in the Hydrocycle', *Acta hydrochimica et hydrobiologia*. doi: 10.1007/978-3-642-69325-0.
- Sharma, V. K., Sohn, M. (2009) 'Aquatic arsenic: Toxicity, speciation, transformations, and remediation', *Environment International*. doi: 10.1016/j.envint.2009.01.005.
- Shimada, N. (1996) 'Geochemical conditions enhancing the solubilization of arsenic into groundwater in Japan', *Applied Organometallic Chemistry*. doi: 10.1002/(SICI)1099-0739(199611)10:9<667::AID-AOC545>3.0.CO;2-I.
- Smedley, P. L., Kinniburgh, D. G. (2002) 'A review of the source, behaviour and distribution of arsenic in natural waters', *Applied Geochemistry*. doi: 10.1016/S0883-2927(02)00018-5.
- Smith, A. H., Lingas, E. O., Rahman, M. (2000) 'Contamination of drinking-water by arsenic in Bangladesh: A public health emergency', *Bulletin of the World Health Organization*. doi: 10.1590/S0042-96862000000900005.
- Smith, E., Smith, J., Naidu, R. (2006) 'Distribution and nature of arsenic along former railway corridors of South Australia', *Science of the Total Environment*. doi: 10.1016/j.scitotenv.2005.05.039.
- Soares, R. (2011) 'Origem, distribuição e biodisponibilidade de metais em águas, sedimentos e solos de um trecho da sub-bacia do rio Paraibuna, MG, Brasil.' *Tese* (Doutorado em Geociências – Geoquímica Ambiental) – Universidade Federal Fluminense, Niterói.
- Sullivan, K. A., Aller, R. C. (1996) 'Diagenetic cycling of arsenic in Amazon shelf sediments', *Geochimica et Cosmochimica Acta*. doi: 10.1016/0016-7037(96)00040-3.
- Telfeyan, K. *et al.* (2017) 'Arsenic, vanadium, iron, and manganese biogeochemistry in a deltaic wetland, southern Louisiana, USA', *Marine Chemistry*. doi: 10.1016/j.marchem.2017.03.010.
- Travassos, M., Baisch, P., Lacerda, L. (1993) 'Geochemistry distribution of heavy metals of the Patos Lagoon Estuary - Brazil'. *Heavy Metals in the Environment*- Toronto, 1, p. 185-188.

- USEPA, U. S. E. P. A. (1991) *Draft analytical method for determination of acid volatile sulfide in sediment*. EPA-821-R-91-100, Washington, DC
- USEPA, U. S. E. P. A. (1996) *Method 3050B - Acid digestion of sediments, sludges, and soils.*, 1996. doi: 10.11117/12.528651.
- USEPA, U.S.E.P.A. (2012) Method – 3051 <http://www.caslab.com/EPA-Method-3051/>
- Vale, C. *et al.* (1990) 'Presence of metal-rich rhizoconcretions on the roots of *Spartina maritima* from the salt marshes of the Tagus Estuary, Portugal', *Science of the Total Environment, The*. doi: 10.1016/0048-9697(90)90265-V.
- Vidal-Durà, A. *et al.* (2018) 'Reoxidation of estuarine sediments during simulated resuspension events: Effects on nutrient and trace metal mobilisation', *Estuarine, Coastal and Shelf Science*. doi: 10.1016/j.ecss.2018.03.024.
- Vilwock, J.A. (1994) 'Geology of the Coastal Province of Rio Grande do Sul, Southern Brazil. A synthesis.' *Pesquisas*, 16:5-49.
- Wallner-Kersanach, M., Mirlean, N., Baumgarten, M.G.Z., Costa, L.F., Baisch, P. (2015) 'Temporal evolution of the contamination in the southern area of the Patos Lagoon estuary, RS, Brazil'. *Journal of Integrated Coastal Zone Management*. DOI: 10.5894/rgci596.
- Wang, S. *et al.* (2012) 'Arsenic retention and remobilization in muddy sediments with high iron and sulfur contents from a heavily contaminated estuary in China', *Chemical Geology*. doi: 10.1016/j.chemgeo.2012.05.005.
- Wang, Y. *et al.* (2012) 'Dynamics of arsenic in salt marsh sediments from Dongtan wetland of the Yangtze River estuary, China', *Journal of Environmental Sciences (China)*. doi: 10.1016/S1001-0742(11)61048-6.
- WHO - World Health Organization. (2011) *Guidelines for drinking-water quality*. 4th ed. Geneva
- Widerlund, A., Ingri, J. (1995) 'Early diagenesis of arsenic in sediments of the Kalix River estuary, northern Sweden', *Chemical Geology*. doi: 10.1016/0009-2541(95)00073-U.
- Windom, H. L., Niencheski, L. F., Smith Jr, R. G. (1999) 'Biogeochemistry of nutrients and trace metals in the estuarine region of the Patos Lagoon (Brazil).' *Estuar. Coast. Shelf Sci.*, 48: 113-123.
- Ying, S. C., Kocar, B. D. and Fendorf, S. (2012) 'Oxidation and competitive retention of arsenic between iron- and manganese oxides', *Geochimica et Cosmochimica Acta*. doi: 10.1016/j.gca.2012.07.013.

Yücel, M. *et al.* (2010) ‘Sulfur speciation in the upper Black Sea sediments’, *Chemical Geology*. doi: 10.1016/j.chemgeo.2009.10.010.

ANEXOS

CAPÍTULO 1 - Testemunho M1								
Prof. (cm)	Amostra	Peso (g)	Fe (g kg^{-1})	Mn (mg kg^{-1})	As (mg kg^{-1})	COT (%)	Finos (%)	Eh (mV)
1	0-2	1,09	12,28	87,74	2,07	1,93	14,63	52,00
3	2-4	1,05	16,88	157,26	3,10	0,68	15,14	180,00
5	4-6	1,05	16,64	256,09	2,78	0,70	15,65	168,00
7	6-8	1,01	18,96	381,97	2,97	0,73	13,63	211,00
9	8-10	1,05	16,33	258,93	2,33	0,86	11,60	98,00
11	10-12	1,04	17,33	199,80	3,78	0,99	11,16	167,00
13	12-14	1,06	15,97	145,56	3,36	1,02	10,72	110,00
15	14-16	1,32	11,94	88,31	2,97	1,05	16,29	65,00
17	16-18	1,10	16,20	103,19	4,14	0,79	21,86	138,00
19	18-20	1,02	19,59	86,74	3,38	0,52	17,70	42,00
21	20-22	1,04	16,53	50,98	3,01	0,73	13,53	-18,00
23	22-24	1,07	15,77	52,73	3,18	0,94	17,99	45,00
25	24-26	1,36	21,37	150,14	4,85	0,88	22,45	27,00
27	26-28	1,02	29,31	220,79	6,96	0,82	23,98	-21,00
29	28-30	1,65	18,73	149,58	4,39	0,74	25,51	21,00
31	30-32	1,09	16,41	121,61	4,02	0,66	20,12	23,00
33	32-34	1,03	15,51	61,14	2,96	0,64	14,73	75,00
35	34-36	1,13	13,05	52,54	2,80	0,62	13,04	37,00
37	36-38	1,01	15,27	48,42	2,99	0,59	11,35	32,00
39	38-40	1,06	15,71	45,74	2,76	0,57	13,45	-1,00
41	40-42	1,01	19,04	45,92	3,55	0,48	15,55	25,00
43	42-44	1,02	15,88	43,24	3,29	0,40	13,33	28,00
45	44-46	1,31	12,50	43,66	3,04	0,41	11,10	-12,00
47	46-48	1,07	13,10	42,59	3,01	0,42	11,52	-61,00
49	48-50	1,18	13,90	40,94	3,19	0,46	11,94	82,00
51	50-52	1,13	14,93	43,13	3,25	0,49	12,35	62,00
53	52-54	1,19	17,49	41,75	2,96	0,51	12,77	126,00
55	54-56	1,05	17,92	39,25	2,93	0,52	15,77	58,00
57	56-58	1,07	14,05	39,31	2,83	0,37	18,77	124,00
59	58-60	1,09	14,87	61,33	3,29	0,23	11,02	22,00
61	60-62	1,10	19,83	98,05	3,63	0,21	3,27	
63	62-64	1,12	19,82	113,80	3,71	0,20	9,04	
		Média	16,7	105,38	3,36	0,66	14,72	63,50
		Max	29,3	381,97	6,96	1,93	25,51	211,00
		Min	11,9	39,25	2,07	0,20	3,27	-61,00
		SD	3,3	80,97	0,85	0,32	4,54	64,54

CAPÍTULO 1 - Testemunho M2								
Prof. (cm)	Amostra	Peso (g)	Fe (g kg ⁻¹)	Mn (mg kg ⁻¹)	As (mg kg ⁻¹)	COT (%)	Finos (%)	Eh (mV)
1	0-2	1,08	14,61	67,67	3,25	5,13	20,84	-252,00
3	2-4	1,15	11,87	63,08	2,79	4,57	26,89	-250,00
5	4-6	1,10	10,91	44,87	2,41	3,51	32,93	-218,00
7	6-8	1,26	14,12	43,14	2,80	2,46	38,77	-212,00
9	8-10	1,01	17,30	40,46	3,02	1,92	44,61	-143,00
11	10-12	1,39	10,78	47,65	2,68	1,39	44,93	-146,00
13	12-14	1,19	15,95	52,88	3,49	1,11	45,26	-82,00
15	14-16	1,14	19,77	59,94	5,40	0,83	46,33	-131,00
17	16-18	1,20	14,30	55,32	3,22	0,77	47,39	-78,00
19	18-20	1,59	13,80	62,09	3,75	0,72	54,28	-69,00
21	20-22	1,12	21,99	81,93	6,44	0,75	61,17	-70,00
23	22-24	1,26	27,54	80,42	9,26	0,78	53,57	-79,00
25	24-26	1,04	20,78	79,88	5,52	0,71	45,98	-98,00
27	26-28	1,33	17,50	60,00	4,73	0,65	41,38	-86,00
29	28-30	1,03	25,48	70,64	5,58	0,57	36,77	-71,00
31	30-32	1,06	26,30	70,22	5,46	0,50	33,18	-74,00
33	32-34	1,35	19,42	71,79	4,36	0,52	29,59	-75,00
35	34-36	1,35	14,94	61,00	3,83	0,54	26,01	-72,00
37	36-38	1,25	22,13	67,66	4,29	0,43	22,44	-79,00
39	38-40	1,35	15,80	58,42	2,88	0,33	23,26	-75,00
41	40-42	1,41	14,79	47,28	2,42	0,34	24,08	-65,00
43	42-44	1,33	15,00	55,81	2,56	0,35	23,32	-72,00
45	44-46	1,16	17,71	53,03	2,82	0,34	22,57	-55,00
47	46-48	1,25	20,16	42,38	3,34	0,33	18,49	-52,00
49	48-50	1,11	18,74	42,51	3,14	0,29	14,41	-48,00
51	50-52	1,07	16,57	41,41	2,92	0,26	14,72	-70,00
53	52-54	1,05	15,55	41,45	2,64	0,26	15,03	-48,00
55	54-56	1,03	17,21	31,88	3,19	0,27	19,59	-36,00
57	56-58	1,17	16,01	38,44	3,08	0,25	24,15	-15,00
59	58-60	1,12	16,94	30,05	2,99	0,24	23,38	-38,00
61	60-62	1,12	12,35	34,23	2,43	0,24	22,61	-51,00
63	62-64	1,03	10,05	36,53	1,59	0,24	21,79	-65,00
	Média	17,07	54,19	3,70	0,99	31,87	92,97	
	Max	27,54	81,93	9,26	5,13	61,17	-15,00	
	Min	10,05	30,05	1,59	0,24	14,41	-252,00	
	SD	4,28	14,50	1,50	1,22	12,82	59,73	

CAPÍTULO 1 - Testemunho M3								
Prof. (cm)	Amostra	Peso (g)	Fe (g kg ⁻¹)	Mn (mg kg ⁻¹)	As (mg kg ⁻¹)	COT (%)	Finos (%)	Eh (mV)
1	0-2	1,04	13,99	83,19	3,33	12,95	87,16	-60,00
3	2-4	1,12	14,11	70,63	3,41	11,76	65,08	-72,00
5	4-6	1,08	13,70	48,71	3,11	9,32	42,99	-134,00
7	6-8	1,09	16,22	60,39	3,55	7,64	41,77	-153,00
9	8-10	1,03	16,82	61,86	3,22	5,96	40,55	-131,00
11	10-12	1,29	12,83	51,28	3,41	5,08	27,44	-230,00
13	12-14	1,15	15,85	65,70	3,88	4,20	14,32	-264,00
15	14-16	1,12	17,17	64,00	5,04	3,79	13,01	-298,00
17	16-18	1,05	16,78	66,77	4,57	3,37	11,69	-277,00
19	18-20	1,08	18,69	148,08	4,90	3,31	12,57	-286,00
21	20-22	1,19	21,06	156,00	4,85	3,25	13,44	-281,00
23	22-24	1,03	26,13	149,83	7,89	2,54	17,42	-293,00
25	24-26	1,04	27,31	178,58	6,48	1,83	21,39	-297,00
27	26-28	1,21	22,00	150,89	6,02	1,67	14,87	-256,00
29	28-30	1,16	24,58	118,24	6,10	1,51	8,35	-132,00
31	30-32	1,10	21,20	131,92	5,12	1,03	6,82	-130,00
33	32-34	1,16	18,30	113,60	4,36	0,54	5,30	-146,00
35	34-36	1,04	21,74	96,18	4,58	0,39	4,37	-133,00
37	36-38	1,10	23,30	100,98	4,34	0,25	3,45	-40,00
39	38-40	1,06	21,43	113,93	3,71	0,25	4,28	-27,00
41	40-42	1,05	19,09	107,84	3,70	0,24	5,11	-25,00
43	42-44	1,23	15,59	105,85	3,22	0,25	5,82	-90,00
45	44-46	1,24	14,97	88,68	3,40	0,26	6,53	-90,00
47	46-48	1,29	15,21	64,91	3,32	0,28	6,52	-90,00
49	48-50	1,29	14,38	63,87	3,25	0,30	6,51	-70,00
51	50-52	1,32	13,21	61,23	3,02	0,29	7,72	-75,00
53	52-54	1,20	15,44	62,76	3,10	0,28	8,93	-54,00
55	54-56	1,15	15,16	67,93	3,28	0,26	8,74	-65,00
57	56-58	1,14	13,16	77,25	3,43	0,25	8,54	-103,00
59	58-60	1,12	12,10	74,43	3,47	0,24	7,36	-163,00
61	60-62	1,14	14,78	78,97	3,24	0,23	6,17	-206,00
63	62-64	1,15	14,29	83,77	3,04	0,24	5,70	-209,00
		Média	17,52	92,76	4,10	2,62	16,87	-152,50
		Max	27,31	178,58	7,89	12,95	87,16	-25,00
		Min	12,10	48,71	3,02	0,23	3,45	-298,00
		SD	4,04	34,49	1,17	3,43	18,82	88,94

CAPÍTULO 1 - Testemunho Z1								
Prof. (cm)	Amostra	Peso (g)	Fe (g kg ⁻¹)	Mn (mg kg ⁻¹)	As (mg kg ⁻¹)	COT (%)	Finos (%)	Eh (mV)
1	0-2	1,05	16,15	48,56	2,25	0,53	28,97	-25,00
3	2-4	1,04	23,09	50,15	2,20	0,43	36,37	-26,00
5	4-6	1,12	21,05	89,70	3,07	0,65	43,77	-41,00
7	6-8	1,01	29,18	132,08	4,28	0,88	58,12	-36,00
9	8-10	1,05	23,90	105,17	4,05	0,88	72,47	-54,00
11	10-12	1,03	25,30	113,17	4,08	0,89	74,17	-66,00
13	12-14	1,01	29,34	152,79	4,79	1,03	75,87	-73,00
15	14-16	1,09	19,31	141,58	4,07	1,17	62,98	-60,00
17	16-18	1,03	23,08	130,92	4,13	0,97	50,10	-98,00
19	18-20	1,08	9,97	52,92	2,47	0,77	54,92	-80,00
21	20-22	1,32	7,87	20,36	1,44	0,41	59,74	-95,00
23	22-24	1,09	9,70	23,83	1,72	0,05	48,03	-150,00
25	24-26	1,20	11,12	32,47	1,76	0,06	36,32	-132,00
27	26-28	1,31	8,43	29,77	1,59	0,07	22,82	-82,00
29	28-30	1,02	11,73	47,49	2,18	0,18	9,31	-57,00
31	30-32	1,01	19,03	126,19	3,55	0,30	7,83	-155,00
33	32-34	1,07	17,25	91,00	2,89	0,38	6,35	-126,00
35	34-36	1,18	13,52	86,51	2,77	0,45	7,09	-139,00
37	36-38	1,10	12,96	58,27	2,33	0,40	7,84	-169,00
39	38-40	1,02	25,30	173,85	3,84	0,34	24,68	-188,00
41	40-42	1,02	31,86	255,70	5,42	0,65	41,52	-187,00
43	42-44	1,04	26,27	189,09	4,02	0,96	34,77	-167,00
45	44-46	1,02	14,69	78,91	2,59	0,72	28,02	-158,00
47	46-48	1,02	15,08	88,56	2,74	0,48	54,25	-128,00
49	48-50	1,10	23,39	178,07	4,36	0,54	80,49	-126,00
51	50-52	1,05	13,89	80,73	2,59	0,60	86,44	-171,00
53	52-54	1,03	11,90	60,10	2,24	0,39	92,39	-147,00
55	54-56	1,01	16,59	88,85	2,72	0,19	86,47	-132,00
57	56-58	1,29	16,60	90,95	2,24	0,33	80,55	-135,00
59	58-60	1,15	13,89	102,90	2,72	0,46	71,93	-137,00
61	60-62	1,10	9,42	43,10	1,89	0,38	63,30	-158,00
63	62-64	1,02	8,64	25,78	1,58	0,30	61,65	-180,00
65	64-66	1,03	9,33	35,29	1,73	0,18	60,00	-165,00
		Média	17,24	91,66	2,92	0,52	49,38	-116,45
		Max	31,86	255,70	5,42	1,17	92,39	-25,00
		Min	7,87	20,36	1,44	0,05	6,35	-188,00
		SD	6,79	54,59	1,04	0,29	25,41	49,52

CAPÍTULO 1 - Testemunho Z2								
Prof. (cm)	Amostra	Peso (g)	Fe (g kg ⁻¹)	Mn (mg kg ⁻¹)	As (mg kg ⁻¹)	COT (%)	Finos (%)	Eh (mV)
1	0-2	1,17	11,82	24,57	2,23	0,30	15,01	-51,00
3	2-4	1,05	17,41	28,66	2,63	0,41	14,40	-53,00
5	4-6	1,11	16,74	34,50	2,78	0,36	13,78	-49,00
7	6-8	1,41	15,36	28,92	2,45	0,32	13,10	-76,00
9	8-10	1,02	17,29	29,71	3,22	0,29	12,42	-70,00
11	10-12	1,49	12,62	21,17	2,20	0,26	13,62	-68,00
13	12-14	1,09	20,77	41,11	3,49	0,26	14,83	-65,00
15	14-16	1,12	16,12	38,52	3,37	0,26	14,53	-55,00
17	16-18	1,05	18,27	40,04	3,51	0,29	14,23	-45,00
19	18-20	1,01	14,27	34,66	2,75	0,31	14,62	-80,00
21	20-22	1,06	13,59	35,94	2,33	0,30	15,01	-129,00
23	22-24	1,20	12,69	44,06	2,20	0,28	17,96	-99,00
25	24-26	1,25	15,49	48,25	2,25	0,31	20,90	-133,00
27	26-28	1,02	14,33	64,40	2,59	0,35	26,24	-179,00
29	28-30	1,09	18,03	54,41	2,65	0,37	31,57	-203,00
31	30-32	1,05	22,22	63,82	3,39	0,39	34,18	-212,00
33	32-34	1,01	25,14	68,55	3,47	0,41	36,80	-237,00
35	34-36	1,20	18,27	72,27	3,28	0,43	36,73	-294,00
37	36-38	1,04	28,92	88,00	4,13	0,52	36,67	-295,00
39	38-40	1,02	27,35	104,20	4,47	0,61	45,52	-301,00
41	40-42	1,07	28,35	89,95	4,44	0,75	54,37	-297,00
43	42-44	1,07	27,54	116,96	3,91	0,88	50,58	-331,00
45	44-46	1,20	22,12	105,64	3,49	0,97	46,78	-324,00
47	46-48	1,18	21,77	116,33	3,25	1,06	45,92	-304,00
49	48-50	1,04	26,80	129,37	4,31	1,09	45,06	-317,00
51	50-52	1,36	14,17	92,68	2,26	1,12	39,17	-371,00
53	52-54	1,06	17,18	72,68	2,64	0,93	33,28	-330,00
55	54-56	1,02	22,45	102,94	3,47	0,73	30,41	-337,00
57	56-58	1,05	22,34	97,39	2,91	0,71	27,53	-354,00
59	58-60	1,07	14,60	74,66	2,65	0,70	27,76	-370,00
61	60-62	1,09	13,57	69,22	2,22	0,66	27,99	-378,00
		Média	18,95	65,60	3,06	0,54	28,10	-206,68
		Max	28,92	129,37	4,47	1,12	54,37	-45,00
		Min	11,82	21,17	2,20	0,26	12,42	-378,00
		SD	5,11	31,18	0,69	0,28	12,94	121,55

CAPÍTULO 1 - Testemunho Z3								
Prof. (cm)	Amostra	Peso (g)	Fe (g kg^{-1})	Mn (mg kg^{-1})	As (mg kg^{-1})	COT (%)	Finos (%)	Eh (mV)
1	0-2	1,37	7,72	129,21	2,03	0,23	7,60	118,00
3	2-4	1,29	9,45	177,00	2,45	0,33	10,43	-88,00
5	4-6	1,06	13,05	124,93	2,56	0,30	13,27	-90,00
7	6-8	1,03	13,06	115,29	2,43	0,25	11,58	-104,00
9	8-10	1,01	9,88	51,11	2,21	0,23	9,90	-124,00
11	10-12	1,10	10,69	55,81	2,10	0,20	10,37	-90,00
13	12-14	1,31	12,03	45,93	2,08	0,20	10,83	-154,00
15	14-16	1,13	13,29	57,66	2,72	0,20	12,96	-111,00
17	16-18	1,12	13,16	79,79	2,73	0,23	15,08	-108,00
19	18-20	1,03	17,44	91,83	2,74	0,27	17,42	-113,00
21	20-22	1,13	16,26	89,84	2,64	0,28	19,75	-91,00
23	22-24	1,09	18,13	116,83	3,07	0,28	21,46	-65,00
25	24-26	1,15	22,03	131,46	3,01	0,31	23,17	-68,00
27	26-28	1,04	17,57	144,46	3,05	0,34	28,04	-155,00
29	28-30	1,05	25,95	188,99	3,33	0,43	32,92	-170,00
31	30-32	1,01	27,20	186,92	3,47	0,52	36,09	-292,00
33	32-34	1,03	31,54	183,31	3,75	0,66	39,26	-230,00
35	34-36	1,14	24,48	219,33	4,03	0,80	45,94	-209,00
37	36-38	1,63	28,28	209,50	3,66	0,84	52,62	-155,00
39	38-40	1,02	29,36	328,73	5,01	0,87	57,22	-346,00
41	40-42	1,04	26,96	346,67	3,76	0,94	61,82	-293,00
43	42-44	1,04	30,92	329,89	4,02	1,01	60,10	-346,00
45	44-46	1,23	30,95	341,23	4,62	0,84	58,39	-361,00
47	46-48	1,20	30,09	309,99	4,02	0,66	64,32	-351,00
49	48-50	1,25	23,93	242,85	3,29	0,76	70,25	-351,00
51	50-52	1,16	20,58	172,39	2,91	0,86	55,88	-365,00
53	52-54	1,04	23,37	171,11	3,14	0,73	41,51	-329,00
55	54-56	1,07	26,87	205,38	3,98	0,59	46,04	-334,00
57	56-58	1,08	23,51	154,50	2,94	0,46	50,57	-282,00
59	58-60	1,01	15,07	101,46	2,45	0,32	50,67	-343,00
61	60-62	1,13	17,17	91,68	2,40	0,57	50,77	-334,00
63	62-64	1,01	18,84	95,73	2,53	0,82	58,00	-334,00
65	64-66	1,04	21,25	99,19	2,57	0,83	65,24	-367,00
		Média	20,31	163,33	3,08	0,52	36,65	-213,18
		Max	31,54	346,67	5,01	1,01	70,25	118,00
		Min	7,72	45,93	2,03	0,20	7,60	-367,00
		SD	7,05	87,03	0,74	0,26	20,32	124,40

CAPÍTULO 2 - Período Polihalino - Sedimento							
Abril/2018		<i>S. alterniflora</i> (SA)			<i>N. granulata</i> (NG)		
Prof. (cm)	Amostra	% Finos	% COT	Eh (mV)	% Finos	% COT	Eh (mV)
1	0-2	32,04	4,32	34,50	20,84	5,13	83,10
3	2-4	35,66	2,63	-220,50	26,89	4,57	54,70
5	4-6	37,87	2,32	-230,70	32,93	3,51	86,70
7	6-8	38,52	2,00	-208,70	38,77	2,46	100,60
9	8-10	40,12	3,11	-145,10	44,61	1,92	134,10
11	10-12	46,34	1,86	-70,30	44,93	1,39	67,30
13	12-14	48,72	1,54	-84,00	45,26	1,11	68,30
15	14-16	47,96	1,23	-74,10	46,33	0,83	14,00
17	16-18	48,35	0,96	-89,80	47,39	0,77	28,30
19	18-20	52,48	0,79	-120,80	54,28	0,72	49,30
21	20-22	58,36	0,75	-141,40	61,17	0,75	5,40
23	22-24	60,41	0,82	-142,60	53,57	0,78	-31,00
25	24-26	53,42	0,65	-199,60	45,98	0,71	-12,20
27	26-28	49,78	0,60	-229,20	41,38	0,65	-75,90
29	28-30	44,36	0,48	-252,60	36,77	0,57	-76,30
31	30-32	42,68	0,66	-291,50	33,18	0,50	-92,70
		Média	46,07	1,55	-154,15	42,14	1,65
		Max	60,41	4,32	34,50	61,17	134,10
		Min	32,04	0,48	-291,50	20,84	0,50
		SD	8,00	1,09	85,27	10,38	1,49
							67,96

CAPÍTULO 2 - Período Polihalino - Nódulos							
<i>S. alterniflora</i> (SA) (Abril/2018)				<i>N. granulata</i> (NG) (Abril/2018)			
Prof (cm)	Mn (mg kg ⁻¹)	As (mg kg ⁻¹)	Fe (%)	Prof (cm)	Mn (mg kg ⁻¹)	As (mg kg ⁻¹)	Fe (%)
1	275,28	144,18	16,13	3	517,15	70,18	9,98
3	232,43	123,74	13,74	6	311,82	31,97	4,74
5	213,77	128,15	14,75	8	270,15	31,47	5,05
7	227,22	94,00	13,87	10	304,76	37,46	6,20
9	148,27	109,29	11,85	12	357,95	51,23	8,62
11	460,15	171,82	16,62	13	592,68	120,24	12,51
13	318,37	111,67	9,07	14	473,23	111,04	12,47
15	305,35	123,70	15,53	15	406,02	149,03	12,74
17	142,31	67,28	12,05	16	224,20	49,76	6,17
19	248,74	116,54	14,96	17	115,90	36,02	4,56
Média	257,19	119,04	13,86	19	193,00	58,50	9,54
Max	460,15	171,82	16,62	Média	342,44	67,90	8,42
Min	142,31	67,28	9,07	Max	592,68	149,03	12,74
SD	91,96	27,90	2,30	Min	115,90	31,47	4,56
				SD	144,83	40,55	3,24

CAPÍTULO 2 - Água Intersticial

<i>S. alterniflora</i> (SA) – Polihalino			<i>N. Granulata</i> (NG) - Polihalino			<i>S. alterniflora</i> (SA) - Oligohalino			<i>N. Granulata</i> (NG) - Oligohalino		
Prof. (cm)	Fe (ug kg ⁻¹)	Mn (ug kg ⁻¹)	Prof.(cm)	Fe (ug kg ⁻¹)	Mn (ug kg ⁻¹)	Prof. (cm)	Fe (ug kg ⁻¹)	Mn (ug kg ⁻¹)	Prof. (cm)	Fe (ug kg ⁻¹)	Mn (ug kg ⁻¹)
3	0,37	0,20	3	0,29	0,02	3	8,01	0,13	3	4,40	0,15
8	60,95	0,85	8	0,15	0,02	8	8,76	0,16	8	4,09	0,13
10	54,66	0,64	10	0,22	0,05	10	2,92	0,10	10	2,40	0,13
12	48,68	0,38	12	0,14	0,09	12	1,08	0,11	12	3,12	0,12
14	38,14	0,41	14	0,12	0,07	14	2,81	0,12	14	2,39	0,12
15	28,23	0,39	15	0,16	0,12	15	3,74	0,14	15	3,90	0,12
16	37,23	0,50	19	0,27	0,18	16	3,81	0,15	19	19,34	0,21
17	39,68	0,76	23	0,37	0,38	17	3,24	0,14	23	43,99	0,21
18	43,81	0,74	28	0,58	0,71	18	7,01	0,18	28	49,85	0,25
20	44,75	0,69	Média	0,26	0,18	20	7,67	0,19	Média	14,83	0,16
24	46,54	0,55	Max	0,58	0,71	24	10,08	0,21	Max	49,85	0,25
28	50,40	0,59	Min	0,12	0,02	28	11,27	0,25	Min	2,39	0,12
Média	41,12	0,56	SD	0,15	0,23	Média	5,87	0,16	SD	19,00	0,05
Max	60,95	0,85				Max	11,27	0,25			
Min	0,37	0,20				Min	1,08	0,10			
SD	15,44	0,19				SD	3,32	0,04			

CAPÍTULO 3 – Sedimento obtido em local ocupado por <i>N. granulata</i> (DA)										
Amostras	Eh (mV)	Mn (mg kg^{-1})			Fe (%)			As (mg kg^{-1})		
		Total	HCl	Reativo	Total	HCl	Reativo	Total	HCl	Reativo
DA-01	175	190,94	24,03	7,74	1,67	0,89	0,27	1,79	0,69	0,49
DA-02	157	183,02	106,51	41,85	2,17	1,77	0,94	4,91	2,97	2,00
DA-03	-20	128,79	25,90	17,95	1,89	1,23	0,27	2,51	0,53	0,28
DA-04	55	911,33	903,45	404,02	3,12	1,65	0,88	8,14	5,48	2,65
DA-05	48	108,22	22,11	16,48	1,85	1,61	0,31	2,89	1,21	0,57
DA-06	88	120,44	19,12	17,97	1,87	1,42	0,42	3,32	1,07	0,86
DA-07	58	125,10	20,92	18,90	1,73	1,01	0,37	1,56	0,77	0,59
DA-08	70	57,01	7,72	6,78	1,72	0,81	0,16	5,28	0,62	0,48
DA-09	75	128,50	15,45	13,03	1,48	0,64	0,31	2,80	1,08	0,51
DA-10	95	671,49	321,82	76,38	3,36	2,39	0,78	8,17	6,11	2,15
DA-11	82	158,01	146,70	25,85	2,05	1,66	0,42	2,64	1,54	0,26
DA-12	115	613,80	398,60	71,53	3,44	2,75	0,59	9,38	7,92	2,78
DA-13	115	86,45	29,62	13,74	1,20	0,40	0,05	0,94	0,41	0,27
DA-14	126	950,95	798,31	108,27	6,24	4,60	1,04	15,46	14,15	3,34
DA-15	123	663,09	305,33	49,25	5,59	4,76	1,10	14,76	10,39	4,59
DA-16	106	164,92	68,57	22,42	2,39	1,66	0,28	2,58	1,66	0,66
DA-17	130	432,25	393,16	17,12	5,92	3,75	1,82	10,65	9,19	6,58
DA-18	140	631,48	511,51	17,10	8,98	7,40	0,98	33,40	31,43	2,96
DA-19	145	420,16	411,04	50,01	5,69	5,11	2,45	23,58	22,76	7,59
DA-20	130	842,13	686,87	85,78	6,61	4,70	1,68	8,70	6,40	2,52
DA-21	108	101,95	22,37	19,11	1,43	0,67	0,14	1,63	0,60	0,27
DA-22	113	85,88	17,39	9,25	1,35	0,46	0,09	1,15	0,38	0,11
DA-23	90	80,75	15,76	8,46	1,31	0,41	0,04	1,03	0,37	0,26
DA-24	100	72,93	18,41	8,67	0,84	0,39	0,02	1,64	0,31	0,28
DA-25	111	86,14	17,17	7,65	1,35	0,38	0,01	1,59	0,45	0,38
DA-26	140	1073,19	733,92	156,73	8,84	5,36	1,89	27,52	26,71	2,83
DA-27	150	932,20	820,04	253,04	10,62	8,05	2,15	28,09	26,82	2,81
DA-28	127	143,62	36,34	14,56	1,67	0,39	0,09	2,50	0,28	0,08
DA-29	90	107,80	33,73	20,38	1,49	0,60	0,10	1,01	0,46	0,43
DA-30	128	591,94	335,64	42,55	4,05	3,12	0,43	5,48	4,92	1,21
DA-31	154	98,94	18,87	11,75	1,41	0,30	0,03	1,20	0,20	0,08
DA-32	156	77,60	19,54	13,64	1,11	0,42	0,09	0,45	0,41	0,33
DA-33	168	931,34	537,92	135,60	7,59	5,01	1,80	26,97	26,57	3,61
DA-34	159	274,51	95,83	44,52	2,56	1,18	0,23	1,37	1,06	0,94
DA-35	193	266,12	126,11	33,96	1,78	1,57	0,58	2,22	1,50	1,34
DA-36	187	254,91	84,64	34,87	1,82	1,55	0,47	2,29	1,33	0,83

CAPÍTULO 3 – Sedimento obtido em local ocupado por <i>S. alterniflora</i> (SA)										
Amostras	Eh (mV)	Mn (mg kg ⁻¹)			Fe (%)			As (mg kg ⁻¹)		
		Total	HCl	Reativo	Total	HCl	Reativo	Total	HCl	Reativo
SA-01	130	173,42	26,67	24,63	1,76	1,50	0,38	2,55	1,58	0,60
SA-02	-20	99,37	35,81	10,25	1,56	1,10	0,28	2,10	1,19	0,55
SA-03	-10	142,71	27,77	8,97	2,38	1,34	0,43	5,69	1,33	0,61
SA-04	25	167,61	37,74	15,78	2,05	1,36	0,47	4,18	1,59	0,51
SA-05	40	105,84	23,30	14,14	1,50	0,68	0,25	1,37	0,64	0,40
SA-06	-35	163,44	43,94	12,68	2,68	2,15	0,56	8,27	1,74	0,81
SA-07	40	298,69	54,01	0,01	2,03	1,44	0,75	3,89	3,39	1,08
SA-08	56	193,94	63,75	16,23	2,32	1,88	0,54	4,25	3,61	0,95
SA-09	67	121,84	49,46	35,05	1,46	0,91	0,34	1,17	1,15	0,47
SA-10	50	213,20	55,17	30,22	2,04	1,51	0,35	3,02	2,18	0,79
SA-11	28	179,44	40,07	14,80	2,07	1,08	0,34	2,23	1,34	0,70
SA-12	60	176,67	94,90	25,48	2,03	1,37	0,44	1,78	1,76	0,72
SA-13	75	871,09	156,07	32,90	4,17	3,62	0,62	6,00	5,76	1,56
SA-14	60	539,25	45,07	32,78	3,60	1,91	0,52	6,74	2,69	1,01
SA-15	85	255,66	134,18	81,86	2,18	1,86	0,56	6,38	5,96	1,11
SA-16	100	533,18	253,13	59,43	3,17	2,43	0,37	3,90	3,12	0,58
SA-17	88	820,77	495,53	18,33	3,12	2,21	0,53	3,18	2,32	1,27
AS-18	115	914,66	113,71	29,93	6,44	3,40	1,00	24,23	22,75	2,64
SA-19	118	97,28	62,09	20,89	0,92	0,22	0,05	0,33	0,14	0,14
SA-20	125	2398,43	517,78	472,80	6,05	2,85	0,87	10,15	4,41	1,57
SA-21	125	510,80	181,78	79,68	3,64	2,74	0,45	3,65	3,41	1,13
SA-22	126	402,42	115,31	23,67	3,29	1,62	0,40	2,57	2,27	1,23